Electron Counting Statistics in Nanostructures

PROEFSCHRIFT

ter verkrijging van
de graad van Doctor aan de Universiteit Leiden,
op gezag van de Rector Magnificus Dr. D. D. Breimer,
hoogleraar in de faculteit der Wiskunde en
Natuurwetenschappen en die der Geneeskunde,
volgens besluit van het College voor Promoties
te verdedigen op woensdag 3 september 2003
te klokke 16.15 uur
door

Markus Kindermann

geboren te Regensburg, Duitsland op 6 augustus 1974

Promotiecommissie:

Promotores:	Prof. dr. C. W. J. Beenakker
	Prof. dr. Yu. V. Nazarov (TU Delft)
Referent:	Prof. dr. ir. W. van Saarloos
Overige leden:	Prof. dr. ir. G. E. W. Bauer (TU Delft)
	Dr. Ya. M. Blanter (TU Delft)
	Prof. dr. M. Büttiker (Geneva)
	Prof. dr. P. H. Kes
	Prof. dr. J. M. van Ruitenbeek

Het onderzoek beschreven in dit proefschrift is uitgevoerd als onderdeel van het wetenschappelijke programma van de Nederlandse Organisatie voor Wetenschappelijk Onderzoek (NWO) en de Stichting voor Fundamenteel Onderzoek der Materie (FOM).

The research described in this thesis has been carried out as part of the scientific program of the Netherlands Organization for Scientific Research (NWO) and the Foundation for Fundamental Research on Matter (FOM).

Meinen Eltern

Contents

1 Introduction

The topic of this thesis originates from quantum optics. The statistics of the number of photons absorbed by a photodetector in a fixed time interval characterizes the quantum state of the electromagnetic field. For example, Poisson statistics is the signature of the coherent state emitted by a laser. An analogous tool in the solid state would be an electron counter. It must be fundamentally different from a photon counter because electrons cannot be absorbed. This provides for a rich new topic of research, to which this thesis is a contribution.

The experimental motivation for this research came from studies of current fluctuations in nanostructures. In macroscopic systems inelastic scattering averages out all non-equilibrium contributions to the fluctuations. Only thermal fluctuations remain, which contain little information about the system. On the nanoscale, however, elastic scattering dominates and current fluctuations contain much information that is not present in the mean current. By studying the statistics of transferred charge we seek to provide a theoretical framework to extract this information from the measured correlators of current fluctuations.

In this introductory chapter we give some background material. We refer to Ref. [1] for a brief tutorial and to Ref. [2] for a comprehensive review.

1.1 Current fluctuations

A photodetector (cf. Fig. 1-1) counts the number n of photons that reach it within a given time τ by absorbing them. By repeating the experiment many times one arrives at the counting distribution $P(n)$.

Electrons in an electrical circuit cannot be absorbed. To obtain the distribution $P(Q)$ of transferred charge Q in a time τ one can use the coupling of the electrical current I to the electromagnetic field. The magnetic field generated by I can be detected in a current meter. Alternatively, the voltage drop induced by

Figure 1-1. Schematic of photodetection.

I over a resistor can be measured by a voltage meter.

Moments of the transferred charge $Q = \int_0^\tau dt\, I(t)$ are related to correlators of the current by

$$\langle Q^n \rangle = \left\langle \left[\int_0^\tau dt\, I(t) \right]^n \right\rangle = \prod_{i=1}^{n} \int_0^\tau dt_1 \cdots \int_0^\tau dt_n \, \langle I(t_1) \cdots I(t_n) \rangle, \qquad (1.1.1)$$

where $\langle \cdots \rangle$ denotes a statistical average. This relation can be rewritten in the frequency domain, as a relation between moments of Q and correlators of the frequency dependent current $I(\omega) = \int dt\, e^{i\omega t} I(t)$. In the limit of a long detection time τ and low frequency $\omega \to 0$ the relation takes the simple form

$$\langle\langle I(\omega_1) \cdots I(\omega_n) \rangle\rangle = \frac{2\pi}{\tau} \delta \left(\sum_{k=1}^{n} \omega_k \right) \langle\langle Q^n \rangle\rangle. \qquad (1.1.2)$$

The double brackets $\langle\langle \cdots \rangle\rangle$ indicate irreducible moments, or cumulants. For $n = 1, 2, 3, 4$ one has

$$\begin{aligned} \langle\langle x_1 \rangle\rangle &= \langle x_1 \rangle, \;\; \langle\langle x_1 x_2 \rangle\rangle = \langle \delta x_1 \delta x_2 \rangle, \;\; \langle\langle x_1 x_2 x_3 \rangle\rangle = \langle \delta x_1 \delta x_2 \delta x_3 \rangle, \\ \langle\langle x_1 x_2 x_3 x_4 \rangle\rangle &= \langle \delta x_1 \delta x_2 \delta x_3 \delta x_4 \rangle - \langle \delta x_1 \delta x_2 \rangle \langle \delta x_3 \delta x_4 \rangle \\ &\quad - \langle \delta x_1 \delta x_3 \rangle \langle \delta x_2 \delta x_4 \rangle - \langle \delta x_1 \delta x_4 \rangle \langle \delta x_2 \delta x_3 \rangle, \qquad (1.1.3) \end{aligned}$$

with $\delta x_i = x_i - \langle x_i \rangle$.

We see that moments of $P(Q)$ can be inferred from a measurement of correlators of current fluctuations. The setup of a typical experiment is shown in Fig. 1-2. A mesoscopic conductor R is connected in series with a macroscopic conductor R_0. Current fluctuations δI produced in R induce voltage fluctuations δV over R_0 that are first passed through a band filter, then amplified and detected. The band filter is typically centered at a frequency of order 1 MHz to eliminate contamination by a high level of background noise. That is mainly due to randomly moving impurities in the conductor and called $1/f$-noise, because of its characteristic frequency dependence. To relate the measured correlators to $P(Q)$ one may still use the low frequency formula (1.1.2), provided that the measurement frequencies ω_i are $\ll \max(eV/\hbar, kT/\hbar)$, with V the voltage applied over the conductor R and T its temperature. (e is the elementary charge, k Boltzmann's constant, and $\hbar$ Planck's constant.)

1.2 Counting statistics

1.2.1 Fermions versus bosons

The counting statistics of non-interacting indistinguishable particles is closely tied to their quantum statistics. Electrons have as fermions an anti-symmetric

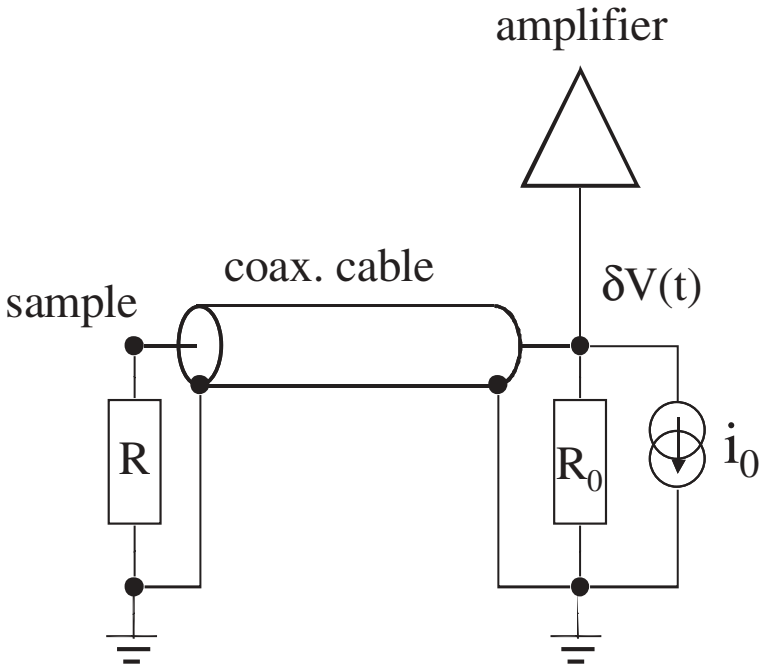

Figure 1-2. Circuit used in the measurement of the third moment of current fluctuations by Reulet, Senzier, and Prober [3].

wavefunction and obey the Pauli exclusion principle, that is, every single-particle quantum state can be occupied by at most one electron. Photons, on the other hand, have as bosons a symmetric wavefunction and are not subject to such a restriction. They tend to "bunch" together in the same quantum state. We begin with an elementary example: The counting statistics for a single source of particles in thermal equilibrium. For photons this applies to black body radiation. For electrons there is no direct application, because we have not yet closed the circuit.

The setup is schematically shown in Fig. 1-3. A single-mode waveguide is connected to a large particle reservoir at temperature T. For simplicity we consider only particles in a narrow energy interval $[E, E + \delta E]$. The single propagating mode in that interval has group velocity $v = \partial E/\partial \hbar k$, with k the longitudinal wave number. Single-particle states in a waveguide of length L are labeled by wave numbers spaced by $\triangle k = 2\pi/L$. Consequently, $N = \delta E/v\hbar\triangle k = \delta E L/hv$ single-particle states in the waveguide take part in the transport.

To obtain the probabilities for n particles to transfer through the waveguide in a time τ it suffices to calculate the probabilities $P(n)$ of having the waveguide occupied with n particles. Since all particles travel at the same velocity v this equals the probability that n particles are transferred during a time $\tau = L/v = Nh/\delta E$. In other words, $N = \tau\delta E/h$. The restriction to integer N is not significant if we assume $N \gg 1$. The (artificial) length L of the waveguide drops out of the final answer.

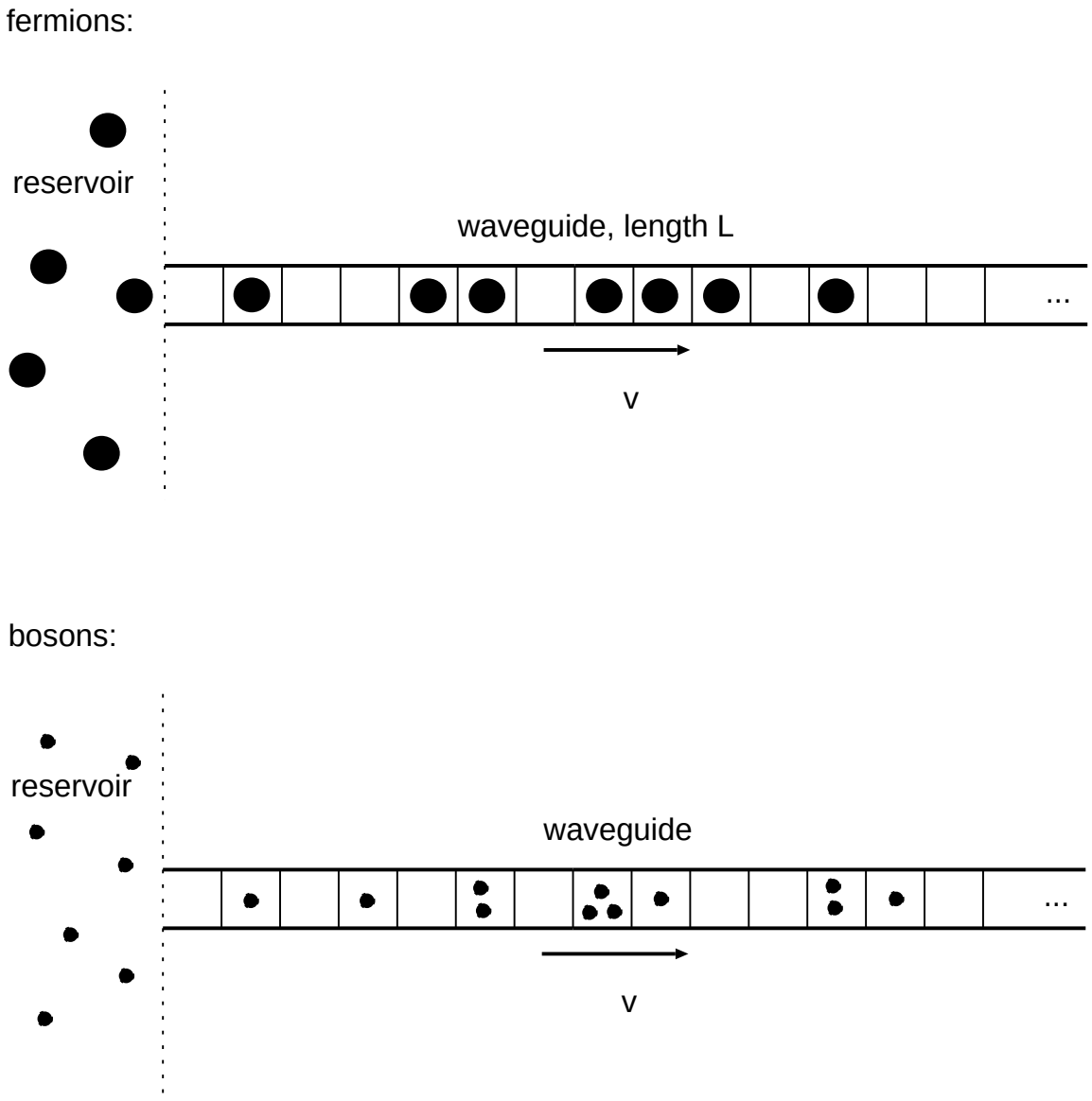

Figure 1-3. Illustration of the difference between fermion and boson counting statistics. A waveguide, containing N discrete single-particle states in an energy range δE, is populated by particles from a reservoir at temperature T. Depending on the quantum statistics individual states can be only singly or also multiply occupied. The upper panel shows the situation for fermions — every state is at most singly occupied. The bottom panel is for bosons. The particles in the waveguide move with velocity v over a length L in a time τ. Then $N = \delta EL/hv = \tau\delta E/h$. The number of transferred particles is distributed according to Eq. (1.2.1) for fermions and to Eq. (1.2.2) for bosons.

In thermal equilibrium each particle configuration with n particles at energy E has weight $\exp(-nE/kT)$. It remains to count how many ways there are to distribute the n particles over the N states of the lead. Fermions occupy every state at most once and the number of configurations is $\binom{N}{n}$. We consequently have

$$P_{\text{fermion}}(n) \propto \binom{\tau\delta E/h}{n} e^{-nE/kT}. \tag{1.2.1}$$

Bosons, on the other hand, may multiply occupy single states and there are $\binom{N+n-1}{n}$ ways to distribute n of them over N states. The probability distribution then becomes

$$P_{\text{boson}}(n) \propto \binom{\tau\delta E/h + n - 1}{n} e^{-nE/kT}. \tag{1.2.2}$$

This is the statistics of radiation emitted by a black body [4]. It is called the negative-binomial distribution.

It is often convenient to characterize a probability distribution $P(n)$ through the generating function $\mathcal{F}$ of its cumulants $\langle\langle n^m \rangle\rangle$,

$$\mathcal{F}(\xi) = \sum_{m=1}^{\infty} \frac{(-i\xi)^m}{m!} \langle\langle n^m \rangle\rangle = \ln \sum_{n=0}^{\infty} P(n) e^{-i\xi n}. \tag{1.2.3}$$

The cumulants are generated by differentiation of $\mathcal{F}$,

$$\langle\langle n^m \rangle\rangle = i^m \frac{d^m}{d\xi^m} \mathcal{F}\Big|_{\xi=0}, \tag{1.2.4}$$

and the probability distribution P can be reconstructed from $\mathcal{F}$ by Fourier transformation,

$$P(n) = \int d\xi \, \exp\left[in\xi + \mathcal{F}(\xi)\right]. \tag{1.2.5}$$

This generalizes the definition of cumulants given in Eq. (1.1.3) to arbitrary order.

The cumulant generating function corresponding to P_{fermion} is

$$\mathcal{F}_{\text{fermion}}(\xi) = \tau \frac{\delta E}{2\pi} \ln\left[1 + f_{\text{fermion}}(E)\left(e^{-i\xi} - 1\right)\right], \tag{1.2.6}$$

with the Fermi-Dirac distribution function $f_{\text{fermion}}(E) = [\exp(E/kT) + 1]^{-1}$. The corresponding result for bosons reads

$$\mathcal{F}_{\text{boson}}(\xi) = -\tau \frac{\delta E}{2\pi} \ln\left[1 - f_{\text{boson}}(E)\left(e^{-i\xi} - 1\right)\right], \tag{1.2.7}$$

with the Bose-Einstein distribution function $f_{\text{boson}}(E) = [\exp(E/kT) - 1]^{-1}$.

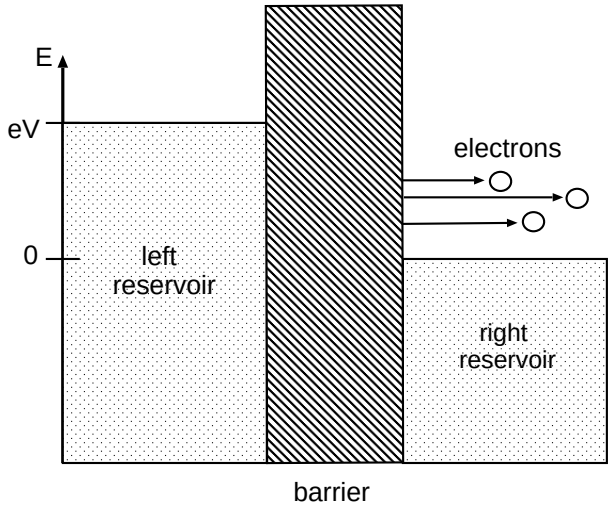

Figure 1-4. Illustration of electrons tunneling through a barrier between two reservoirs at zero temperature, with a voltage difference V. The currents due to electron states below the Fermi energy $E = 0$ cancel each other pairwise, so they need not be considered.

1.2.2 Electron gas at zero temperature

For the electron counting statistics in a closed electrical circuit we need to consider a second reservoir. This is easiest at zero temperature, as illustrated in Fig. 1-4. Since all states originating from the reservoirs are either filled or empty at $T = 0$, the reservoirs are noiseless. Current fluctuations arise from scattering events in the conductor that connects the two reservoirs. We assume for simplicity that this scattering is described by a single transmission probability Γ, in an energy interval $\delta E = eV$ above the Fermi level. Particle transfer is in this case a Bernoulli process [5]: $N = \tau eV/h$ particles try to pass the barrier independently of each other in a time τ and each of them succeeds with probability Γ. The number n of transmitted particles for a given number of trials N has binomial statistics, with distribution

$$P_{\rm binomial}(n) = \binom{N}{n}\Gamma^n(1-\Gamma)^{N-n}. \tag{1.2.8}$$

The cumulant generating function is

$$\mathcal{F}_{\rm binomial}(\xi) = N\ln\left[1+\Gamma\left(e^{-i\xi}-1\right)\right]. \tag{1.2.9}$$

The first few cumulants are

$$\langle\langle n^2\rangle\rangle = N\Gamma(1-\Gamma) \tag{1.2.10}$$

$$\langle\langle n^3\rangle\rangle = N\Gamma(1-\Gamma)(1-2\Gamma). \tag{1.2.11}$$

If the transmission probability Γ is $\ll 1$, the transfer of a particle through the barrier is a rare event. In this limit the quantum statistics of the particles is

irrelevant and the counting statistics follows the Poisson distribution,

$$P_{\text{Poisson}}(n) = \frac{\langle n\rangle^n}{n!} e^{-\langle n\rangle}, \tag{1.2.12}$$

where $\langle n\rangle = N\Gamma = \tau eV\Gamma/h$ is the mean number of transferred particles. The Poisson distribution has the cumulant generating function

$$\mathcal{F}_{\text{Poisson}}(\xi) = \langle n\rangle \left(e^{-i\xi} - 1\right), \tag{1.2.13}$$

with all cumulants equal to $\langle n\rangle$.

All these distributions tend to a Gaussian distribution in the limit $N \to \infty$, as a consequence of the central limit theorem. Since a Gaussian has a quadratic cumulant generating function, all cumulants higher than the second are suppressed in this limit. This makes the measurement of higher order cumulants difficult. For example, the ratio $\langle\langle n^3\rangle\rangle^{1/3}/\langle\langle n^2\rangle\rangle^{1/2}$ vanishes as $N^{-1/6}$ for large N. Nevertheless, it is possible to extract higher order cumulants from measurements of current fluctuations, as demonstrated by a recent experiment [3].

1.2.3 Electron gas at finite temperature

At a finite temperature of the electron reservoirs the statistics of charge transfer through the conductor depicted in Fig. 1-4 is more complicated. Current fluctuations originating from both reservoirs are mixed by the scattering at the barrier.

The statistics simplifies, however, if the transmission probability Γ through the barrier is $\ll 1$. This is typical for a tunnel junction. At zero temperature the statistics of charge transfer is then Poissonian, cf. Eq. (1.2.12). At finite temperature electron states on both sides of the barrier can be partially filled and the charge transfer consists of two independent Poisson processes [6]. One of them transfers electrons from the left side of the tunnel junction to the right side with rate $r_{L\to R}$, and the other one from right to left with rate $r_{R\to L}$. The statistics of transferred charge $Q = en$ has in this case the cumulant generating function

$$\mathcal{F}_{\text{tunnel}}(\xi) = \tau\left[r_{L\to R}(e^{-ie\xi} - 1) + r_{R\to L}(e^{ie\xi} - 1)\right]. \tag{1.2.14}$$

The rates are given by

$$r_{L\to R} = \Gamma\frac{eV}{h}\frac{1}{1-\exp(-eV/kT)}, \quad r_{R\to L} = e^{-eV/kT} r_{L\to R}. \tag{1.2.15}$$

From Eq. (1.2.14) we obtain the cumulants of charge transfer,

$$\langle\langle Q^{2n}\rangle\rangle = \tau e^{2n}[r_{L\to R} + r_{R\to L}], \tag{1.2.16}$$

$$\langle\langle Q^{2n+1}\rangle\rangle = \tau e^{2n+1}[r_{L\to R} - r_{R\to L}]. \tag{1.2.17}$$

At zero temperature $r_{R\to L}$ vanishes and we have the result $\langle\langle Q^2\rangle\rangle = e\langle Q\rangle$ for the second cumulant. At finite temperature $\langle\langle Q^2\rangle\rangle > e\langle Q\rangle$, because of thermal noise. The zero temperature contribution is known as "shot noise", because it is entirely due to the discreteness of the electron charge. Its experimental signature is the linear dependence on the applied voltage V. It dominates thermal noise if $eV \gg kT$. Shot noise was first studied in 1918 by Schottky [7], who proposed to measure the elementary charge from the ratio of the second moment to the mean current. The same idea was used 70 years later [8] in the quantum Hall effect, to measure the fractional charge of the tunneling particles (there e is replaced by an effective e^*). Levitov and Reznikov [6] proposed to use the third cumulant for a charge measurement at high temperature. According to Eq. (1.2.17), $\langle\langle Q^3\rangle\rangle = e^{*2}\langle Q\rangle$ regardless of the temperature of the conductor.

1.2.4 Multichannel generalization

So far we have assumed for simplicity that there is only a single transmission probability Γ. More generally, one has M transmission channels in the energy range δE, each with a different transmission probability Γ_k, $k = 1, 2, \cdots M$. These numbers are defined as the eigenvalues of the transmission matrix product $tt^\dagger$.

The multi-channel generalization of the binomial distribution of charge transfer at zero temperature is a multinomial distribution. It has the cumulant generating function

$$\mathcal{F}_{\rm fermion}(\xi) = \frac{eV\tau}{h}\sum_{k=1}^{M}\ln\left[1+\Gamma_k\left(e^{-ie\xi}-1\right)\right], \tag{1.2.18}$$

which reduces to Eq. (1.2.9) for $M = 1$. For later reference we also give the full finite-temperature result of Levitov and Lesovik [5],

$$\mathcal{F}(\xi) = \tau\int\frac{d\varepsilon}{h}\sum_{k=1}^{M}\ln\left\{1+\Gamma_k\left[(e^{-ie\xi}-1)f_{\rm L}(1-f_{\rm R})+(e^{ie\xi}-1)f_{\rm R}(1-f_{\rm L})\right]\right\}, \tag{1.2.19}$$

with the electron distribution functions $f_L(\varepsilon) = [e^{(\varepsilon-eV)/kT}+1]^{-1}$ and $f_R(\varepsilon) = (e^{\varepsilon/kT}+1)^{-1}$ in the left and the right reservoirs. In the tunneling limit $\Gamma_k \ll 1$ this reduces to the bi-directional Poisson distribution of Sec. 1.2.3.

1.3 Microscopic theory

In this section we outline how the results obtained in the previous section from intuitive physical arguments and combinatorics can be derived more rigorously.

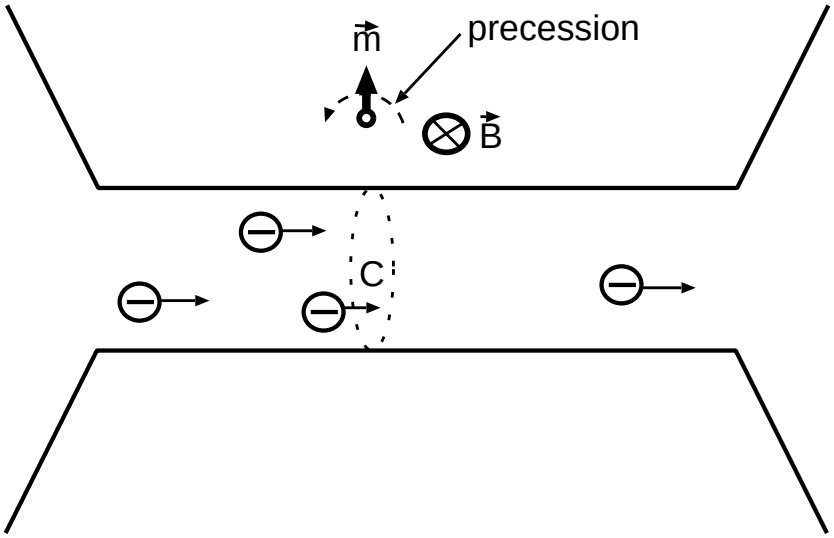

Figure 1-5. Simple model of an electron counter. The magnetic moment $\vec{m}$ precesses in the field $\vec{B}$ produced by the current I through a nearby conductor. The total precession angle after a time τ is a direct measure for the number of electrons that have passed $\vec{m}$ during τ. This model was analysed in Ref. [5].

The first attempt in the literature [9] to evaluate the counting statistics of electrons flowing through a mesoscopic conductor was a straight forward calculation of expectation values $\left\langle \left[\int_0^\tau dt\, I(t) \right]^m \right\rangle$. However, for $m > 2$ this leads to unphysical results. The electron counting statistics obtained in this way for a conductor of non-interacting electrons suggests that the charge transfer involves carriers with a fraction of the electron charge.

The underlying problem was identified and solved in Ref. [5]. There the correct statistics was found by analyzing a simple model of a current meter, the magnetic moment of a spin-1/2 (cf. Fig. 1-5). See Fig. 1-5. The model has been reviewed in Ref. [10]. Here we follow an alternative route [11] to find the proper expression for the charge transfer statistics.

For this we study the statistics of charge Q on one side of the cross-section C (at $x = 0$) of a conductor through which the charge transfer takes place, see Fig. 1-6. If Q is known at time 0, the statistics of $Q(\tau)$ at time τ corresponds to the statistics of the charge Q that has traversed C in the time interval $[0, \tau]$.

The operator of electric charge to the right of the cross-section C is $Q = e\theta(x)$, with $\theta(x) = 1$ for $x > 0$ and $\theta(x) = 0$ for $x \leq 0$. . The generating function of cumulants of $Q(\tau)$ reads

$$\mathcal{F}_c(\xi) = \sum_{m=1}^{\infty} \frac{(-i\xi)^m}{m!} \langle\langle Q^m(\tau) \rangle\rangle = \ln \left\langle e^{-i\xi Q(\tau)} \right\rangle = \ln \left\langle e^{iH\tau} e^{-i\xi Q} e^{-iH\tau} \right\rangle . \quad (1.3.1)$$

Here H is the Hamiltonian of the conductor and the average is taken over the

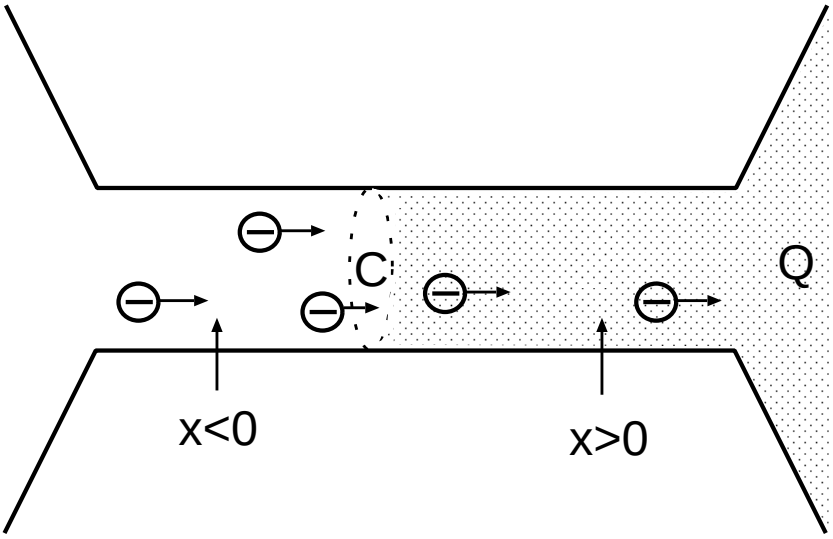

Figure 1-6. The amount of charge Q to the right of the cross-section C is related to the number of electrons that is transferred through C. The generating function of Q is given by Eq. (1.3.6), in agreement with Ref. [5].

initial density matrix of the conductor. For ease of notation we set $\hbar = 1$ from now on.

Using the identity

$$e^{i\xi Q/2} e^{A} e^{-i\xi Q/2} = \exp(e^{i\xi Q/2} A e^{-i\xi Q/2}), \tag{1.3.2}$$

we rewrite Eq. (1.3.1) as

$$\begin{aligned} \mathcal{F}(\xi) &= \ln \left\langle e^{-i\xi Q/2} \exp\left(i e^{i\xi Q/2} H e^{-i\xi Q/2} \tau \right) \right. \\ &\qquad \left. \times \exp\left(-i e^{-i\xi Q/2} H e^{i\xi Q/2} \tau \right) e^{-i\xi Q/2} \right\rangle . \end{aligned} \tag{1.3.3}$$

The charge operator Q commutes with all position operators $\mathbf{x}$ contained in the Hamiltonian $H = H(\mathbf{p}, \mathbf{x})$. It does not, however, commute with the momentum operators $\mathbf{p}$. As a consequence, momentum operators are transformed as

$$\mathbf{p} \to e^{-i\xi Q/2} \mathbf{p} e^{i\xi Q/2} = \mathbf{p} - \frac{e}{2} \xi \nabla \theta(x) \equiv \mathbf{p}_\xi . \tag{1.3.4}$$

The term $\frac{e}{2}\xi\nabla\theta(x)$ plays the role of a fictitious vector potential. We define a new Hamiltonian $H_\xi = H(\mathbf{p}_\xi, \mathbf{x})$. The cumulant generating function then takes the form

$$\mathcal{F}(\xi) = \ln \left\langle e^{-i\xi Q/2} e^{iH_{-\xi}\tau} e^{-iH_\xi \tau} e^{-i\xi Q/2} \right\rangle . \tag{1.3.5}$$

If the initial state of the conductor is an eigenstate of charge with eigenvalue Q_0, the two factors $e^{-i\xi Q/2}$ in Eq. (1.3.6) merely account for the initial charge Q_0. The generating function then becomes

$$\mathcal{F}(\xi) = \ln \left\langle e^{iH_{-\xi}\tau} e^{-iH_\xi \tau} \right\rangle - i\xi Q_0, \tag{1.3.6}$$

in agreement with Ref. [5].

In the semiclassical approximation to the kinetic energy of the electrons one may expand $H_\xi = H + \xi I/2 + \mathcal{O}(\xi^2)$. The counting variable ξ couples to the current I through the conductor. Eq. (1.3.6) may then be rewritten as an expectation value of time-ordered exponentials,

$$\mathcal{F}(\xi) = \ln \left\langle \overleftarrow{T}\ e^{-i\int dt\, \xi I(t)/2}\, \overrightarrow{T} e^{-i\int dt\, \xi I(t)/2} \right\rangle , \tag{1.3.7}$$

where we have used the identity

$$e^{-i(H+\xi I/2)t} = e^{-iHt}\overrightarrow{T} \exp\left[-i\xi \int_0^t dt'\, I(t')/2 \right], \tag{1.3.8}$$

with $I(t) = e^{iHt} I e^{-iHt}$. The symbols $(\overleftarrow{T})\,\overrightarrow{T}$ denote (inverse) time ordering. In this form of $\mathcal{F}$ it is explicit that moments of the transferred charge Q are indeed given by averages over powers of $\int_0^\tau dt\, I(t)$ as one would immediately guess. In contrast to what might be the first guess, however, the current operators $I(t)$ in such powers have to be time-ordered as in Eq. (1.3.7). This time ordering cures the spurious fractional charges found in Ref. [9]. The charge transfer statistics (1.3.7) evaluated for a normal metal mesoscopic conductor takes the form of Eq. (1.2.19) [5] with all the special cases that we have found from intuitive arguments before.

1.4 Keldysh formulation of counting statistics

Starting with the seminal paper of Levitov and Lesovik [5] a variety of techniques have been developed over the years to calculate the charge transfer statistics (1.3.6). In Refs. [12, 13] a cascaded Langevin approach to higher order moments of current fluctuations in diffusive wires and chaotic cavities has been proposed. A semiclassical theory of counting statistics has been put forward in Ref. [14], based on a stochastic path integral. In this thesis we predominantly employ the Keldysh approach to counting statistics due to Nazarov [15].

The generating function $\mathcal{F}$ of the statistics of charge transfer Eq. (1.3.6) has the form of a Keldysh partition function. It contains one time development exponential that propagates the system forward in time and one that evolves backwards. This is particularly evident in the form of Eq. (1.3.7). In the analogous Keldysh partition function the two time evolution operators in Eq. (1.3.7) correspond to the forward and the backward part of the Keldysh time contour c_K (see Fig. 1-7). Based on this formal analogy Nazarov proposed to evaluate $\mathcal{F}$ with an extension of the Keldysh Green function technique [15]. (A general review of the Keldysh Green function technique can be found in [16].) In chapters 2 and 3 we develop a path integral representation of the statistics of various observables in electrical circuits. Dealing with a system that is brought out of

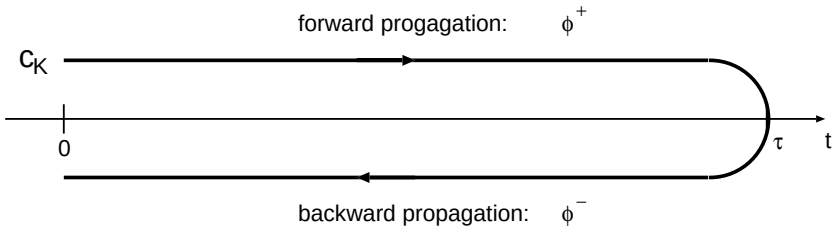

Figure 1-7. Keldysh time contour c_K on the time interval $[0,\tau]$. In a Keldysh path integral fields on the two parts of the contour, here ϕ^+ and ϕ^-, propagate the system forward and backward in time respectively.

thermal equilibrium (usually by an applied voltage) we employ also for this the Keldysh approach. The resulting Keldysh path integral is taken over two sets of integration fields, one responsible for the propagation of the system forward in time and one for backward propagation. An introductory text on this topic can be found in [17]. Also in our path integral approach objects very similar to the $\mathcal{F}$ of Eq. (1.3.7) play a central role. For this reason we outline in this section how we evaluate them using the Green function approach of Ref. [15].

In this approach, we treat phase-coherent conductors, characterized by a scattering matrix S. We take S to be energy independent. This is justified for energies (voltages) smaller than the Thouless energy, which is the inverse dwell time of electrons in the conductor [18]. The scattering region is connected to two reservoirs that contain electrons in local thermal equilibrium. We assume the electrons to be non-interacting.

The source ξ enters the Hamiltonian H_ξ as the fictitious vector potential introduced in Eq. (1.3.4). We choose this coupling here in a slightly more general form,

$$H_\xi = H[\mathbf{p} - e\mathbf{A}_\xi(x)], \quad \mathbf{A}_\xi(x) = \frac{1}{2}\mathbf{e}_{||}a(x)\xi. \tag{1.4.1}$$

The vector potential A_ξ with the normalization $\int dx\, a(x) = 1$, points along the direction of current flow $\mathbf{e}_{||}$ and depends only on the coordinate along the conductor x. It is chosen a pure gauge. For a time-dependent $\xi(t)$ it introduces, however, an additional voltage $V(t)$ over the conductor. The corresponding phase $\phi(t) = \int^t dt'\, V(t')$ is $\phi(t) = \int dx\, \mathbf{e}_{||}\mathbf{A}_\xi(x,t) = \xi(t)/2$.

To express $\mathcal{F}$ in terms of Keldysh Green functions we collect the time ordered and the anti-time ordered exponential in Eq. (1.3.7) into one contour ordered exponential along a contour c_K that is the usual Keldysh contour restricted to a finite time interval $[0,\tau]$ (see Fig. 1-7).

We write the many-electron states of the system in second quantized form, defining one electron field operator per transport channel m, direction of motion $\sigma \in \{-1,1\}$ (left $(-)$ or right $(+)$), and time direction on the Keldysh contour $\gamma \in \{+,-\}$ (forward contour $(+)$ and backward contour $(-)$). We collect those fields into a vector $\phi^\gamma_{m,\sigma}(x)$. The vector $\psi^\gamma_{m,\sigma}(x) = \exp(-i\sigma k_m x)\phi^\gamma_{m,\sigma}(x)$ is its

semiclassical counterpart, k_m being the Fermi wavevector of the m-th channel. With this notation we have

$$\mathcal{F}(\xi) = \ln \langle \mathcal{T}_\pm U_\xi \rangle , \quad U_\xi = e^{-i\int_0^\tau dt \int dx\, \psi^\dagger(x,t)\tilde{\tau}_3 \tilde{H}_\xi \psi(x,t)} \tag{1.4.2}$$

with the Hamiltonian

$$\tilde{H}_\xi = -i\tilde{v}\partial_x + e\xi\tilde{v}\tilde{\tau}_3 a(x) + \tilde{V}(x). \tag{1.4.3}$$

The notation $\mathcal{T}_\pm$ denotes the Keldysh time ordering: operators with Keldysh index $-$ stand to the left of $+$-operators, earlier $-$-operators to the left of later ones, earlier $+$-operators to the right of later $+$-operators. Matrices in the product space of mode, direction and Keldysh space are denoted by a tilde, for example $\tilde{H}$. We have applied the semiclassical approximation to the kinetic energy of the electrons. The matrix $\tilde{\tau}_3$ acts as the third Pauli matrix in the Keldysh space. We have further defined the matrix $\tilde{v}_{m\sigma,n\sigma'} = \sigma v_m \delta_{m,n}\delta_{\sigma,\sigma'}$ of the Fermi velocity v_m in the m-th channel. The potential $\tilde{V}$ represents the scattering potential for electrons inside the conductor. The matrix $\tilde{\tau}_3$ that multiplies H_ξ in Eq. (1.4.2) accounts for the sign difference between the exponents of the two time development operators in Eq. (1.3.7). The $\tilde{\tau}_3$ in the source term of Eq. (1.4.3) appears because the sign of the source ξ differs for forward and backward propagation. Differentiating both sides of Eq. (1.4.2) with respect to ξ,

$$\frac{d}{d\xi}\mathcal{F}(\xi) = -i\frac{\left\langle \mathcal{T}_\pm \int_0^\tau dt \int dx\, e\, a(x)\psi^\dagger(x,t)\tilde{v}\psi(x,t)U_\xi \right\rangle}{\langle \mathcal{T}_\pm U_\xi \rangle}, \tag{1.4.4}$$

we relate $\mathcal{F}$ to the semiclassical Keldysh Green function

$$\tilde{G}^{\gamma\gamma'}_{\xi\, m\sigma n\sigma'}(x,t;x',t') = -i\gamma\frac{\left\langle \mathcal{T}_\pm \psi^\gamma_{m\sigma}(x,t)\psi^{\gamma'\dagger}_{n\sigma'}(x',t')U_\xi \right\rangle}{\langle \mathcal{T}_\pm U_\xi \rangle}. \tag{1.4.5}$$

The matrix $\tilde{G}_\xi$ is related to the exact Green function $\tilde{\mathcal{G}}^{\gamma\gamma'}_{\xi\, m\sigma n\sigma'}(x,t;x',t')$ as

$$\tilde{\mathcal{G}}^{\gamma\gamma'}_{\xi\, m\sigma n\sigma'}(x,x') = \sum_{\sigma,\sigma'=\pm1} e^{-i\sigma k_m x + i\sigma' k_n x'} \tilde{G}^{\gamma\gamma'}_{\xi\, m\sigma n\sigma'}(x,x'). \tag{1.4.6}$$

Eqs. (1.4.4) together with (1.4.5) imply that

$$\frac{\partial}{\partial\xi}\mathcal{F} = e\int_0^\tau dt \int dx\; a(x)\mathrm{Tr}\;\tilde{\tau}_3\tilde{v}\tilde{G}_\xi(x,t;x,t). \tag{1.4.7}$$

The trace in Eq. (1.4.7) is taken over mode, direction, and Keldysh indices. The problem is therefore reduced to computing an electron Green function $\tilde{G}_\xi$ in the presence of the source field ξ.

We evaluate $\tilde{G}_\xi$ by solving its equation of motion. It turns out that $\tilde{G}_\xi(x,x')$ is determined by the condition that it does not grow exponentially with respect

to its relative coordinate $x - x'$ inside the reservoirs. In the calculation that proceeds very closely along the lines of [19] we assume that the mechanism that isotropizes the direction of motion of the electrons inside the reservoirs is scattering from point defects. The matrix $\tilde{G}_\xi$ turns out to depend on the semiclassical Green functions G_R and G_L of the electrons in the two reservoirs to the right and to the left of the conductor,

$$G_{\rm L} = \begin{pmatrix} 1 - 2f_{\rm L}(\omega_k) & 2f_{\rm L}(\omega_k) \\ 2[1 - f_{\rm L}(\omega_k)] & 2f_{\rm L}(\omega_k) - 1 \end{pmatrix}, \tag{1.4.8}$$

and correspondingly G_R. The functions f_L and f_R are the energy dependent occupation numbers of electron states in the two reservoirs. The two matrices G_R and G_L enter the expression through the self-energy of the impurity scattering process. Integrating Eq. (1.4.7) with the resulting G_ξ one finds that

$$\mathcal{F}(\xi) = \frac{1}{2}\sum_k {\rm Tr}\,\ln\left[1 + \frac{1}{4}\Gamma_k\left(\left\{\tilde{G}_{\rm L}, G_{\rm R}\right\} - 2\right)\right]. \tag{1.4.9}$$

The trace is taken over Keldysh indices, $\{,\}$ denotes the anti-commutator, and the Green function of the left reservoir is rotated,

$$\tilde{G}_{\rm L} = e^{-ie\xi\tau_3/2} G_{\rm L} e^{ie\xi\tau_3/2}. \tag{1.4.10}$$

After having performed the trace one ends up with Eq. (1.2.19).

The generating functional for finite frequency current correlators

$$\mathcal{Z}_{\rm con}[\phi^+, \phi^-] = \left\langle \overleftarrow{T}\; e^{i\int dt\, \phi^-(t) I(t)} \overrightarrow{T} e^{-i\int dt\, \phi^+(t) I(t)} \right\rangle \tag{1.4.11}$$

can be derived along the same lines with a time-dependent vector potential $\mathbf{A}^\pm(\mathbf{x}, t) = \mathbf{e}_{||} a(x)\phi^\pm(t)$ instead of the $\mathbf{A}_\xi$ of Eq. (1.4.1). It can be again cast in the form of Eq. (1.4.9). The trace, however, includes then also frequency indices and the rotated Green function $\tilde{G}_{\rm L}$ reads

$$\tilde{G}_{\rm L}(t, t') = \begin{bmatrix} e^{-ie\phi^+(t)} & 0 \\ 0 & e^{-ie\phi^-(t)} \end{bmatrix} G_{\rm L}(t - t') \begin{bmatrix} e^{ie\phi^+(t')} & 0 \\ 0 & e^{ie\phi^-(t')} \end{bmatrix} \tag{1.4.12}$$

in the time domain. The functional (1.4.11) is what enters the path integral formulation of counting statistics that we develop in chapters 2 and 3.

1.5 This thesis

1.5.1 Chapter 2: Counting statistics of a general observable

In Ref. [20] the charge transfer statistics (1.3.6) has been evaluated for a Josephson junction between two superconductors. The corresponding probability distribution turned out to be negative for certain values of the transmitted charge

Q. The reason for this is that in Ref. [20] the Josephson junction has been assumed to be in a phase eigenstate. The step from Eq. (1.3.5) to Eq. (1.3.6) in our derivation of the counting statistics formula is then unjustified.

In the original derivation of Eq. (1.3.6) of Ref. [5] a quasi-classical assumption has been made. By the paradoxical result of the "negative probabilities" one is led to believe that this assumption breaks down for superconductors. In chapter 2 we confirm this by studying a model of a charge detector that does not rely on quasi-classical assumptions.

We analyze the process of current measurement with a linear detector. The electrons in a conductor couple to their environment, including any current detector, only by the electromagnetic interaction. The current through an electrical conductor couples in the low frequency regime to the phase $\phi(t) = \int^t dt'\, V(t')$, where V is the voltage drop over the conductor. It is related to the vector potential $\mathbf{A}$ inside the conductor through an integral $\phi = \int_{\mathcal{L}} d\mathbf{l}\, \mathbf{A}(\mathbf{l})$ along a line $\mathcal{L}$ through the conductor. We choose this coupling field to be a part of the current detector. The Hamiltonian of the problem reads then

$$H = H_{\text{conductor}} + \phi I + H_{\text{detector}}, \tag{1.5.1}$$

with the operator ϕ corresponding to the phase $\phi(t)$. A simple example of a current detector is a capacitor that stores the charge flowing through the conductor. It has Hamiltonian $H_{\text{detector}} = Q^2/2C$. The charge Q on the capacitor is the variable conjugated to ϕ, with commutation relation $[Q, \phi] = i\hbar$ [21]. The equation of motion $\dot{Q}(t) = i[H, Q(t)]/\hbar = I(t)$, written in the Heisenberg picture, confirms that Q is a direct measure for the charge transfer $Q = \int_0^\tau dt\, I(t)$ through the conductor. This is the detection model we analyze in chapter 2.

The detector influences the conductor by the coupling term ϕI in Eq. (1.5.1). One would like to achieve that $\phi = 0$ to minimize this influence. As a consequence of the Heisenberg uncertainty principle, this is impossible, however, without loosing all information about the detector variable Q that one wants to measure. This charge-phase duality turns out to be the clue to understand the "negative probabilities". An analysis of the detector influence on the conductor is therefore a central part of chapter 2.

This detector influence is treated in a path integral formulation. We employ a formalism pioneered by Feynman and Vernon [22] to express the time evolution of the conductor coupled to a detector as a path integral over detector degrees of freedom. The dynamics of the conductor enters the path integral in the form of a so-called "influence functional". In this formalism the final detector density matrix ρ^f at time τ is related to the initial density matrix ρ^{in} at time 0 by the path integral

$$\rho^f(\phi^+, \phi^-) = \int_{\phi^+(\tau)=\phi^+,\, \phi^-(\tau)=\phi^-} \mathcal{D}[\phi^+]\ \mathcal{D}[\phi^-]\ e^{-iS_{\text{det}}[\phi^+,\phi^-]}\, \mathcal{Z}_{\text{con}}[\phi^+, \phi^-]\, \rho^{in}[\phi^+(0), \phi^-(0)], \tag{1.5.2}$$

with detector action

$$S_{\mathrm{det}}[\phi^+,\phi^-] = -\int_0^\tau dt\,\frac{C}{2}[(\dot{\phi}^+)^2 - (\dot{\phi}^-)^2]. \tag{1.5.3}$$

The influence functional $\mathcal{Z}_{\mathrm{con}}$ of the conductor is given in Eq. (1.4.11). Eq. (1.5.2) has the structure of a Keldysh path integral. The integration over ϕ^+ propagates the detector forward in time, while that over ϕ^- is responsible for the backward propagation (see Fig. 1-7).

The fluctuating phase in Eq. (1.5.2) influences the electrons in the conductor. In the limit of a static detector, $C \to \infty$, the phase undergoes no time-dependent fluctuations and only the initial phase uncertainty of the detector remains. In this limit the influence functional $\mathcal{Z}_{\mathrm{con}}$ is a generalization of the generating function (1.3.7) to two arguments ϕ^+ and ϕ^-. We identify a quasi-classical limit in which $\mathcal{Z}_{\mathrm{con}}$ reduces to $\mathcal{F}$ and is associated with a positive probability distribution. We suggest schemes that allow to access $\mathcal{Z}_{\mathrm{con}}$ experimentally in the general case when no correspondence to a probability distribution exists. All of this analysis is done for the measurement of time integrals of an arbitrary observable A, with $A = I$ as a special case.

1.5.2 Chapter 3: Counting statistics in electrical circuits

The detection model that we employ in chapter 2 is not yet realistic. The device that we describe with the path integral (1.5.2), a capacitor in series with the conductor, is not of great practical use as a current meter. Any capacitor with a finite capacitance develops a counter voltage in response to the charge stored on it and one would not be able to measure current flow in a steady state of the conductor. We therefore improve on this detection model in chapter 3, such that it allows us to describe an arbitrary linear detector.

A linear system has a quadratic Hamiltonian that can be diagonalized. Any linear device is therefore represented by a set of non-interacting bosons. Caldeira and Leggett [23] showed that such systems may be efficiently described through a path integral that is formulated in terms of relevant degrees of freedom only. Having a Gaussian action, all degrees of freedom that do not interact with the outside world can be integrated over easily. The procedure is applicable to many macroscopic systems. Due to the large number of degrees of freedom that are involved in their dynamics, each one of them typically needs to be displaced only infinitesimally in order to accomplish a macroscopic displacement of the entire system. The equations of motion of all the constituent degrees of freedom may therefore often safely be linearized. Taking our current detector to be macroscopic and assuming that it obeys linear equations of motion we can accordingly still express the dynamics of the conductor coupled to the detector as a path integral of the form (1.5.2). The relevant detector degree of freedom for which we formulate the path integral is again the phase that couples the

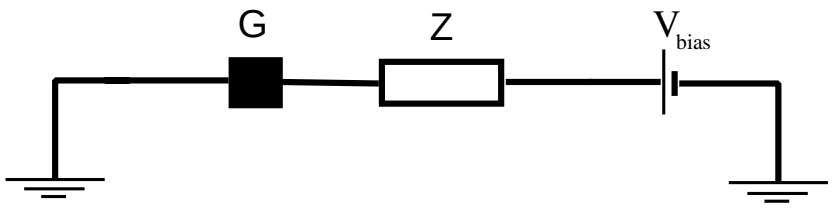

Figure 1-8. Electric circuit studied in chapter 3. The conductor G has a series impedance Z, its "electromagnetic environment". A current or a voltage meter is part of the electromagnetic environment.

detector to the current through the conductor. The effective detector action that one finds after integrating out all internal degrees of freedom depends only on the classical response functions (impedance matrix) of the detector and its temperature.

So far we have been referring to everything outside the conductor as "the detector". In reality, the environment to a conductor consists of an electrical circuit around it, equivalent to a series impedance (see Fig. 1-8). What one would really call the detector is just a part of this electromagnetic environment. It still holds true, however, that the electrons in the conductor couple to the outside world only through the electromagnetic interaction. At low frequencies, the coupling of the conductor to the electromagnetic field is well approximated by the interaction term ϕI. Provided the environment to the conductor is macroscopic and linear we can therefore describe also the series circuit of Fig. 1-8 by the path integral (1.5.2). (The linearity of the environment manifests itself by a linear current-voltage characteristic and by current and voltage fluctuations that are Gaussian and independent of the voltage applied to the circuit. The environment does not produce shot noise, but only thermal noise.) The generating function $\mathcal{Z}(\xi)$ of moments of the measured quantity is obtained from the density matrix at the time of observation ρ^f of Eq. (1.5.2). Evaluated for a thermal initial state ρ^{in} it takes the form

$$\mathcal{Z}(\xi) = \int \mathcal{D}\vec{\phi}\, e^{-iS_e[\xi,\vec{\phi}]}\, \mathcal{Z}_{con}[\vec{\phi}], \tag{1.5.4}$$

with an action S_e that depends on the impedance of the electromagnetic environment and its temperature. Here we have collected the phases on the two branches of the Keldysh contour into a vector $\vec{\phi} = (\phi^+, \phi^-)$.

The static detector of the previous section influenced the measured conductor in a subtle quantum mechanical way by a vector potential that was a pure gauge. In the infinite capacitance limit there is no classical back action of a

capacitor in series with the conductor. A dynamical detector, or, equivalently, a general series impedance, produces a time-dependent vector potential that has a voltage $V = \dot{\phi}$ associated with it. By this voltage the detector has a robust, classical back action on the conductor. We study the effect of this back action on the statistics of charge transfer through the conductor. In other words, we assess with our approach the effect on the statistics of current flow of interactions of electrons inside the conductor with electrons in its environment. The environment electrons create an effective electric field for the conductor electrons that we account for by the additional voltage $V = \dot{\phi}$ over the conductor.

Ohm's law states that a macroscopic resistor with impedance Z in series with a conductor of conductance G reduces the mean current through the conductor by a factor of $(1 + ZG)^{-1}$. One might surmise that this rescaling carries over to current fluctuations, such that the correlator $\langle \delta I^n \rangle$ would be reduced by a factor $(1 + ZG)^{-n}$. This is indeed true for the variance, $n = 2$. We find, however, that it is not valid for $n > 2$. Lower order cumulants mix in because the effect of the feedback of the series impedance is nonlinear. We explore the consequences of this nonlinear feedback in chapters 4 (at zero temperature) and 5 (at nonzero temperature).

In chapters 3, 4, and 5 we analyze Eq. (1.5.4) in saddle point approximation. The procedure is justified if the impedance of the circuit at the characteristic frequency Ω of charge transfer through the conductor is small compared to h/e^2, which is the case in many experiments. For $kT \lesssim eV$ the scale Ω is set by the smallest of $\bar{I}/e$ and eV/h.

1.5.3 Chapter 4: Charge versus phase statistics

A conductor is current biased when the current flowing through it is not allowed to fluctuate. Experimentally a current source is implemented by a voltage source in series with a resistor that has much larger resistance than the conductor to be biased. The magnitude of the current through the conductor is then dictated by the macroscopic resistor of the current source and does not fluctuate. A conductor under current bias corresponds therefore to the circuit in Fig. 1-8 in the limit of a large series impedance Z. We can describe it by the path integral (1.5.4) in the limit of $Z \to \infty$.

As a result of the nonlinear feedback of the series impedance discussed in chapter 3, the statistics of fluctuations under current bias is fundamentally different from that under voltage bias. We find that the statistics of phase increments $\phi = \int_0^\tau dt\, V(t)$ in a conductor under current bias I_0 obeys the Pascal-distribution

$$P_{\text{Pascal}}(N') = \binom{N'-1}{n'-1} \Gamma^{n'} (1-\Gamma)^{N'-n'}, \tag{1.5.5}$$

with $N' = e\phi/h$ and $n' = I_0\tau/e$. The Pascal distribution of voltage fluctuations under current bias is to be contrasted with the binomial distribution (1.2.8) of

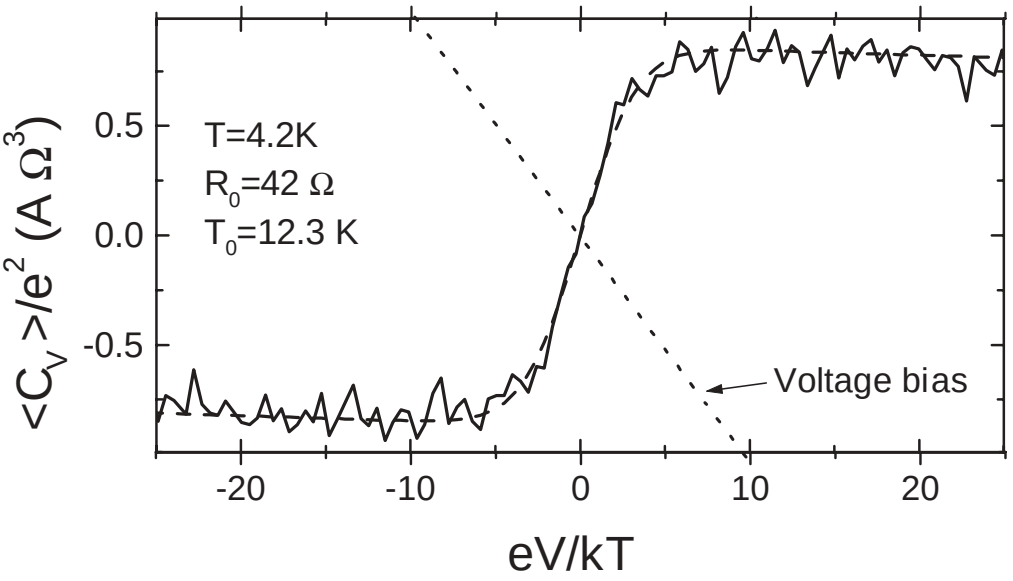

Figure 1-9. Measurement of the third moment of voltage fluctuations over a tunnel contact by Reulet, Senzier, and Prober [3]. Voltage fluctuations over a tunnel junction of resistance $R = 87\,\Omega$ were measured with an amplifier of input impedance $R_0 = 42\,\Omega$, that constitutes the main part of the electromagnetic environment to the junction. The temperature T of the sample was $4.2\,\mathrm{K}$ and the effective amplifier temperature T_0 seen by the sample $12.3\,\mathrm{K}$. The experimental curve (solid) is quantitatively fitted by our theoretical prediction (dashed curve). The short-dashed line is the result without feedback from the environment ("Votage bias").

charge fluctuations under voltage bias. It has the following intuitive interpretation.

As explained in section 1.3, charge transfer at zero temperature under voltage bias V_0 represents a Bernoulli process with $N = eV_0\tau/h$ attempted transfers and individual success probability Γ. The binomial distribution (1.2.8) gives then the probabilities to have n successful attempts in this process. Under current bias the dynamics of the process is changed by the series impedance Z. The number n' of electrons that are transferred in the detection time is fixed to $n' = I_0\tau/e$. For this to be achieved, Z regulates the voltage V over the conductor, such that the number of attempted transfers N' may fluctuate. This physical picture harmonizes with the statistical interpretation of the Pascal distribution as giving probabilities of the number of attempts N' that are needed to achieve $I_0\tau/e$ successes in a Bernoulli experiment.

1.5.4 Chapter 5: Temperature dependence

The second moment (1.2.10) of the shot noise at a tunnel barrier becomes unobservable on the background of thermal current noise for $kT \gtrsim eV$. This makes experiments difficult, since high voltages tend to heat up the conductor. To cir-

cumvent this problem, Levitov and Reznikov [6] suggested instead to measure the third cumulant. As shown in Eq. (1.2.17), odd-order cumulants in a tunnel junction are strictly proportional to the applied voltage V, regardless of the temperature of the conductor.

The first experiment to test this theoretical prediction gave a completely different picture, as shown in Fig. 1-9. The third cumulant of voltage fluctuations over a tunnel junction is not a linear function of V. Even the sign is different from the prediction. In chapter 5 we explain the experiment by including the feedback effect of the environment. This could be done directly from the path integral method of chapter 3, but as an alternative we present in chapter 5 a technically simpler Langevin approach that yields the same result. A detailed comparison of our theory with the experimental data has been carried out by the authors of Ref. [3]. As shown in Fig. 1-9, there is good agreement between theory and experiment.

1.5.5 Chapter 6: Interaction effects

The path integral (1.5.4) accounts for the interaction of electrons in a nanoscale conductor with those in a macroscopic series resistor Z (cf. Fig. 1-8). In chapters 3, 4, and 5 we have been solving it in saddle point approximation. This approximation breaks down when the impedance at the characteristic frequency scale Ω for charge transfer through the conductor is not small, $Z(\Omega) \gtrsim h/e^2$, $\Omega = \min(eV/h, \bar{I}/e)$. In this regime the impedance can react fast enough to affect the dynamics of the transfer of a single electron. This phenomenon is called the "environmental Coulomb blockade", the resulting corrections to quantities evaluated at the saddle point "fluctuation" or "quantum" corrections [21, 24].

An impedance falls off at high frequencies. We denote by Λ the frequency scale where Z has dropped below h/e^2. Quantum corrections are then negligible at sufficiently high voltages, where $eV > \Lambda$, while they become important for a small bias voltage V and temperature T, where $kT \ll eV \ll \Lambda$. As a consequence mesoscopic conductors exhibit a "zero bias anomaly". The current at bias voltages that are low enough for quantum corrections to be important no longer increases linearly with V. For a tunnel junction with a macroscopic series resistor Z the current at low voltage follows the power law [24],

$$I(eV) \propto (eV/\Lambda)^{2z+1} \text{ for } z < 1. \tag{1.5.6}$$

Here it is assumed that the impedance $z = Z(\omega)e^2/h$ is constant up to the cut-off $\Lambda \gg eV$.

In our path integral approach the physics of the zero-bias anomaly is described by time-dependent fluctuations around the saddle point. To treat them we need the influence functional $\mathcal{Z}_{\rm con}$ at finite frequencies. We evaluate it as outlined in section 1.4, with the result (1.4.9). Using a perturbative renormalization group analysis of Eq. (1.5.4), we then quantify the zero bias anomaly of

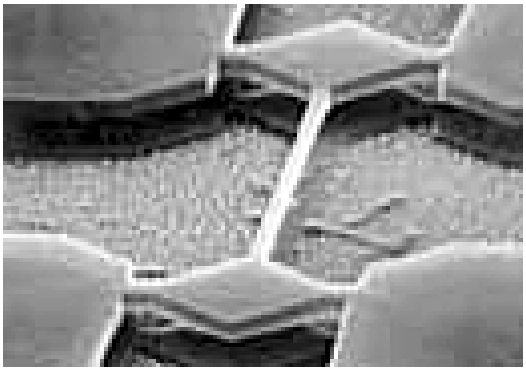

Figure 1-10. Freely suspended wire fabricated by M. L. Roukes.

the counting statistics of charge transfer. We find the fluctuation corrections to this statistics for arbitrary nanoscale conductors with a series resistor of not too large impedance Z. We find that a power law current-voltage characteristic like Eq. (1.5.6) emerges at small voltages not only for a tunnel barrier, but generically for mesoscopic conductors. The scaling behaviour at small applied voltage divides such conductors into two broad classes. For a first class of conductors $I(eV)$ scales like the current through a tunnel barrier, according to Eq. (1.5.6). A second class of conductors, including two tunnel barriers in series and diffusive conductors, exhibits scaling with the exponent $z+1$ instead of $2z+1$.

1.5.6 Chapter 7: Momentum transfer statistics

In chapter 7 of this thesis we study a mechanical aspect of charge transport through nanowires. An active line of research in the field of nanomechanics is the fabrication of very small mechanical oscillators that have high vibration frequencies. It is the aim to study such mechanical degrees of freedom at their quantum limit. These oscillators not only have high resonance frequencies, they are also very light. For this reason they are sensitive force detectors. A common design for such oscillators is a free-standing bridge between two solid metal banks [25], cf. Fig. 1-10. The bridge constitutes a freely suspended nanowire and one can drive electrical currents through it. We address the question whether and how strongly the electrons that flow then through the oscillator and exert forces on it can excite vibrations. This has been studied before for a diffusive wire using a Boltzmann equation approach [26]. In chapter 7 we treat phase-coherent conductors in a quantum mechanical framework. We compute the probability distribution of displacements of the wire in response to an applied voltage.

The effect is naturally small due to the small ratio of the electron mass to the mass of the oscillator. Still, the result is, that at sufficiently (and experimentally achievably) low temperatures, the vibration induced by the current flow domin-

ates the thermal background excitation. The non-Gaussian character of the displacement distribution induced by this mechanism distinguishes it additionally from thermal motion. The sensitivity of present day position detectors should be high enough to observe the effect.

1.5.7 Chapter 8: Optical analogy

In the last chapter of the thesis we close the circle and turn back to the counting statistics of photons. We compare it with the statistics of a comparable electronic system. We focus on chaotic radiation with a high filling factor f of modes. (The term "chaotic"means that there is no phase coherence between different photons such as in the light emitted by a laser.) The wave character of the light then becomes apparent and deviations from the electronic behaviour are to be expected. We propose one specific experiment in which the signature of the quantum statistics should be particularly pronounced. In that experiment light should first be passed through one barrier with a very small transmission probability $\Gamma \ll 1$. The measured probability distribution of photocounts should then be compared with the situation of two such barriers after one another. For the single barrier the photon noise is comparable to the mean number of transferred photons, as is to be expected for a Poisson process. In the two barrier system, resonances are formed. As a result, there are some modes k for which the probabilities of photon transfer are high, $\Gamma_k \simeq 1$. The prediction is then, that the variance of the photon count is not of the order of its mean anymore. Instead, it is enhanced by a factor proportional to the filling factor f of the modes. In the wave regime $f \gg 1$ the photon noise in the two barrier system is therefore much larger than that in the situation with a single barrier, although the mean photo-count in both situations is comparable. No such effect exists for electrons, since then $f \leq 1$.

Bibliography

[1] C. W. J. Beenakker and C. Schönenberger, Physics Today **56** (5), 37 (2003).

[2] Ya. M. Blanter and M. Büttiker, Phys. Rep. **336**, 1 (2000).

[3] B. Reulet, J. Senzier, and D. E. Prober, cond-mat/0302084.

[4] L. Mandel and E. Wolf, *Optical Coherence and Quantum Optics* (Cambridge University Press, Cambridge, 1995).

[5] L. S. Levitov and G. B. Lesovik, JETP Lett. **58**, 230 (1993); L. S. Levitov, H. W. Lee, and G. B. Lesovik, J. Math. Phys. **37**, 4845 (1996).

[6] L. S. Levitov and M. Reznikov, cond-mat/0111057.

[7] W. Schottky, Ann. Phys. (Leipzig) **57**, 541 (1918).

[8] L. Saminadayar, D. C. Glattli, Y. Jin, and B. Etienne, Phys. Rev. Lett. **79**, 2526 (1997); R. de-Piciotto, M. Reznikov, M. Heiblum, V. Umansky, G. Bunin, and D. Mahalu, Nature **389**, 162 (1997).

[9] L. S. Levitov and G. B. Lesovik, JETP Lett. **55**, 555 (1992).

[10] L. S. Levitov, in *Quantum Noise*, edited by Yu. V. Nazarov and Ya. M. Blanter, NATO Science Series II Vol. 97 (Kluwer, Dordrecht, 2003); cond-mat/0210284.

[11] M. Kindermann and Yu. V. Nazarov, in *Quantum Noise*, edited by Yu. V. Nazarov and Ya. M. Blanter, NATO Science Series II Vol. 97 (Kluwer, Dordrecht, 2003); cond-mat/0303590.

[12] K. E. Nagaev, Phys. Rev. B **66**, 075334 (2002).

[13] K. E. Nagaev, P. Samuelsson, and S. Pilgram, Phys. Rev. B **66**, 195318 (2002).

[14] S. Pilgram, A. N. Jordan, E. V. Sukhorukov, and M. Büttiker, Phys. Rev. Lett. **90**, 206801 (2003).

[15] Yu. V. Nazarov, Ann. Phys. (Leipzig) **8** SI-193, 507 (1999).

[16] J. Rammer and H. Smith, Rev. Mod. Phys. **58**, 323 (1986).

[17] A. Kamenev, in *Strongly Correlated Fermions and Bosons in Low-Dimensional Disordered Systems*, edited by I. V. Lerner, B. L. Altshuler, V. I. Fal'ko, and T. Giamarchi, NATO Science Series II Vol. 72 (Kluwer, Dordrecht, 2002); cond-mat/0109316.

[18] C. W. J. Beenakker, Rev. Mod. Phys. **69**, 731 (1997).

[19] Yu. V. Nazarov, Superlattices and Microstructures **25**, 1221 (1999).

[20] W. Belzig and Yu. V. Nazarov, Phys. Rev. Lett. **87**, 197006 (2001).

[21] G.-L. Ingold and Yu. V. Nazarov, in *Single Charge Tunneling*, edited by H. Grabert and M. H. Devoret, NATO ASI Series B294 (Plenum, New York, 1992).

[22] R. P. Feynman and F. L. Vernon, Ann. Phys. **24**, 118 (1963).

[23] A. O. Caldeira and A. J. Leggett, Ann. Phys. **149**, 374 (1983).

[24] M. H. Devoret, D. Esteve, H. Grabert, G.-L. Ingold, H. Pothier, and C. Urbina, Phys. Rev. Lett. **64**, 1824 (1990).

[25] M. L. Roukes, Phys. World **14**, 25 (2001); cond-mat/0008187.

[26] A. V. Shytov, L. S. Levitov, and C. W. J. Beenakker, Phys. Rev. Lett. **88**, 228303 (2002).

2 Full counting statistics of a general quantum mechanical variable

2.1 Introduction

The measurement paradigm in quantum mechanics assumes that a measurement is done instantly. [1] This is to be contrasted with a realistic measurement of, say, electric current, where the result of measurement is averaged over a sufficiently long time interval. If one intends to measure a variable A, the individual measurement gives $\int_0^\tau A(t)dt/\tau$. The reason for this is obvious: any measurement has to be accurate. The integration over time averages over instant fluctuations of $A(t)$ resulting in a more accurate outcome of an individual measurement of this sort. The dispersion of the probability distribution of the outcomes is supposed to vanish in the limit of $\tau \to \infty$. In this chapter we focus on the problems related to the determination of this probability distribution, the statistics of the measurement results.

Several years ago Levitov and Lesovik [2–4] have made a significant step in the understanding of this fundamental issue. They have introduced the concept of full counting statistics (FCS) of electric current and have found this statistics for the generic case of a one-mode mesoscopic conductor. The word "counting"reflects the discreteness of the electric charge. If electrons were classical particles, one could just count electrons traversing a conductor. The FCS could be readily defined in terms of the probability to have N electrons transferred through the conductor during a time interval τ, $P_\tau(N)$. With this distribution function one calculates the average current $\langle N\rangle/\tau$, current noise $(\langle N\rangle^2 > -\langle N\rangle^2)/\tau$ and all higher cumulants of the current. A non-trivial value of interest is the probability to have big deviations from the average value. This can be measured with a threshold detector. The probability distribution $P_\tau(N)$ would be the goal of a quantum-mechanical calculation.

The operator of electric current through a conductor, $\hat{I}$, is well-defined in the Fock space spanned by the scattering states of electrons. The initial idea of Lesovik and Levitov [2] was to define an operator of transferred charge by means of a seemingly obvious relation

$$\hat{Q}_{tr} = \int_0^\tau dt\, \hat{I}(t). \tag{2.1.1}$$

To this operator one applies the general paradigm of quantum measurement [1]: The probability to have a certain charge q transferred equals the square of the projection of the wave function of the system on the eigenstate of $\hat{Q}_{tr}$

with eigenvalue q. Lesovik and Levitov were able to perform the challenging calculation of these projections. However, they were hardly satisfied with the results. For instance, the transferred charge was not quantized in units of the elementary charge.

This is why in the subsequent paper [3] the same authors have proposed another method of evaluating $P_\tau(N)$. Their scheme invoked a measuring device. As a model device, they chose a precessing spin-$1/2$ whose precession angle should be proportional to the transferred charge. The measurement paradigm is then applied to the device. In this way they were able to obtain a satisfactory definition of the statistics $P_\tau(N)$ with an integer number of charges transferred. The details of the calculation and a thorough discussion are presented in [4].

It was clear to the authors of [4] that their definition of the FCS does not depend on a specific measurement scheme. However, this fact was not explicitly evident. For several years this hindered the impact of these outstanding contributions.

One of the authors has recently proposed a slightly different calculation scheme of FCS that does not invoke any measuring device but still leads to the same results [5]. The observation was that the cumulants of the current can be obtained as non-linear responses of a system to a fictitious field that can only be defined in the framework of the Keldysh diagrammatic technique [6]. The calculation of FCS can be accomplished with a slight extension of the Keldysh technique. This meant some progress since the methods of the Keldysh technique are well elaborated and can be readily applied to a variety of physical systems and situations.

More recently, it has been shown, that a statistics very similar to the one defined in [4] can be obtained also without explicitly modeling a charge detector, as a property of the current conductor only [7].

In [8] the charge transfer between two superconductors has been addressed. The problem can be tackled with an extension of the above-mentioned Keldysh technique. The expressions for $P_\tau(N)$ were obtained. Albeit the authors have encountered a significant difficulty with understanding the results in classical terms, using the schemes proposed in [3,7]. The calculation gave *negative* probabilities. This indicates that the results cannot be interpreted without invoking a quantum description of a detector.

All this suggests that the quantum mechanical concept of counting statistics shall be refined and the generality of previously used definitions shall be accessed. This is done in the present article.

To preserve generality, we analyze the counting statistics of an arbitrary quantum mechanical variable A. Then the result does not have to be discrete, and, strictly speaking, no counting takes place. We keep the term "counting"for historical reasons.

We introduce a detector whose read-off we can interpret as the statistics of $\int dt\, \hat{A}(t)$ and we determine its quantum mechanical time evolution. It turns

out, that the answer does not depend on details of the detector. This allows for a formal separation of the measured system from the measuring device. We develop an exact quantum mechanical description of the measurement setup in terms of a path integral over detector variables and derive our results from this description. We show that a classical interpretation of FCS is only possible in the presence of a certain symmetry. For the FCS of the electric current, this symmetry is gauge invariance. In superconductors gauge invariance is broken and the FCS must be interpreted along quantum mechanical lines.

It is the main message of the present chapter that this interpretation problem does not make the concept of full counting statistics useless and/or unphysical. We show that it is the FCS that completely determines the evolution of the density matrix of the detector. We show that thereby the statistics is observable in experiments. We propose and discuss two concrete measuring schemes.

The chapter is organized as follows. We start with a general compact discussion of the interpretation problems. We present our detection model in section 2.3. It is analyzed in the subsequent section. Section 2.5 defines the FCS and gives its interpretation. The subsequent sections provide examples of the FCS for a system in the ground state, a normal conductor and a harmonic oscillator. We characterize the FCS in sections 2.9 and 2.10 where two concrete schemes are discussed that allow to measure it experimentally.

2.2 General discussion

It is not a priori clear why the operator definition (2.1.1) produces senseless results. We list below possible intuitive reasons for this. To start with, the paradigm concerns an *instant* measurement. The operator definition (2.1.1) is not local in time and accumulates information about the quantum state of the system for a (long) interval of time. The applicability of the paradigm is therefore not obvious. For instance, the averages of powers of $\hat{Q}_{tr}$ can be expressed in terms of correlators of currents

$$\langle \hat{Q}_{tr}^N \rangle = \int_0^\tau dt_1 ... dt_N \langle \hat{I}(t_1)\hat{I}(t_2)...\hat{I}(t_N)\rangle. \tag{2.2.1}$$

Usually causality comes into quantum mechanics via time ordering of operator products. There is no time ordering of current operators in (2.2.1). This may indicate implicit problems with causality. The second reason is as follows. It seems obvious that the time integral of $\hat{I}$ can be associated with a physical operator of charge. For an arbitrary operator $\hat{A}$ it may be difficult to find such a physical associate. Still, integrals of $\hat{A}$ can be measured, and the statistics of them can be accumulated.

In view of this problem it seems to be necessary to model the measurement process in order to define a statistics of time averages. This has been done in [3] by introducing the spin-1/2 detector. Since within this detection model

the described interpretation problems ("negative probabilities") [8] arose, we refine now the model [9]. We adopt a detector model that has already been used by John von Neumann in an analysis of the quantum measurement process [10]. We introduce a detector variable x, whose operator $\hat{x}$ commutes with all operators of the system to be measured. We assume that the canonically conjugated variable, q, ($[\hat{x},\hat{q}] = i$, in units with $\hbar = 1$) can be measured according to the paradigm. Next we introduce an interaction between the system and the detector in a way that in the time interval $(0,\tau)$ the Heisenberg equation of motion reads

$$\dot{\hat{q}}(t) = \hat{A}(t), \tag{2.2.2}$$

simulating Eq. (2.1.1). In this way we avoid all possible difficulties with misinterpretations of the paradigm. The integral of $A(t)$ is now correctly associated with an operator that can *a priori* be measured.

Albeit there is a price to pay. As we show below, the FCS can be defined in this way as an operator that relates the density matrices of the detector before and after the measurement. In general, it is not the same as the probability distribution of shifts of the detector momentum which can be associated with probabilities of $\int_0^\tau dt\, \hat{A}(t)$ in the classical limit. The FCS can be interpreted in such terms only under certain conditions, which are satisfied for the statistics of current in normal metal conductors.

To make the detector more realistic and thus to show the generality of the results, one shall introduce internal dynamics of the detector variable. This dynamics would make the detector a non-ideal one: the readings may differ from the definitions (2.1.1) and (2.2.2). The path integral approach we describe below provides the most convenient way to incorporate this internal dynamics.

2.3 Model

The detector in our model consists of one degree of freedom x (with conjugated variable q) with the Hamiltonian $\hat{q}^2/2m$. The system shall be coupled to the position x of the detector during the time interval $[0,\tau]$ and be decoupled adiabatically for earlier and later times. For this we introduce a smooth coupling function $\alpha_\tau(t)$ that takes the value 1 in the time interval $[0,\tau]$ and is zero beyond the interval $[t_1,t_2]$ ($t_1 < 0$ and $t_2 > \tau$). The values for $t_1 < t < 0$ and $\tau < t < t_2$ are chosen in a way that provides an adiabatic switching. The entire Hamiltonian reads then

$$H(t) = \hat{H}_{\rm sys} - \alpha_\tau(t)\hat{x}\hat{A} + \frac{\hat{q}^2}{2m}. \tag{2.3.1}$$

The Heisenberg equation of motion for the detector momentum q

$$\dot{\hat{q}}(t) = \alpha_\tau(t)\hat{A}(t) \tag{2.3.2}$$

suggests, that the statistics of outcomes of measurements of the detector's momentum after having it uncoupled from the system corresponds to the statistics of the time average $\int_0^\tau dt\, \hat{A}(t)$ that we are interested in.

The coupling term can be viewed as a disturbance of the system measured by the detector. To minimize this disturbance, one would clearly like to concentrate the detector wave function around $x = 0$. The uncertainty principle forbids, however, to localize it completely. Thereby one would loose all information about the detector momentum, which is to be measured. This is a fundamental limitation imposed by quantum mechanics, and we are going to explore its consequences step by step. To discern it form a classical back action of the detector we take the limit of a static detector with $m \to \infty$, such that $\dot{\hat{x}} = 0$ and any classical back action is ruled out.

2.4 Approach

To predict the statistics of measurement outcomes in our detection model we need the reduced density matrix of the detector after the measurement, at $t > t_2$. If there were no system to measure we could readily express it in the form of a path integral in the (double) variable $x(t)$ over the exponential of the detector action. This is still possible in the presence of a system coupled to the detector [11]. The information about the system to be measured can be compressed into an extra factor in this path integral, the so-called influence functional. This makes the separation between the detector and the measured system explicit. To make contact with [4], we write the influence functional as an operator expression that involves system degrees of freedom only. We denote the initial detector density matrix (at $t < t_1$) by $\rho^{in}(x^+, x^-)$ and the final one (at $t > t_2$, after having traced out the system's degrees of freedom) by $\rho^f(x^+, x^-)$. $\hat{R}$ denotes the initial density matrix of the system. The entire initial density matrix is assumed to factorize, $\hat{D} = \hat{R}\hat{\rho}^{in}$.

We start out by inserting complete sets of states into the expression for the time development of the density matrix

$$\begin{aligned}\rho^f(x^+, x^-) \;=\; & \underset{\text{System}}{Tr}\, \langle x^+ | \overrightarrow{T} e^{-i\int_{t_1}^{t_2} dt\, \left[\hat{H}_{\text{sys}} - \alpha_\tau(t)\hat{x}\hat{A} + \hat{q}^2/2m\right]} \hat{D} \\ & \overleftarrow{T} e^{i\int_{t_1}^{t_2} dt\, \left[\hat{H}_{\text{sys}} - \alpha_\tau(t)\hat{x}\hat{A} + \hat{q}^2/2m\right]} | x^- \rangle. \end{aligned} \tag{2.4.1}$$

Here, $(\overleftarrow{T})\overrightarrow{T}$ denote (inverse) time ordering. As the complete sets of states we choose product states of any complete set of states of the system and alternatingly complete sets of eigenstates of the position or the momentum operator of the detector. Those intermediate states allow us to replace the position and momentum operators in the time development exponentials by their eigenvalues. We can then do the integrals over the system states as well as the momentum

integrals and arrive at the expression

$$\begin{aligned}\rho^f(x^+,x^-) &= \int \underset{x^+(t_2)=x^+}{\mathcal{D}[x^+]} \underset{x^-(t_2)=x^-}{\mathcal{D}[x^-]} \rho^{in}[x^+(t_1),x^-(t_1)]\, e^{-iS_{\rm Det}([x^+],[x^-])} \\ &\quad \underset{\rm System}{Tr}\, \overrightarrow{T} e^{-i\int_{t_1}^{t_2} dt\left[\hat{H}_{\rm sys}-\alpha_\tau(t)x^+(t)\hat{A}\right]} R\, \overleftarrow{T} e^{i\int_{t_1}^{t_2} dt\left[\hat{H}_{\rm sys}-\alpha_\tau(t)x^-(t)\hat{A}\right]}\end{aligned} \tag{2.4.2}$$

with the detector action

$$S_{\rm Det}([x^+],[x^-]) = -\int_{t_1}^{t_2} dt\, \frac{m}{2}[(\dot{x}^+)^2-(\dot{x}^-)^2]. \tag{2.4.3}$$

We rewrite the expression as

$$\rho^f(x^+,x^-) = \int dx_1^+ dx_1^-\, K(x^+,x^-;x_1^+,x_1^-,\tau)\rho^{in}(x_1^+,x_1^-) \tag{2.4.4}$$

with the kernel

$$\begin{aligned}K(x^+,x^-;x_1^+,x_1^-,\tau) &= \int \underset{x^+(t_2)=x^+,x^+(t_1)=x_1^+}{\mathcal{D}[x^+]} \underset{x^-(t_2)=x^-,x^-(t_1)=x_1^-}{\mathcal{D}[x^-]} \\ &\quad \mathcal{Z}_{\rm Sys}([\alpha_\tau x^+],[\alpha_\tau x^-])\, e^{-iS_{\rm Det}([x^+],[x^-])}\end{aligned} \tag{2.4.5}$$

that contains the influence functional

$$\mathcal{Z}_{\rm Sys}([\chi^+],[\chi^-]) = \underset{\rm System}{Tr}\, \overrightarrow{T} e^{-i\int_{t_1}^{t_2} dt\left[\hat{H}_{\rm sys}-\chi^+(t)\hat{A}\right]}\, \hat{R}\, \overleftarrow{T}\, e^{i\int_{t_1}^{t_2} dt\left[\hat{H}_{\rm sys}-\chi^-(t)\hat{A}\right]}. \tag{2.4.6}$$

Taking the limit of an infinite detector mass now, we find that $S_{\rm Det}$ in Eq. (2.4.5) suppresses all fluctuations in the path integral. In the appendix we show that the kernel $K(x^+,x^-,x_1^+,x_1^-,\tau)$ becomes local in position space,

$$K(x^+,x^-,x_1^+,x_1^-,\tau) = \delta(x^+-x_1^+)\,\delta(x^--x_1^-)\;P(x^+,x^-,\tau) \tag{2.4.7}$$

with

$$P(x^+,x^-,\tau) = \underset{\rm System}{Tr}\, \overrightarrow{T} e^{-i\int_{t_1}^{t_2} dt\left[\hat{H}_{\rm sys}-\alpha_\tau(t)x^+\hat{A}\right]} \hat{R}\, \overleftarrow{T} e^{\,i\int_{t_1}^{t_2} dt\left[\hat{H}_{\rm sys}-\alpha_\tau(t)x^-\hat{A}\right]}. \tag{2.4.8}$$

It is constructive to rewrite now the density matrices in Wigner representation

$$\rho(x,q) = \int \frac{dz}{2\pi}\, e^{-iqz}\, \rho(x+\frac{z}{2},x-\frac{z}{2}) \tag{2.4.9}$$

and define

$$P(x,q,\tau) = \int \frac{dz}{2\pi} e^{-iqz}\, P(x+\frac{z}{2},x-\frac{z}{2},\tau). \tag{2.4.10}$$

This gives the convenient relation

$$\rho^f(x,q) = \int dq_1\, P(x,q-q_1,\tau)\, \rho^{in}(x,q_1). \tag{2.4.11}$$

2.5 Interpretation of the FCS

We adopt the relations (2.4.8), (2.4.10) and (2.4.11) as the definition of the FCS of the variable A. Let us see why. First let us suppose that we can treat the detector classically. Then the density matrix of the detector in the Wigner representation can be interpreted as a classical probability distribution $\Pi(x,q)$ to be at a certain position x with momentum q. This allows for a classical interpretation of $P(x,q,\tau)$ as the probability to have measured $q = \int_0^\tau A(t)$. Indeed, one sees from (2.4.10) that the final $\Pi(x,q)$ is obtained from the initial one by shifts in q, $P(x,q,\tau)$ being the probability distribution of those shifts.

In general, the density matrix in the Wigner representation cannot be interpreted as a probability to have a certain position and momentum since it is not positive. Concrete calculations given below illustrate that $P(x,q,\tau)$ does not have to be positive either. Consequently, it cannot be interpreted as a probability distribution. Still it predicts the results of measurements according to Eq. (2.4.11).

There is, however, an important case when the FCS can indeed be interpreted as a probability distribution. It is the case that $P(x,q,\tau)$ does not depend on x, $P(x,q,\tau) \equiv P(q,\tau)$. Then, integrating Eq. (2.4.11) over x, we find

$$\Pi^f(q) = \int dq'\, P(q-q',\tau)\, \Pi^{in}(q') \tag{2.5.1}$$

with $\Pi(q) \equiv \int dx\, \rho(x,q)$. Therefore, the FCS in this special case is the kernel that relates the probability distributions of the detector momentum before and after the measurement, $\Pi^{in}(q)$ and $\Pi^f(q)$, to each other. Those distributions are positive and so is $P(q,\tau)$.

When studying the FCS of a stationary system and the measurement time τ exceeds time scales associated with the system, the operator expression in Eq. (2.4.8) can be seen as a product of terms corresponding to time intervals. Therefore in this limit of $\tau \to \infty$ the dependence on the measuring time can be reconciled into

$$P(x^+,x^-,\tau) = e^{-\mathcal{I}(x^+,x^-)\tau} \tag{2.5.2}$$

where the expression in the exponent is supposed to be large. Then the integral (2.4.10) that defines the FCS can be done in the saddle point approximation. Defining the time average $\bar{A} = q/\tau$, that is, $\bar{A}$ is the result of a measurement of $\int_0^\tau A(t)dt/\tau$, the FCS can be recast into the from

$$P(x,\bar{A},\tau) = e^{-\tilde{\mathcal{I}}(x,\bar{A})\tau} \tag{2.5.3}$$

where $\tilde{\mathcal{I}}$ is defined as the (complex) extremum with respect to (complex) z:

$$\tilde{\mathcal{I}} = \operatorname*{extr}_z \{\mathcal{I}(x+\frac{z}{2}, x-\frac{z}{2}) + i\bar{A}z\}. \tag{2.5.4}$$

The average value of $\bar{A}$ and its variance (noise) can be expressed in terms of derivatives of $\mathcal{E}$:

$$\langle \bar{A} \rangle = -\lim_{z\to 0} \frac{\partial \mathcal{E}(x+z/2, x-z/2)}{i\partial z}; \;\; \tau \langle\langle \bar{A}^2 \rangle\rangle = \lim_{z\to 0} \frac{\partial^2 \mathcal{E}(x+z/2, x-z/2)}{\partial z^2}. \tag{2.5.5}$$

More generally, the quantity $P(x^+, x^-, \tau)$ is the generating function of moments of q. It is interesting to note that in general this function may generate a variety of moments that differ in the time order of operators involved, for instance,

$$\begin{aligned} Q_M^N &= (-1)^M i^N \lim_{x^\pm \to 0} \frac{\partial^M}{\partial (x^-)^M} \frac{\partial^{N-M}}{\partial (x^+)^{N-M}} P(x^+, x^-, \tau) \\ &= \int_0^\tau dt_1 ... dt_N \, \langle \overleftarrow{T}\{A(t_1)...A(t_M)\} \overrightarrow{T}\{A(t_{M+1})...A(t_N)\} \rangle. \end{aligned} \tag{2.5.6}$$

The moments of (the not necessarily positive) $P(0, q, \tau)$ are expressed through these moments and binomial coefficients,

$$Q^{(N)} \equiv \int dq \, q^N P(0, q, \tau) = 2^{-N} \sum_M \binom{N}{M} Q_M^N. \tag{2.5.7}$$

2.6 FCS of a system in the ground state

To acquire a better understanding of the general relations obtained we consider now an important special case. We will assume that the system considered is in its ground state $|g\rangle$, so that its initial density matrix is $\hat{R} = |g\rangle\langle g|$. In this case the FCS is easily calculated. We have assumed that the coupling between the system and the detector is switched on adiabatically. Then the time development operators in (2.4.8) during the time interval $t_1 < t < 0$ adiabatically transfer the system from $|g\rangle$ into the ground state $|g(x^\pm)\rangle$ of the new Hamiltonian $\hat{H}_{\rm sys} - x^\pm \hat{A}$. In the time interval $0 < t < \tau$ the time evolution of the resulting state has then the simple form

$$e^{-it(\hat{H}_{\rm sys} - x^\pm \hat{A})} \, |g(x^\pm)\rangle \;=\; e^{-itE(x^\pm)} \, |g(x^\pm)\rangle. \tag{2.6.1}$$

Here, $E(x^\pm)$ are the energies corresponding to $|g(x^\pm)\rangle$. This gives the main contribution to the FCS if the measurement time is large and the phase acquired during the switching of the interaction can be neglected in comparison with this contribution,

$$P(x^+, x^-, \tau) = e^{-i\tau[E(x^+) - E(x^-)]}. \tag{2.6.2}$$

We now assume the function $E(x)$ to be analytic and expand it in its Taylor series. We also re-scale q as above, $\bar{A} = q/\tau$. We have then for the FCS

$$P(x, \bar{A}, \tau) = \int dz \, e^{-iz\bar{A}\tau} \cdot e^{-i\tau[E'(x)z + E'''(x)z^3/24 + ...]}. \tag{2.6.3}$$

First we observe that $P(x, \bar{A}, \tau)$ is a real function in this case, since the exponent in (2.6.3) is anti-symmetric in z. A first requirement for being able to interpret it as a probability distribution is therefore fulfilled. However, the same asymmetry assures that all *even* cumulative moments of $\bar{A}$ are identically zero, whereas the odd ones need not. On one hand, since the second moment corresponds to the noise and the ground state cannot provide any, this makes sense. On the other hand, this would be impossible if $P(0, \bar{A}, \tau)$ were a positive probability distribution unless it had no dispersion at all.

Belzig and Nazarov [8] encountered this situation analyzing the FCS of a super-conducting junction. In a certain limit the junction becomes a Josephson junction in its ground state. In this limit the interpretation of the FCS as a probability distribution does not work any longer. Fortunately enough, the relation (2.4.11) allows us to interpret the results obtained.

In the limit $\tau \to \infty$ of Eq. (2.6.3) terms involving higher derivatives of $E(x)$ are negligible and we have

$$\lim_{\tau\to\infty} P(x, \bar{A}, \tau) = \delta[\bar{A} + E'(x)]. \tag{2.6.4}$$

According to the Hellman-Feynman theorem $E'(x) = -\langle g(x)|\hat{A}|g(x)\rangle$. As one would expect, in this limit the measurement gives the expectation value of the operator $\hat{A}$ in a ground state of the system that is somewhat altered by its interaction with the detector at position x. Therefore the resulting dispersion of A will be determined by the *initial* quantum mechanical spread of the detector wave function. The error of the measurement stems from the interaction with the detector rather than from the intrinsic noise of the measured system.

2.7 FCS of electrical current in a normal conductor

A complementary example is a normal conductor biased at finite voltage. This is a stationary *non-equilibrium* system far from being in its ground state. Here we do not intend to go to microscopic details of the derivation. Our immediate aim is to make contact with the approaches of Refs. [4, 5]. We keep the original notations of the references wherever it is possible.

The starting points of the approaches differ much. Levitov and Lesovik propose a detector model where the z-component of a spin-1/2 creates a local vector potential felt by the electrons. This corresponds to a total Hamiltonian of the form

$$\hat{H} = \hat{H}_{\text{sys}} - \frac{\lambda}{2e}\hat{\sigma}_z\hat{I}$$

which is studied at different coupling constants λ. Reference [5] starts with an extension of the Keldysh technique to only formally defined systems where the evolution of the wave function in different time directions is governed by two different Hamiltonians

$$\hat{H}^{\pm} = \hat{H}_{\text{sys}} \pm \chi\hat{I} \tag{2.7.1}$$

and shows that the so defined Green functions can be used to generate moments of $\hat{I}$. This is to be compared with our detection model.

Despite different starting points, all three approaches quickly concentrate on the calculation of the quantity

$$\langle \exp[-i(\hat{H}_{\rm sys} - x^+\hat{I})\tau] \exp[-i(\hat{H}_{\rm sys} - x^-\hat{I})\tau]\rangle. \tag{2.7.2}$$

This quantity is denoted by $\chi(\lambda)$ in [4] and by $\exp[-S(\chi)]$ in [5]. It corresponds to our definition of the FCS Eq. (2.4.8) and we see now that the final result does not depend on the starting point.

As a concrete example we consider the FCS of the current in a phase-coherent conductor which is characterized by a set of transmission coefficients T_n [Eq. (37) of [3]]. In general, the answer is expressed in terms of energy-dependent electron filling factors $f_{R(L)}$ on the right (left) side of the conductor,

$$\begin{aligned} \ln P(x^+,x^-,\tau) &= \frac{\tau}{2\pi}\sum_n \int_{-\infty}^{+\infty} d\varepsilon \, \ln[1 + T_n(e^{ie(x^- - x^+)} - 1)f_R(1-f_L) \\ &\quad + T_n(e^{ie(x^+ - x^-)} - 1)f_L(1-f_R)]. \end{aligned} \tag{2.7.3}$$

This expression depends on $x^+ - x^-$ only. This is a direct consequence of gauge invariance. Indeed, in each of the Hamiltonians the coupling term is the coupling to a vector potential localized in a certain cross-section of the conductor. The gauge transform that shifts the phase of the wave functions by $ex^{\pm}$ on the right side of the conductor, eliminates this coupling term. This transform was explicitly implemented in [5]. Since there are *two* Hamiltonians in the expression, the coupling terms cannot be eliminated simultaneously provided that $x^+ \neq x^-$. However, the gauge transform with the phase shift $e(x^+ + x^-)/2$ makes the coupling terms depending on $x^+ - x^-$ only.

Since $P(x^+,x^-,\tau)$ depends on $x^+ - x^-$ only, the FCS $P(x,q,\tau)$ does not depend on x. As we have seen in section 2.5, this enables one to interpret the FCS as a probability distribution.

Superconductivity breaks gauge invariance, thus making such an interpretation impossible.

2.8 FCS of a harmonic oscillator

Let us now illustrate the proposed measuring process with a simple example. We consider the measurement of the position of a harmonic oscillator in its ground state. The Hamiltonian of the system is then $\hat{H}_0 = \frac{\hat{Q}^2}{2M} + \frac{1}{2}M\omega^2\hat{X}^2$ and $\hat{A} = \hat{X}$ shall be measured. The entire Hamiltonian in the measurement period reads then

$$\hat{H} = \frac{\hat{Q}^2}{2M} + \frac{1}{2}M\omega^2\hat{X}^2 - \hat{x}\,\hat{X}. \tag{2.8.1}$$

The perturbed ground state $|g(x)\rangle$ is in this simple example obtained by shifting the original ground state wave function by $x/M\omega^2$ in X-representation. Its energy is $E_g(x) = E_g(0) - \frac{1}{2M\omega^2}\, x^2$. We then find from (2.6.4), that

$$P(x,q,\tau) = \delta(q - x\tau/M\omega^2). \tag{2.8.2}$$

Following our first classical interpretation of $P(0,q,\tau)$ we would now conclude, that a harmonic oscillator in its ground state does not transmit any fluctuations of its position variable to the detector and that the detector's wave function is not altered by the oscillator. Calculating, however, the read-off of the detector with a Gaussian wave of uncertainty $\triangle q$ in the momentum as the initial state of the detector,

$$\rho^{in}(x,q) = \exp[-\frac{q^2}{2(\triangle q)^2} - 2(\triangle q)^2 x^2], \tag{2.8.3}$$

we find for the final momentum distribution

$$\Pi^f(q) = \exp[-\frac{q^2}{2(\triangle q)^2 + \tau^2/2M^2\omega^4(\triangle q)^2}]. \tag{2.8.4}$$

The uncertainty $\triangle q^f$ of the final detector momentum increases in time,

$$(\triangle q^f)^2 = (\triangle q)^2 + \frac{\tau^2}{4M^2\omega^4(\triangle q)^2}, \tag{2.8.5}$$

in contradiction to our first interpretation of Eq. (2.8.2). A $\triangle q^f$ that is growing with the detection time τ seems to imply that the detector does sense noise in the oscillator variable X. The true origin of this is, however, the interaction of the measured system with the detector. The detector position is spread over an interval $\triangle x \gtrsim 1/2\triangle q$. Since the oscillator is in its ground state the resulting disturbance drives it into ground states of new Hamiltonians $\hat{H}_0 + x\hat{X}$. For every detector influence x a different expectation value $E'(x) = \langle g(x)|\hat{X}|g(x)\rangle$ is measured. The read-off of the detector will then be a superposition of measurement outcomes corresponding to all those different influences. As a result, the uncertainty in the detector momentum grows with time, $(\triangle q^f)_{\triangle x} \approx \tau\triangle x\ \partial\langle g(x)|\hat{X}|g(x)\rangle/\partial x$. We conclude that the the quantum fluctuations of the detector set an upper bound on the accuracy of the measurement process. It vanishes if the FCS is x-independent and a classical interpretation of the process is possible.

2.9 Characterization of the FCS. First scheme

As we have already seen, the statistics $P(x,q,\tau)$ proposed above allows to predict the outcomes of measurements within our detection model and it resolves

inconsistencies that arose in earlier interpretations. It remains to be shown now, that it is real in the sense that it is experimentally observable.

For a first scheme of measuring the FCS we start from relation (2.4.11) between the initial and the final density matrix. Writing this equation in (x^+, x^-)-space, we find that

$$P(x^+, x^-, \tau) = \frac{\rho^f(x^+, x^-)}{\rho^{in}(x^+, x^-)} \tag{2.9.1}$$

or

$$P(x, q, \tau) = \int \frac{dz}{2\pi}\, e^{iqz}\, \frac{\rho^f(x + z/2, x - z/2)}{\rho^{in}(x + z/2, x - z/2)}. \tag{2.9.2}$$

We would already be done if we could measure all elements of the detector's final and initial density matrices. This is not possible in general, however. By successively measuring a certain observable we can measure the diagonal elements of the density matrix in a basis of eigenstates of that observable, but not the off-diagonal entries. We can therefore measure the functions $\Pi(q)$, but not $\hat{\rho}$ itself.

The key idea that we will pursue to solve this problem is to repeat the same measurement many times for shifted but otherwise identical initial detector density matrices. We suggest to repeat the measurement of the final momentum distribution $\Pi^f(q)$ for a number of initial density matrices that differ only in the expectation value x_0 of the position of the detecting particle and define the function

$$\Gamma^f(x_0, q, \tau) = \int dx\, dq'\, P(x, q - q', \tau)\, \rho^{in}(x - x_0, q'). \tag{2.9.3}$$

This way we expose the system during the measurement to different detector influences and one can hope that by doing so this influence can be identified and eliminated by a deconvolution procedure. Defining the Fourier transform of $\Gamma^f(x_0, q, \tau)$ with respect to both of its variables

$$\tilde{\Gamma}^f(q_0, z, \tau) \equiv \frac{1}{2\pi} \int dx_0\, dq\, e^{ix_0 q_0 - izq}\, \Gamma^f(x_0, q, \tau) \tag{2.9.4}$$

we find, that the FCS can indeed be reconstructed from this function by means of the relation

$$P(x, q, \tau) = \frac{1}{2\pi} \int dq_0\, dz\, e^{iqz - iq_0 x}\, \frac{\tilde{\Gamma}^f(q_0, z, \tau)}{\tilde{\rho}^{in}(q_0, z)} \tag{2.9.5}$$

where

$$\tilde{\rho}(q_0, z) \equiv \int dx\, e^{iq_0 x}\, \rho(x + \frac{z}{2}, x - \frac{z}{2}). \tag{2.9.6}$$

To interpret the result of the measurement, we still have to know the full initial density matrix of the detector. This should be feasible, however. One might either prepare the detector initially in a specific, well-known state, or one might let the detector equilibrate with an environment. The initial density matrix is

then stationary, $0 = [\hat{\rho}^{in}, \hat{H}] \propto [\hat{\rho}^{in}, \hat{q}^2]$, it is diagonal in a basis of momentum eigenstates and can be determined by a momentum measurement only. We conclude that the FCS is an observable.

To illustrate the procedure we apply it now to the example of a harmonic oscillator. The final momentum distribution with shifted initial detector states is

$$\Gamma^f(x_0, q, \tau) = \exp[-\frac{(q - x_0\tau/M\omega^2)^2}{(2(\triangle q)^2 + \tau^2/2M^2\omega^4(\triangle q)^2)}]. \tag{2.9.7}$$

On transforming this into Fourier space it becomes

$$\tilde{\Gamma}^f(q_0, z, \tau) = \exp[-\frac{(\triangle q)^2 z^2}{2} - \frac{\tau^2 z^2}{8M^2\omega^4(\triangle q)^2}] \;\; \delta(q_0 - \tau z/M\omega^2). \tag{2.9.8}$$

Employing now Eq. (2.9.5) with $\tilde{\rho}^{in}(q_0, z) = \exp[-(\triangle q)^2 z^2/2 - q_0^2/8(\triangle q)^2]$ we indeed recover the desired FCS Eq. (2.8.2).

2.10 Second scheme

If the system is in one state only, for example its ground state, or in a mixture of a limited number of discrete states, one can measure the FCS without knowledge of the initial detector state. We first assume that the system is in its ground state. Then we have the explicit expression (2.6.2) for the time evolution and we find, that

$$\Gamma^f(x_0, q, \tau) = \int dx \; dz \; dq' \; e^{-iz(q-q') - i\tau(E'(x)\, z + \frac{1}{24}E'''(x)\, z^3 + \ldots)} \; \rho^{in}(x - x_0, q'), \tag{2.10.1}$$

$\Gamma^f(x_0, q, \tau)$ again being the final momentum distribution for shifted initial detector wave functions. In the limit of large τ we find with (2.6.4) that

$$\lim_{\tau \to \infty} \Gamma^f(x_0, q, \tau) \propto \int dx \; \rho^{in}(x - x_0, q + \tau E'(x)). \tag{2.10.2}$$

This formula suggests that one can measure the function $E'(x)$ arbitrarily exactly in the limit of a long measurement time τ by determining the peak of the final momentum distribution. The only assumption we have to make about the initial detector density matrix now is, that it is well centered around $x = 0$ and that it falls off sufficiently fast for momenta higher than some arbitrary $\triangle q$. We want $\hat{\rho}^{in}$ to be peaked in x-space such that $E'(x)$ is measured at the point x_0 only (E(x) is assumed to be analytic). Of course, this means, that the width $\triangle q$ in momentum space of $\hat{\rho}^{in}$ and therefore also of $\hat{\rho}^f$ will be wide. For big τ, however, the peak position, that increases linearly in time, can still be detected with arbitrary precision.

Integrating $E'(x)$ we can then reconstruct the FCS for arbitrary detection times,

$$P(x,q,\tau) = \int \frac{dz}{2\pi}\, \exp\left\{-iqz - i\tau \int_{x-z/2}^{x+z/2} dx'\, E'(x')\right\}. \tag{2.10.3}$$

When the system is in a mixture of N distinct states, the expression for $P(x,q,\tau)$ is a sum of terms of the form (2.6.2) with different functions $E_n(x)$. There appear in general N distinct peaks in the final momentum distribution allowing to record all N functions $E_n'(x)$. Again, one can reconstruct $P(x,q,\tau)$ for arbitrary τ.

2.11 Conclusions

We have been studying the statistics of time averages of a quantum mechanical variable A. A simple model describing a detector without internal dynamics has been employed. The formalism that we have presented is, however, general enough to allow for the description of a generic detector. In our approach, the measurement outcome is expressed in terms of an object that we have called full counting statistics (FCS) of the variable A. It is an extension of another function proposed earlier in this context. This extension basically consists of accounting for the detector influence on the measured system. We find that the interplay of this influence with the quantum nature of the detector hampers in general a classical interpretation of the detector read-off. This way we have been able to remove inconsistencies that arose in earlier interpretations. Finally, we have shown, that this FCS is not only a theoretical construct that predicts results of measurements, but that it is an observable itself.

Appendix A:

Here we give a detailed derivation of the infinite mass limit of the kernel (2.4.5).

First, we define a Fourier transformed influence functional

$$\tilde{F}[k^+,k^-,\tau] = \int D[x^+]D[x^-]F[x^+,x^-,\tau]e^{i\int_{t_1}^{t_2} dt\,\left[x^+k^+ - x^-k^-\right]} \tag{A.1}$$

and correspondingly

$$\begin{aligned}\tilde{K}(q^+,q^-,q_1^+,q_1^-,\tau) \;=\; & \int dx^+\, dx^-\, dx_1^+\, dx_1^-\; e^{ix^+q^+ - ix^-q^- - ix_1^+q_1^+ + ix_1^-q_1^-} \\ & K(x^+,x^-,x_1^+,x_1^-,\tau).\end{aligned} \tag{A.2}$$

The $k^\pm$ are functions on the interval $[t_1,t_2]$. Inserting the identity

$$\exp\left\{i\int_{t_1}^{t_2} dt\,\frac{m}{2}\,\dot{x}^2\right\} = \int D[q]\,\exp\left\{i\int_{t_1}^{t_2} dt\,\left[-\frac{q^2}{2m} - q\dot{x}\right]\right\} \tag{A.3}$$

and using (2.4.5) we derive then

$$\tilde{K}(q^+,q^-,q_1^+,q_1^-,\tau) = \int\limits_{q^+(t_2)=q^+,q^+(t_1)=q_1^+} D[q^+] \int\limits_{q^-(t_2)=q^-,q^-(t_1)=q_1^-} D[q^-]\ \tilde{F}[\dot{q}^+,\dot{q}^-,\tau] \exp\left\{ i\int_{t_1}^{t_2} dt\ \frac{q^{+2}}{2m} - \frac{q^{-2}}{2m}\right\}. \quad \text{(A.4)}$$

In the infinite mass limit, the kinetic term in this expression disappears. Now, we change integration variables from $D[q^\pm]$ to $D[\dot{q}^\pm]$ and call $k^\pm = \dot{q}^\pm$. Then,

$$\tilde{K}(q^+,q^-,q_1^+,q_1^-,\tau) = \int\limits_{\int_{t_1}^{t_2} dt\ k^+=q^+-q_1^+} D[k^+] \int\limits_{\int_{t_1}^{t_2} dt\ k^-=q^--q_1^-} D[k^-]\ \tilde{F}[k^+,k^-,\tau]. \quad \text{(A.5)}$$

We can represent the functions $k^\pm$ by their Fourier series, $k^\pm(t) = \sum_{n=0}^{\infty} k_n^\pm \cos n\pi(t-t_1)/(t_2-t_1)$. Changing the integration variables in (A.5) to the coefficients $k_n^\pm$ in this expansion, we notice, that only the integrals over the zeroth components $k_0^\pm$ are constrained by the boundary conditions. We can therefore do all the integrals over higher Fourier modes in (2.4.5) and obtain

$$\tilde{K}(q^+,q^-,q_1^+,q_1^-,\tau) = \int \prod_{n\neq 0} D[k_n^+]\ D[k_n^-]\ D[x_n^+]\ D[x_n^-]\ F[x^+,x^-,\tau] \exp\left\{ i\frac{t_2-t_1}{2}\sum_{n=1}^{\infty}(k_n^+x_n^+ - k_n^-x_n^-) + i[x_0^+(q^+-q_1^+) - x_0^-(q^--q_1^-)]\right\}. \quad \text{(A.6)}$$

We have also expanded the functions $x^\pm$ in Fourier series now, $x^\pm(t) = \sum_{n=0}^{\infty} x_n^\pm \cos n\pi(t-t_1)/(t_2-t_1)$.

We see, that the $k_n^\pm$-integrations result in δ-functions that constrain the $x_n^\pm$, $n \neq 0$, to zero and allow us to do the corresponding $x_n^\pm$ - integrals:

$$\tilde{K}(q^+,q^-,q_1^+,q_1^-,\tau) = \int dx_0^+\ dx_0^-\ e^{i\left[x_0^+(q^+-q_1^+)-x_0^-(q^--q_1^-)\right]} \underset{\text{System}}{Tr}\ \overrightarrow{T}\ \exp\left\{-i\int_{t_1}^{t_2} dt[\hat{H}_{\text{sys}} - \alpha_\tau x_0^+\hat{A}]\right\}\ \hat{R}\ \overleftarrow{T}\ \exp\left\{ i\int_{t_1}^{t_2} dt[\hat{H}_{\text{sys}} - \alpha_\tau x_0^-\hat{A}]\right\} \quad \text{(A.7)}$$

or

$$K(x^+,x^-,x_1^+,x_1^-,\tau) = \delta(x^+-x_1^+)\ \delta(x^--x_1^-)\ P(x^+,x^-,\tau) \quad \text{(A.8)}$$

with

$$P(x^+,x^-,\tau) = \underset{\text{System}}{Tr}\ \overrightarrow{T}\ e^{-i\int_{t_1}^{t_2} dt\left[\hat{H}_{\text{sys}}-\alpha_\tau x^+\hat{A}\right]}\ \hat{R}\ \overleftarrow{T}\ e^{\,i\int_{t_1}^{t_2} dt\left[\hat{H}_{\text{sys}}-\alpha_\tau x^-\hat{A}\right]}. \quad \text{(A.9)}$$

This establishes the locality of the kernel $K(x^+,x^-,x_1^+,x_1^-,\tau)$.

Bibliography

[1] D. J. Griffiths, *Introduction to Quantum Mechanics*, Prentice Hall, New Jersey, 1995.

[2] L. S. Levitov and G. B. Lesovik, JETP Lett. 55, 555 (1992).

[3] L. S. Levitov and G. B. Lesovik, JETP Lett. 58, 230 (1993).

[4] L. S. Levitov, H. W. Lee, and G. B. Lesovik, Journ. Math. Phys. **37**, 4845 (1996).

[5] Yu. V. Nazarov, Ann. Phys. (Leipzig) **8** Spec. Issue SI-193, 507 (1999).

[6] J. Rammer and H. Smith, Rev. Mod. Phys. **58**, 323 (1986).

[7] A. Shelankov and J. Rammer, cond-mat/0207343 (2002).

[8] W. Belzig and Yu. V. Nazarov, Phys. Rev. Lett. **87**, 197006 (2001).

[9] This has emerged from discussions with L. S. Levitov.

[10] J. v. Neumann, *Die mathematischen Grundlagen der Quantenmechanik*, Springer Verlag, Berlin (1932).

[11] R.P. Feynman and F.L. Vernon, Ann. Phys.(N.Y.) **24**, 118 (1963).

3 Feedback of the electromagnetic environment on current and voltage fluctuations out of equilibrium

3.1 Introduction

A mesoscopic conductor is part of a macroscopic electrical circuit that influences its transport properties. This electromagnetic environment is a source of decoherence and plays a central role for single-electron effects [1–5]. Most studies address time-averaged properties. Time-dependent fluctuations of the electrical current are also affected by the environment, which reduces the low-frequency fluctuations by a feedback loop: A current fluctuation δI induces a counter-acting voltage fluctuation $\delta V = -Z\delta I$ over the conductor, which in turn reduces the current by an amount $-G\delta V$. (Here G and Z are, respectively, the conductance of the mesoscopic system and the equivalent series impedance of the macroscopic voltage-biased circuit.)

At zero temperature the macroscopic circuit does not generate any noise itself, and the feedback loop is the only way it affects the current fluctuations in the mesoscopic conductor, which persist at zero temperature because of the shot noise effect [6–8]. In the second cumulant $C^{(2)}$, or shot-noise power, the feedback loop may be accounted for by a rescaling of the current fluctuations: $\delta I \to (1 + ZG)^{-1}\delta I$. For example, the Poisson noise $C^{(2)} = e\bar{I}(1 + ZG)^{-2}$ of a tunnel junction is simply reduced by a factor $(1 + ZG)^{-2}$ due to the negative feedback of the series impedance. We have recently discovered that this textbook result breaks down beyond the second cumulant [9]. Terms appear which depend in a nonlinear way on lower cumulants, and which can not be incorporated by any rescaling with powers of $1 + ZG$. In the example of a tunnel junction the third cumulant at zero temperature takes the form $C^{(3)} = e^2\bar{I}(1 - 2ZG)(1 + ZG)^{-4}$.

Ref. [9] was restricted to zero temperature. In Ref. [10] we removed this restriction and showed that the nonlinear feedback of the electromagnetic environment drastically modifies the temperature dependence of $C^{(3)}$. Earlier theory [11–13] assumed an isolated mesoscopic conductor and predicted a temperature-independent $C^{(3)}$ for a tunnel junction. The coupling to an environment introduces a temperature dependence, which can even change the sign of $C^{(3)}$ as the temperature is raised. No such effect exists for the second cumulant. The predicted temperature dependence has been measured in a recent experiment [14]. The method we used in Ref. [10] to arrive at these results was phenomenological. The nonlinear feedback was inserted by hand into the Langevin equation,

through a cascade assumption [13]. The purpose of the present chapter is to provide a fully quantum mechanical derivation. Our results agree with Ref. [10], thereby justifying the Langevin approach.

The outline of this chapter is as follows. In Secs. 3.2 and 3.3 we present the general quantum mechanical framework within which we describe a broad class of electrical circuits that consist of mesoscopic conductors embedded in a macroscopic electromagnetic environment. The basis is a path integral formulation of the Keldysh approach to charge counting statistics [15, 16]. It allows us to compute correlators and cross-correlators of currents and voltages at arbitrary contacts of the circuit. The method is technically involved, but we give an intuitive interpretation of the results in terms of "pseudo-probabilities". Within this framework we study in Secs. 3.4 and 3.5 series circuits of two conductors. For concrete results we specialize to a low-frequency regime where the path integrals over fluctuating quantum fields can be taken in saddle-point approximation. The conditions of validity for this approximation are discussed. We obtain general relations between third order correlators in a series circuit and correlators of the individual isolated conductors. We specialize to the experimentally relevant case of a single mesoscopic conductor in series with a macroscopic conductor that represents the electromagnetic environment. Most experiments measure voltage correlators. In Sec. 3.6 we propose an experimental method to obtain current correlators, using the Hall voltage in a weak magnetic field. The fundamental difference between current and voltage correlators rests on whether the variable measured is odd or even under time reversal. In Sec. 3.7 we relax the low-frequency approximation by addressing Coulomb blockade effects from the environment [17–19]. We conclude in Sec. 3.8.

3.2 Description of the circuit

We consider a circuit consisting of electrical conductors G_i, a macroscopic electromagnetic environment [with impedance matrix $Z(\omega)$], plus ideal current and voltage meters M_i. The current meter (zero internal impedance) is in series with a voltage source, while the voltage meter (infinite internal impedance) is in parallel to a current source. Any finite impedance of meters and sources is incorporated in the electromagnetic environment. In Fig. 3-1 we show examples of such circuits.

The electromagnetic environment is assumed to produce only thermal noise. To characterize this noise we consider the circuit without the mesoscopic conductors, see Fig. 3-2. Each pair of contacts to the environment is now attached to a current source and a voltage meter. The impedance matrix is defined by

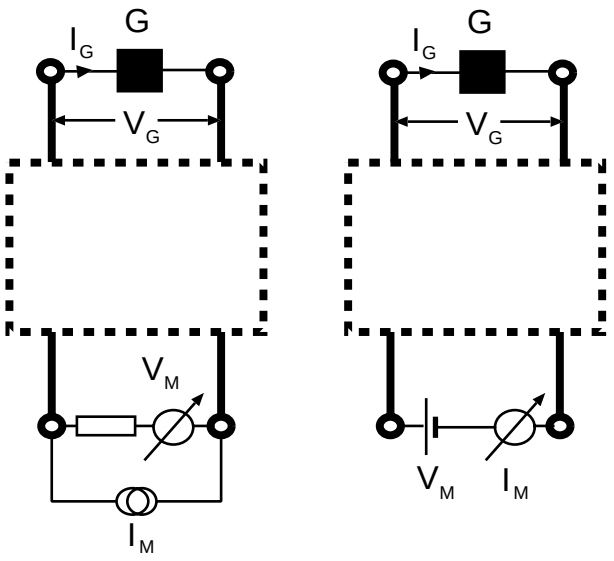

Figure 3-1. Electrical circuits studied in this chapter. The black boxes represent conductors embedded in an electromagnetic environment (dashed rectangle). A voltage source is present at the contacts for a current measurement (right circuit) and a current source at the contacts for a voltage measurement (left circuit). The two circuits can also be combined into one larger circuit containing two conductors and both a current and a voltage meter.

partial derivatives of voltages with respect to currents,

$$\boldsymbol{Z} = \begin{pmatrix} Z_{GG} & Z_{GM} \\ Z_{MG} & Z_{MM} \end{pmatrix} = \begin{pmatrix} \frac{\partial V_G}{\partial I_G}\Big|_{I_M} & \frac{\partial V_G}{\partial I_M}\Big|_{I_G} \\ \frac{\partial V_M}{\partial I_G}\Big|_{I_M} & \frac{\partial V_M}{\partial I_M}\Big|_{I_G} \end{pmatrix}. \tag{3.2.1}$$

(All quantities are taken at the same frequency ω.) If there is more than one pair of contacts of type G or M, then the four blocks of $\boldsymbol{Z}$ are themselves matrices. Positive and negative frequencies are related by $Z_{\alpha\beta}(-\omega) = Z^*_{\alpha\beta}(\omega)$. We also note the Onsager-Casimir [20] symmetry $Z_{\alpha\beta}(B,\omega) = Z_{\beta\alpha}(-B,\omega)$, in an external magnetic field B. The thermal noise at each pair of contacts is Gaussian. The covariance matrix of the voltage fluctuations δV_α is determined by the fluctuation-dissipation theorem,

$$\langle \delta V_\alpha(\omega)\delta V_\beta(\omega')\rangle = \pi\delta(\omega+\omega')\hbar\omega\coth\left(\frac{\hbar\omega}{2kT}\right)[Z_{\alpha\beta}(\omega) + Z^*_{\beta\alpha}(\omega)], \tag{3.2.2}$$

with T the temperature of the environment.

We seek finite frequency cumulant correlators of the variables measured at the current and voltage meters,

$$\langle\langle X_1(\omega_1)\cdots X_n(\omega_n)\rangle\rangle = 2\pi\delta\left(\sum_{k=1}^{n}\omega_k\right) C^{(n)}_{\mathbf{X}}(\omega_1,\cdots,\omega_n). \tag{3.2.3}$$

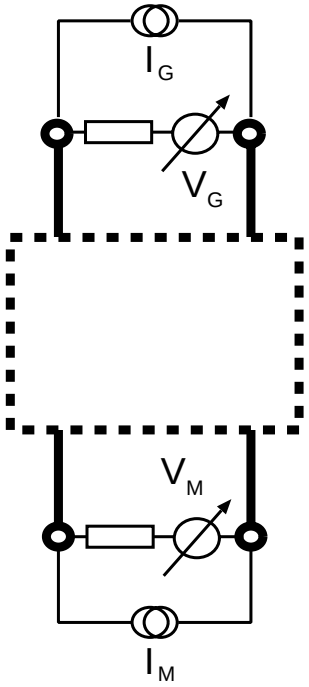

Figure 3-2. Circuit used to characterize the impedance matrix of the electromagnetic environment. All contacts are now connected to a voltage meter plus a current source.

Here X_i stands for either V_M or I_M. Fourier transforms are defined by $X_i(\omega) = \int dt\, \exp(i\omega t) X_i(t)$. Our aim is to relate the correlators at the measurement contacts to the correlators one would measure at the conductors if they were isolated from the environment.

3.3 Path integral formulation

Correlators of currents I_M and voltages V_M at the measurement contacts are obtained from the generating functional

$$\mathcal{Z}_X[\vec{\boldsymbol{j}}] = \left\langle T_- e^{i\int dt\, [H + \boldsymbol{j}^-(t) X]} T_+ e^{-i\int dt\, [H + \boldsymbol{j}^+(t) X]} \right\rangle . \tag{3.3.1}$$

They contain moments of outcomes of measurements of the variable X (equal to I_M or V_M) at different instants of time. The symbols $T_+ (T_-)$ denote (inverse) time ordering, different on the forward and the backward part of the Keldysh contour. The exponents contain source terms $j^\pm$ and a Hamiltonian H, which we discuss separately.

The source term $j^\pm(t)$ is a charge $Q_M = \int^t dt'\, I_M(t')$ if $X = V_M$, whereas it is a phase $\Phi_M = \int^t dt'\, V_M(t')$ if $X = I_M$. (We have set $\hbar$ to unity.) The superscript $\pm$ determines on which part of the Keldysh contour the source is effective. The

vector $\vec{\boldsymbol{j}} = (\boldsymbol{j^{cl}}, \boldsymbol{j^{q}})$ indicates the linear combinations

$$\boldsymbol{j^{cl}} = \frac{1}{2}\frac{\partial}{\partial t}(\boldsymbol{j}^{+} + \boldsymbol{j}^{-}), \quad \boldsymbol{j^{q}} = \boldsymbol{j}^{+} - \boldsymbol{j}^{-}. \tag{3.3.2}$$

We denote vectors in this two-dimensional "Keldysh space" by a vector arrow. The "classical" source fields $\boldsymbol{j^{cl}} = (j_1^{cl}, j_2^{cl}, \cdots)$ account for current or voltage sources at the measurement contacts. Cumulant correlators of the measured variables are generated by differentiation of $\ln \mathcal{Z}_X$ with respect to the "quantum" fields $\boldsymbol{j^{q}} = (j_1^{q}, j_2^{q}, \cdots)$:

$$\left\langle\!\left\langle \prod_{k=1}^{n} X_k(t_k) \right\rangle\!\right\rangle = \prod_{k=1}^{n} \frac{\delta}{-i\delta j_k^{q}(t_k)} \ln \mathcal{Z}_X \Big|_{\boldsymbol{j^{q}}=0}. \tag{3.3.3}$$

The Hamiltonian consists of three parts,

$$H = H_e + \sum_i H_{G_i} - \boldsymbol{\Phi_G} \boldsymbol{I_G}. \tag{3.3.4}$$

The term $H_e = \sum_j \Omega_j a_j^{\dagger} a_j$ represents the electromagnetic environment, which we model by a collection of harmonic oscillators at frequencies Ω_j. The conductors connected to the environment have Hamiltonians H_{G_i}. The interaction term couples the phases $\boldsymbol{\Phi_G}$ (defined by $i[H_e, \boldsymbol{\Phi_G}] = \boldsymbol{V_G}$) to the currents $\boldsymbol{I_G}$ through the conductors. The phases $\boldsymbol{\Phi_G}$, as well as the measured quantities $\mathbf{X}$, are linear combinations of the bosonic operators a_j of the electromagnetic environment,

$$\boldsymbol{\Phi_G} = \sum_j \left(\boldsymbol{c_j^G} a_j + \boldsymbol{c_j^{G*}} a_j^{\dagger} \right), \tag{3.3.5}$$

$$\boldsymbol{X} = \sum_j \left(\boldsymbol{c_j^X} a_j + \boldsymbol{c_j^{X*}} a_j^{\dagger} \right). \tag{3.3.6}$$

The coefficients c_j^G and c_j^X depend on the impedance matrix of the environment and also on which contacts are connected to a current source and which to a voltage source.

To calculate the generating functional we use a path integral formulation in Keldysh space [16, 21]. We first present the calculation for the case of a voltage measurement at all measurement contacts (so $X_k = V_{M_k}$ and $j_k = Q_{M_k}$ for all k). We will then show how the result for a current measurement can be obtained from this calculation. The path integral involves integrations over the environmental degrees of freedom a_j weighted with an influence functional $\mathcal{Z}_{\boldsymbol{I_G}}$ due to the conductors. Because the conductors are assumed to be uncoupled in the absence of the environment, this influence functional factorizes:

$$\mathcal{Z}_{\boldsymbol{I_G}}[\vec{\boldsymbol{\Phi}}_{\boldsymbol{G}}] = \prod_i \mathcal{Z}_{I_{G_i}}[\vec{\Phi}_{G_i}]. \tag{3.3.7}$$

An individual conductor has influence functional

$$\mathcal{Z}_{I_{G_i}} = \left\langle T_- \, e^{i\int dt \left[H_{G_i}+\Phi^-_{G_i}(t) I_{G_i}\right]} T_+ e^{-i\int dt \left[H_{G_i}+\Phi^+_{G_i}(t) I_{G_i}\right]} \right\rangle . \tag{3.3.8}$$

Comparing Eq. (3.3.8) with Eq. (3.3.1) for $\mathbf{X} = \boldsymbol{I_M}$, we note that the influence functional of a conductor G_i is just the generating functional of current fluctuations in G_i when connected to an ideal voltage source without electromagnetic environment. That is why we use the same symbol $\mathcal{Z}$ for influence functional and generating functional.

The integrals over all environmental fields except $\vec{\boldsymbol{\Phi}}_{\boldsymbol{G}}$ are Gaussian and can be done exactly. The resulting path integral expression for the generating functional $\mathcal{Z}_{V_M}$ takes the form

$$\mathcal{Z}_{V_M}[\vec{\boldsymbol{Q}}_{\boldsymbol{M}}] = \int \mathcal{D}[\vec{\boldsymbol{\Phi}}_{\boldsymbol{G}}] \exp\left\{-iS_e[\vec{\boldsymbol{Q}}_{\boldsymbol{M}}, \vec{\boldsymbol{\Phi}}_{\boldsymbol{G}}]\right\} \mathcal{Z}_{I_G}[\vec{\boldsymbol{\Phi}}_{\boldsymbol{G}}], \tag{3.3.9}$$

up to a normalization constant [22]. We use for the integration fields $\vec{\boldsymbol{\Phi}}_{\boldsymbol{G}}$ the same vector notation as for the source fields: $\vec{\boldsymbol{\Phi}}_{\boldsymbol{G}} = (\boldsymbol{\Phi}^{\boldsymbol{cl}}_{\boldsymbol{G}}, \boldsymbol{\Phi}^{\boldsymbol{q}}_{\boldsymbol{G}})$ with $\boldsymbol{\Phi}^{\boldsymbol{cl}}_{\boldsymbol{G}} = \frac{1}{2}(\partial/\partial t)(\boldsymbol{\Phi}^+_{\boldsymbol{G}} + \boldsymbol{\Phi}^-_{\boldsymbol{G}})$ and $\boldsymbol{\Phi}^{\boldsymbol{q}}_{\boldsymbol{G}} = \boldsymbol{\Phi}^+_{\boldsymbol{G}} - \boldsymbol{\Phi}^-_{\boldsymbol{G}}$. The Gaussian environmental action S_e is calculated in App. A. The result is given in terms of the impedance matrix $\boldsymbol{Z}$ of the environment,

$$S_e[\vec{\boldsymbol{Q}}_{\boldsymbol{M}}, \vec{\boldsymbol{\Phi}}_{\boldsymbol{G}}] = \frac{1}{2}\int \frac{d\omega}{2\pi} \left[\vec{\boldsymbol{Q}}^*_{\boldsymbol{M}} \check{\boldsymbol{Z}}_{\boldsymbol{MM}} \vec{\boldsymbol{Q}}_{\boldsymbol{M}} + \left(\vec{\boldsymbol{\Phi}}^*_{\boldsymbol{G}} - \vec{\boldsymbol{Q}}^*_{\boldsymbol{M}} \check{\boldsymbol{Z}}_{\boldsymbol{MG}}\right) \check{\boldsymbol{Y}} \left(\vec{\boldsymbol{\Phi}}_{\boldsymbol{G}} - \check{\boldsymbol{Z}}_{\boldsymbol{GM}} \vec{\boldsymbol{Q}}_{\boldsymbol{M}}\right) \right], \tag{3.3.10}$$

$$\check{\boldsymbol{Y}}(\omega) = \begin{pmatrix} 0 & \boldsymbol{Z}^{\dagger -1}_{\mathbf{GG}}(\omega) \\ \boldsymbol{Z}^{-1}_{\mathbf{GG}}(\omega) & -\frac{i}{2}\omega[2N(\omega)+1][\boldsymbol{Z}^{-1}_{\mathbf{GG}}(\omega) + \boldsymbol{Z}^{\dagger -1}_{\mathbf{GG}}(\omega)] \end{pmatrix}, \tag{3.3.11}$$

$$\check{\boldsymbol{Z}}_{\boldsymbol{MM}}(\omega) = \begin{pmatrix} 0 & \boldsymbol{Z}^{\dagger}_{\mathbf{MM}}(\omega) \\ \boldsymbol{Z}_{\boldsymbol{MM}}(\omega) & -\frac{i}{2}\omega[2N(\omega)+1][\boldsymbol{Z}_{\boldsymbol{MM}}(\omega) + \boldsymbol{Z}^{\dagger}_{\mathbf{MM}}(\omega)] \end{pmatrix}, \tag{3.3.12}$$

$$\check{\boldsymbol{Z}}_{\boldsymbol{MG}}(\omega) = \begin{pmatrix} -\boldsymbol{Z}^{\dagger}_{\mathbf{GM}}(\omega) & 0 \\ \frac{i}{2}\omega[2N(\omega)+1][\boldsymbol{Z}_{\boldsymbol{MG}}(\omega) + \boldsymbol{Z}^{\dagger}_{\mathbf{GM}}(\omega)] & \boldsymbol{Z}_{\boldsymbol{MG}}(\omega) \end{pmatrix} = \check{\boldsymbol{Z}}^{T}_{\mathbf{GM}}(-\omega), \tag{3.3.13}$$

with the Bose-Einstein distribution $N(\omega) = [\exp(\omega/kT) - 1]^{-1}$. We have marked matrices in the Keldysh space by a check, for instance $\check{\mathbf{Y}}$.

When one substitutes Eq. (3.3.10) into Eq. (3.3.9) and calculates correlators with the help of Eq. (3.3.3), one can identify two sources of noise. The first source of noise is current fluctuations in the conductors that induce fluctuations of the measured voltage. These contributions are generated by differentiating the terms of S_e that are linear in $\vec{\boldsymbol{Q}}_{\boldsymbol{M}}$. The second source of noise is the environment itself, accounted for by the contributions quadratic in $\vec{\boldsymbol{Q}}_{\boldsymbol{M}}$.

Generating functionals $\mathcal{Z}_{I_M}$ for circuits where currents rather than voltages are measured at some of the contacts can be obtained along the same lines with modified response functions. It is also possible to obtain them from $\mathcal{Z}_{V_M}$ through the functional Fourier transform derived in App. B,

$$\mathcal{Z}_{I_M}[\vec{\Phi}_M] = \int \mathcal{D}[\vec{Q}_M]\, e^{-i\vec{Q}_M\times\vec{\Phi}_M}\, \mathcal{Z}_{V_M}[\vec{Q}_M]. \tag{3.3.14}$$

We have defined the cross product

$$\vec{Q}\times\vec{\Phi} \equiv \int dt\, (Q^{cl}\Phi^q - \Phi^{cl}Q^q). \tag{3.3.15}$$

This transformation may be applied to any pair of measurement contacts to obtain current correlators from voltage correlators.

Eq. (3.3.14) ensures that the two functionals

$$\mathcal{P}[V,I] = \int \mathcal{D}[q]\, e^{i\int dt\, qV}\, \mathcal{Z}_V\left[\vec{Q}=(I,q)\right], \tag{3.3.16}$$

$$\mathcal{P}'[V,I] = \int \mathcal{D}[\varphi]\, e^{i\int dt\, \varphi I}\, \mathcal{Z}_I\left[\vec{\Phi}=(V,\varphi)\right], \tag{3.3.17}$$

are identical: $\mathcal{P}[V,I] = \mathcal{P}'[V,I]$. This functional $\mathcal{P}$ has an intuitive probabilistic interpretation. With the help of Eq. (3.3.3) we obtain from $\mathcal{P}$ the correlators

$$\langle V(t_1)\cdots V(t_n)\rangle_I = \frac{\int \mathcal{D}[V]\, V(t_1)\cdots V(t_n)\mathcal{P}[V,I]}{\int \mathcal{D}[V]\,\mathcal{P}[V,I]}, \tag{3.3.18}$$

$$\langle I(t_1)\cdots I(t_n)\rangle_V = \frac{\int \mathcal{D}[I]\, I(t_1)\cdots I(t_n)\mathcal{P}[V,I]}{\int \mathcal{D}[I]\,\mathcal{P}[V,I]}. \tag{3.3.19}$$

This suggests the interpretation of $\mathcal{P}[V,I]$ as a joint probability distribution functional of current and voltage fluctuations. Yet, $\mathcal{P}$ can not properly be called a probability since it need not be positive. In the low frequency approximation introduced in the next section it is positive for normal metal conductors. However, for superconductors, it has been found to take negative values [23]. It is therefore more properly called a "pseudo-probability".

We conclude this section with some remarks on the actual measurement process. The time-averaged correlators (3.2.3) may be measured in two different ways. In the first way the variable X is measured repeatedly and results at different times are correlated afterwards. In the second way (and this is how it is usually done [24]) one uses a detector that measures directly time integrals of X (for example, by means of a spectral filter). The correlators measured in the

first way are obtained from the generating functional according to Eq. (3.3.3),

$$2\pi\delta\left(\sum_{k=1}^{n}\omega_k\right)C_{\mathbf{X}}^{(n)}(\omega_1,\cdots,\omega_n)$$
$$=\prod_k\left[\int_{-\infty}^{\infty}dt\,e^{i\omega_k t}\frac{\delta}{-i\delta j_k^q(t)}\right]\ln\mathcal{Z}_X\Big|_{j^q=0}. \qquad (3.3.20)$$

The second way of measurement is modelled by choosing cross-impedances that ensure that an instantaneous measurement at one pair of contacts yields a time average at another pair, for example $Z_{MG}(\omega)\propto\delta(\omega-\omega_0)$. The resulting frequency dependent correlators do not depend on which way of measurement one uses.

3.4 Two conductors in series

We specialize the general theory to the series circuit of two conductors G_1 and G_2 shown in Fig. 3-3 (lower panel). We derive the generating functional $\mathcal{Z}_{V,I}$ for correlators of the voltage drop $V\equiv V_{M_1}$ over conductor G_1 and the current $I\equiv I_{M_2}$ through both conductors. (The voltage drop over conductor G_2 equals $V_{M_2}-V_{M_1}\equiv V_{\rm bias}-V$, with $V_{\rm bias}$ the non-fluctuating bias voltage of the voltage source.) To apply the general relations of the previous section we embed the two conductors in an electromagnetic environment, as shown in the top panel of Fig. 3-3. In the limit of infinite resistances R_1, R_2, and R_3 this 8-terminal circuit becomes equivalent to a simple series circuit of G_1 and G_2. We take the infinite resistance limit of Eq. (3.3.9) in App. C. The result

$$\mathcal{Z}_{V,I}[\vec{Q},\vec{\Phi}]=\int\mathcal{D}[\vec{\Phi}']\,e^{-i\vec{\Phi}'\times\vec{Q}}\,\mathcal{Z}_1[\vec{\Phi}']\mathcal{Z}_2[\vec{\Phi}-\vec{\Phi}'] \qquad (3.4.1)$$

shows that the generating functional of current and voltage correlators in the series circuit is a functional integral convolution of the generating functionals $\mathcal{Z}_1\equiv\mathcal{Z}_{I_{G_1}}$ and $\mathcal{Z}_2\equiv\mathcal{Z}_{I_{G_2}}$ of the two conductors G_1 and G_2 defined in Eq. (3.3.8).

Eq. (3.4.1) implies a simple relation between the pseudo-probabilities $\mathcal{P}_{G_1+G_2}$ of the series circuit (obtained by means of Eq. (3.3.17) from $\mathcal{Z}_{V,I}|_{\vec{Q}=0}$) and the pseudo-probabilities $\mathcal{P}_{G_k}$ of the individual conductors (obtained by means of Eq. (3.3.17) from $\mathcal{Z}_k$). We find

$$\mathcal{P}_{G_1+G_2}[V,I]=\int\mathcal{D}V'\,\mathcal{P}_{G_1}[V-V',I]\mathcal{P}_{G_2}[V',I]. \qquad (3.4.2)$$

This relation is obvious if one interprets it in terms of classical probabilities: The voltage drop over G_1+G_2 is the sum of the independent voltage drops over G_1 and G_2, so the probability $\mathcal{P}_{G_1+G_2}$ is the convolution of $\mathcal{P}_{G_1}$ and $\mathcal{P}_{G_2}$. Yet the relation (3.4.2) is for quantum mechanical pseudo-probabilities.

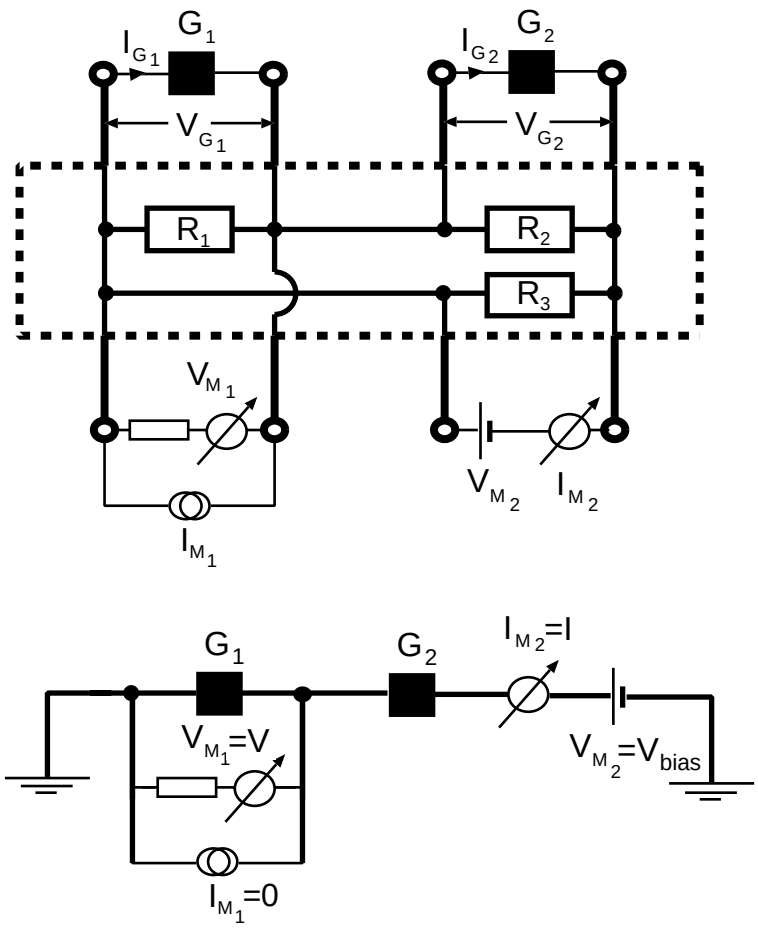

Figure 3-3. Top panel: Circuit of two conductors G_1, G_2 in an electromagnetic environment modelled by three resistances R_1, R_2, R_3. In the limit $R_1, R_2, R_3 \to \infty$ the circuit becomes equivalent to the series circuit in the lower panel.

We evaluate the convolution (3.4.1) in the low-frequency regime, when the functionals $\mathcal{Z}_1$ and $\mathcal{Z}_2$ become local in time,

$$\ln \mathcal{Z}_k[\vec{\Phi}] \equiv -iS_k[\vec{\Phi}] = -i \int dt\, S_k(\vec{\Phi}(t)). \tag{3.4.3}$$

We then do the path integration in saddle-point approximation, with the result

$$\ln \mathcal{Z}_{V,I}[\vec{Q}, \vec{\Phi}] = -i \operatorname*{extr}_{[\vec{\Phi}']} \Big\{ \vec{\Phi}' \times \vec{Q} + \int dt\, [S_1(\vec{\Phi}'(t)) + S_2(\vec{\Phi}(t) - \vec{\Phi}'(t))] \Big\}. \tag{3.4.4}$$

The notation "extr" indicates the extremal value of the expression between curly brackets with respect to variations of $\vec{\Phi}'(t)$. The validity of the low-frequency and saddle-point approximations is addressed at the end of this section.

We will consider separately the case that both conductors G_1 and G_2 are mesoscopic conductors and the case that G_1 is mesoscopic while G_2 is a macroscopic conductor. The action of a macroscopic conductor with impedance Z is

quadratic,

$$S_{\rm macro}[\vec{\Phi}] = \frac{1}{2}\int \frac{d\omega}{2\pi}\,\vec{\Phi}^\dagger \check{Y}\vec{\Phi}, \tag{3.4.5}$$

corresponding to Gaussian current fluctuations. The matrix $\check{Y}$ is given by Eq. (3.3.11), with a scalar $Z_{GG} = Z$. The corresponding pseudo-probability $\mathcal{P}_{\rm macro}$ is positive,

$$\mathcal{P}_{\rm macro}[V,I] = \exp\left\{-\int \frac{d\omega}{4\pi\omega}\,\frac{|V-ZI|^2}{{\rm Re}\,Z}\tanh\left(\frac{\omega}{2kT}\right)\right\}. \tag{3.4.6}$$

Substitution of $\mathcal{P}_{\rm macro}$ for $\mathcal{P}_{G_2}$ in Eq. (3.4.2) gives a simple result for $\mathcal{P}_{G_1+G_2}$ at zero temperature,

$$\mathcal{P}_{G_1+G_2}[V,I] = \mathcal{P}_{G_1}[V-ZI,I], \quad \text{if } T=0. \tag{3.4.7}$$

The feedback of the macroscopic conductor on the mesoscopic conductor amounts to a negative voltage $-ZI$ produced in response to a current I.

The action of a mesoscopic conductor in the low-frequency limit is given by the Levitov-Lesovik formula [25,26],

$$\begin{aligned} S_{\rm meso}(\vec{\Phi}) \;=\; & \frac{1}{2\pi}\sum_{n=1}^{N}\int d\varepsilon\,\ln[1+\Gamma_n(e^{ie\varphi}-1)n_R(1-n_L) \\ & +\Gamma_n(e^{-ie\varphi}-1)n_L(1-n_R)], \end{aligned} \tag{3.4.8}$$

with $\vec{\Phi} = (V,\varphi)$. The Γ_n's ($n = 1,2,\cdots N$) are the transmission eigenvalues of the conductor. The two functions $n_L(\varepsilon,T) = [\exp(\varepsilon/kT)+1]^{-1}$ and $n_R(\varepsilon,T) = n_L(\varepsilon+eV,T)$ are the filling factors of electron states at the left and right contacts, with V the voltage drop over the conductor and T its temperature.

The criterion for the applicability of the low-frequency and saddle-point approximations to the action of a mesoscopic conductor depends on two time scales. The first scale $\tau_1 = \min(1/eV, 1/kT)$ is the mean width of current pulses due to individual transferred electrons. The second scale $\tau_2 = e/I \simeq (e^2/G)\tau_1$ is the mean time between current pulses. At frequencies below $1/\tau_1$ the action of the conductor becomes local in time. Below the second scale $1/\tau_2$ the action of the conductor is large for values of $\vec{\Phi}$ where the nonlinearities become important. This justifies the saddle-point approximation. The nonlinearities in $S_{\rm meso}$ become relevant for $\varphi \simeq 1/e$, so for time scales $\tau \gg \tau_2$ we indeed have $S_{\rm meso} \simeq \tau I\varphi \simeq \tau I/e \simeq \tau/\tau_2 \gg 1$.

These two approximations together are therefore justified if fluctuations with frequencies ω above $\Lambda \simeq \min(1/\tau_1, 1/\tau_2)$ are suppressed by a small effective impedance: $Z(\omega) \ll h/e^2$ for $\omega \gtrsim \Lambda$. A small impedance acts as a heavy mass term in Eq. (3.4.1), suppressing fluctuations. This is seen from Eq. (3.4.5) for a macroscopic conductor and it carries over to other conductors. In Sec. 3.7 we will examine the Coulomb blockade effects that appear if $Z(\omega)$ is not small at high frequencies.

3.5 Third cumulants

3.5.1 Two arbitrary conductors in series

We use the general formula (3.4.4) to calculate the third order cumulant correlator of current and voltage fluctuations in a series circuit of two conductors G_1 and G_2 at finite temperature. We focus on correlators at zero frequency (finite frequency generalizations are given later).

The zero-frequency correlators $C_{\mathrm{X}}^{(n)}(\overline{V})$ depend on the average voltage $\overline{V}$ over G_1, which is related to the voltage V_{bias} of the voltage source by $\overline{V} = V_{\mathrm{bias}}(1 + G_1/G_2)^{-1}$. The average voltage over G_2 is $V_{\mathrm{bias}} - \overline{V} = V_{\mathrm{bias}}(1 + G_2/G_1)^{-1}$. Our goal is to express $C_{\mathrm{X}}^{(n)}(\overline{V})$ in terms of the current correlators $C_1^{(n)}(V)$ and $C_2^{(n)}(V)$ that the conductors G_1 and G_2 would have if they were isolated and biased with a non-fluctuating voltage V. These are defined by

$$\langle\langle I_i(\omega_1)\cdots I_i(\omega_n)\rangle\rangle_V = 2\pi\delta\left(\sum_{k=1}^{n}\omega_k\right)C_i^{(n)}(V), \tag{3.5.1}$$

where I_i is the current through conductor i at fixed voltage V.

To evaluate Eq. (3.4.4) it is convenient to discretize frequencies $\omega_n = 2\pi n/\tau$. The Fourier coefficients are $f_n = \tau^{-1}\int_0^\tau dt\, e^{i\omega_n t} f(t)$. The detection time τ is sent to infinity at the end of the calculation. For zero-frequency correlators the sources at non-zero frequencies vanish and there is a saddle point configuration such that all fields at non-zero frequencies vanish as well. We may then write Eq. (3.4.4) in terms of only the zero-frequency fields $\vec{\Phi}_0 = (V_0, \varphi_0)$, $\vec{\Phi}_0' = (V_0', \varphi_0')$, and $\vec{Q}_0 = (I_0, q_0)$, with actions

$$\tau^{-1}S_k(\vec{\Phi}_0') = G_k\varphi_0'V_0' + i\sum_{n=2}^{\infty}\frac{(-i\varphi_0')^n}{n!}C_k^{(n)}(V_0'). \tag{3.5.2}$$

For $\vec{\Phi}_0 = (V_{\mathrm{bias}}, 0)$ and $\vec{Q}_0 = (0,0)$ the saddle point is at $\vec{\Phi}_0' = (\overline{V}, 0)$. For the third order correlators we need the extremum in Eq. (3.4.4) to third order in φ_0 and q_0. We have to expand S_k to third order in the deviation $\delta\vec{\Phi}_0' = \vec{\Phi}_0' - (\overline{V}, 0)$ from the saddle point at vanishing sources. We have to this order

$$\begin{aligned}
\tau^{-1}S_1(\vec{\Phi}_0') &= G_1\varphi_0'(\overline{V} + \delta V_0') - \frac{i}{2}C_1^{(2)}(\overline{V})\varphi_0'^2 - \frac{1}{6}C_1^{(3)}(\overline{V})\varphi_0'^3 \\
&\quad - \frac{i}{2}\frac{d}{d\overline{V}}C_1^{(2)}(\overline{V})\delta V_0'\varphi_0'^2 + \mathcal{O}(\delta\vec{\Phi}_0'^4), \qquad (3.5.3)\\
\tau^{-1}S_2(\vec{\Phi}_0 - \vec{\Phi}_0') &= G_2\varphi_0'(V_{\mathrm{bias}} - \overline{V} - \delta V_0') - \frac{i}{2}C_2^{(2)}(V_{\mathrm{bias}} - \overline{V})\varphi_0'^2 \\
&\quad - \frac{1}{6}C_2^{(3)}(V_{\mathrm{bias}} - \overline{V})\varphi_0'^3 + \frac{i}{2}\frac{d}{d\overline{V}}C_2^{(2)}(V_{\mathrm{bias}} - \overline{V})\delta V_0'\varphi_0'^2 + \mathcal{O}(\delta\vec{\Phi}_0'^4).
\end{aligned} \tag{3.5.4}$$

Minimizing the sum $S_1(\vec{\Phi}_0') + S_2(\vec{\Phi}_0 - \vec{\Phi}_0')$ to third order in q_0 and φ_0 we then find the required relation between the correlators of the series circuit and the correlators of the isolated conductors. For the second order correlators we find

$$C_{II}^{(2)}(\overline{V}) = (R_1+R_2)^{-2}[R_1^2 C_1^{(2)}(\overline{V}) + R_2^2 C_2^{(2)}(V_{\rm bias}-\overline{V})], \tag{3.5.5a}$$

$$C_{VV}^{(2)}(\overline{V}) = (R_1+R_2)^{-2}(R_1R_2)^2[C_1^{(2)}(\overline{V}) + C_2^{(2)}(V_{\rm bias}-\overline{V})], \tag{3.5.5b}$$

$$C_{IV}^{(2)}(\overline{V}) = (R_1+R_2)^{-2}R_1R_2[R_2 C_2^{(2)}(V_{\rm bias}-\overline{V}) - R_1 C_1^{(2)}(\overline{V})], \tag{3.5.5c}$$

with $R_k = 1/G_k$. The third order correlators contain extra terms that depend on the second-order correlators,

$$C_{III}^{(3)}(\overline{V}) = (R_1+R_2)^{-3}[R_1^3 C_1^{(3)}(\overline{V}) + R_2^3 C_2^{(3)}(V_{\rm bias}-\overline{V})] + 3C_{IV}^{(2)}\frac{d}{d\overline{V}}C_{II}^{(2)}, \tag{3.5.6a}$$

$$C_{VVV}^{(3)}(\overline{V}) = (R_1+R_2)^{-3}(R_1R_2)^3[C_2^{(3)}(V_{\rm bias}-\overline{V}) - C_1^{(3)}(\overline{V})] + 3C_{VV}^{(2)}\frac{d}{d\overline{V}}C_{VV}^{(2)}, \tag{3.5.6b}$$

$$C_{VVI}^{(3)}(\overline{V}) = (R_1+R_2)^{-3}(R_1R_2)^2[R_1 C_1^{(3)}(\overline{V}) + R_2 C_2^{(3)}(V_{\rm bias}-\overline{V})] + 2C_{VV}^{(2)}\frac{d}{d\overline{V}}C_{IV}^{(2)} + C_{IV}^{(2)}\frac{d}{d\overline{V}}C_{VV}^{(2)}, \tag{3.5.6c}$$

$$C_{IIV}^{(3)}(\overline{V}) = (R_1+R_2)^{-3}R_1R_2[R_2^2 C_2^{(3)}(V_{\rm bias}-\overline{V}) - R_1^2 C_1^{(3)}(\overline{V})] + 2C_{IV}^{(2)}\frac{d}{d\overline{V}}C_{IV}^{(2)} + C_{VV}^{(2)}\frac{d}{d\overline{V}}C_{II}^{(2)}. \tag{3.5.6d}$$

These results agree with those obtained by the cascaded Langevin approach [10].

3.5.2 Mesoscopic and macroscopic conductor in series

An important application is a single mesoscopic conductor G_1 embedded in an electromagnetic environment, represented by a macroscopic conductor G_2. A macroscopic conductor has no shot noise but only thermal noise. The third cumulant $C_2^{(3)}$ is therefore equal to zero. The second cumulant $C_2^{(2)}$ is voltage independent, given by [7]

$$C_2^{(2)}(\omega) = \omega\coth\left(\frac{\omega}{2kT_2}\right)\mathrm{Re}\,G_2(\omega), \tag{3.5.7}$$

at temperature T_2. We still assume low frequencies $\omega \ll \max(e\overline{V}, kT_1)$, so the frequency dependence of S_1 can be neglected. We have retained the frequency dependence of S_2, because the characteristic frequency of a macroscopic conductor is typically much smaller than of a mesoscopic conductor.

From Eq. (3.5.6) (and a straightforward generalization to frequency dependent correlators) we can obtain the third cumulant correlators by setting $C_2^{(3)} = 0$ and substituting Eq. (3.5.7). We only give the two correlators $C_{III}^{(3)}$ and $C_{VVV}^{(3)}$,

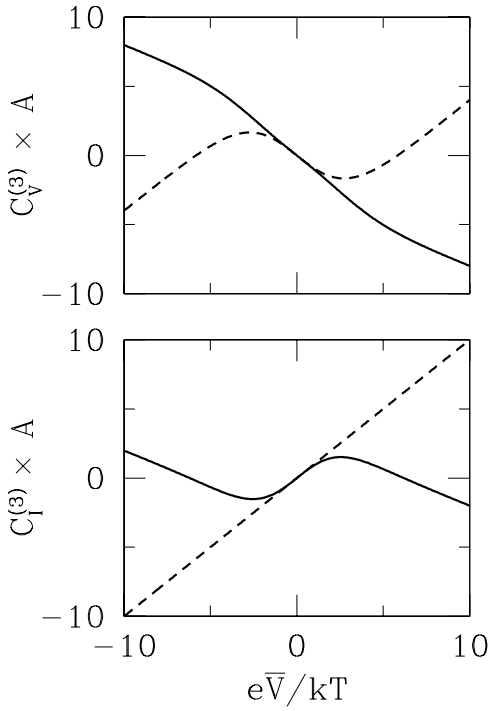

Figure 3-4. Third cumulant of voltage and current fluctuations of a tunnel junction (conductance G) in an electromagnetic environment (impedance Z, assumed frequency independent). Both $C_I^{(3)}$ and $C_V^{(3)}$ are multiplied by the scaling factor $A = (1+ZG)^3/eGkT$. The two curves correspond to different values of ZG (solid curve: $ZG = 1$; dashed curve: $ZG = 0$). The temperatures of the tunnel junction and its environment are chosen the same, $T_1 = T_2 = T$.

since these are the most significant for experiments. To abbreviate the formula we denote $G = G_1$ and $Z(\omega) = 1/G_2(\omega)$. We find

$$C_{III}^{(3)}(\omega_1,\omega_2,\omega_3) = \frac{1}{[1+Z(\omega_1)G][1+Z(\omega_2)G][1+Z(\omega_3)G]}\Big\{C_1^{(3)}(\overline{V}) - \frac{dC_1^{(2)}(\overline{V})}{d\overline{V}}\sum_{j=1}^{3} Z(-\omega_j)[C_1^{(2)}(\overline{V}) - GZ(\omega_j)C_2^{(2)}(\omega_j)][1+Z(-\omega_j)G]^{-1}\Big\}, \tag{3.5.8}$$

$$-\frac{C_{VVV}^{(3)}(\omega_1,\omega_2,\omega_3)}{Z(\omega_1)Z(\omega_2)Z(\omega_3)} = \frac{1}{[1+Z(\omega_1)G][1+Z(\omega_2)G][1+Z(\omega_3)G]} \times \Big\{C_1^{(3)}(\overline{V}) - \frac{dC_1^{(2)}(\overline{V})}{d\overline{V}}\sum_{j=1}^{3} Z(-\omega_j)[C_1^{(2)}(\overline{V}) + C_2^{(2)}(\omega_j)][1+Z(-\omega_j)G]^{-1}\Big\}. \tag{3.5.9}$$

We show plots for two types of mesoscopic conductors: a tunnel junction and a diffusive metal. In both cases it is assumed that there is no inelastic scattering,

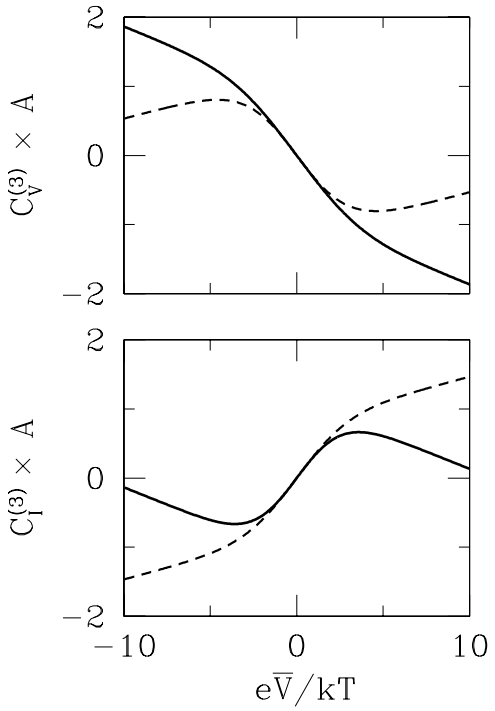

Figure 3-5. Same as Fig. 3-4, but now for a diffusive metal.

which is what makes the conductor mesoscopic. The plots correspond to global thermal equilibrium ($T_1 = T_2 = T$) and to a real and frequency-independent impedance $Z(\omega) \equiv Z$. We compare $C_I^{(3)} \equiv C_{III}^{(3)}$ with $C_V^{(3)} \equiv -C_{VVV}^{(3)}/Z^3$. (The minus sign is chosen so that $C_I^{(3)} = C_V^{(3)}$ at $T = 0$.)

For a tunnel junction one has

$$C_1^{(2)}(V) = GeV \coth \frac{eV}{2kT}, \quad C_1^{(3)}(V) = Ge^2V. \tag{3.5.10}$$

The third cumulant of current fluctuations in an isolated tunnel junction is temperature independent [11], but this is changed drastically by the electromagnetic environment [10]. Substitution of Eq. (3.5.10) into Eqs. (3.5.8) and (3.5.9) gives the curves plotted in Fig. 3-4 for $ZG = 0$ and $ZG = 1$. The slope $dC_V^{(3)}(\overline{V})/d\overline{V}$ becomes strongly temperature dependent and may even change sign when kT becomes larger than $e\overline{V}$. This is in qualitative agreement with the experiment of Reulet, Senzier, and Prober [14]. In Ref. [14] it is shown that Eq. (3.5.9) provides a quantitative description of the experimental data.

For a diffusive metal we substitute the known formulas for the second and

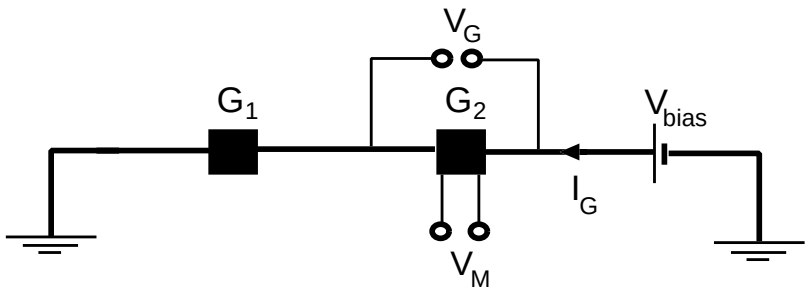

Figure 3-6. Four-terminal voltage measurement.

third cumulants without electromagnetic environment [12,13],

$$C_1^{(2)}(V) = \frac{1}{3}GeV\left(\coth p + 2/p\right), \tag{3.5.11}$$

$$C_1^{(3)}(V) = e^2GV\frac{p(1-26e^{2p}+e^{4p})-6(e^{4p}-1)}{15p(e^{2p}-1)^2}. \tag{3.5.12}$$

We have abbreviated $p = eV/2kT$. Plots for $ZG = 0$ and $ZG = 1$ are shown in Fig. 3-5. The diffusive metal is a bit less striking than a tunnel junction, since the third cumulant is already temperature dependent even in the absence of the electromagnetic environment. In the limit $ZG \to \infty$ we recover the result for $C_V^{(3)}$ obtained by Nagaev from the cascaded Langevin approach [27].

3.6 How to measure current fluctuations

In Fig. 3-4 we have plotted both current and voltage correlators, but only the voltage correlator has been measured [14]. At zero temperature of the macroscopic conductor there is no difference between the two, as follows from Eqs. (3.5.8) and (3.5.9): $C_{III}^{(3)} = -C_{VVV}^{(3)}/Z^3$ if $C_2^{(2)} = 0$, which is the case for a macroscopic conductor G_2 at $T_2 = 0$. For $T_2 \neq 0$ a difference appears that persists in the limit of a non-invasive measurement $Z \to 0$ [10]. Since V and I in the series circuit with a macroscopic G_2 are linearly related and linear systems are known to be completely determined by their response functions and their temperature, one could ask what it is that distinguishes the two measurements, or more practically: How would one measure $C_{III}^{(3)}$ instead of $C_{VVV}^{(3)}$?

To answer this question we slightly generalize the macroscopic conductor to a four-terminal, rather than two-terminal configuration, see Fig. 3-6. The voltage V_M over the extra pair of contacts is related to the current I_G through the series circuit by a cross impedance, $\partial V_M/\partial I_G = Z_{MG}$. The full impedance matrix $\mathbf{Z}$ is defined as in Eq. (3.2.1). For simplicity we take the zero-frequency limit. For this

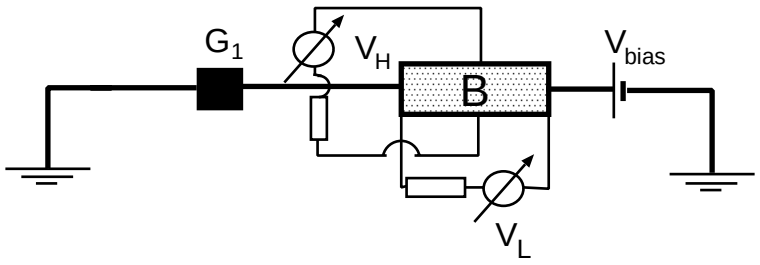

Figure 3-7. Hall bar that allows one to measure the voltage correlator $C_V^{(3)} \propto \langle\langle V_L^3 \rangle\rangle$ as well as the current correlator $C_I^{(3)} \propto \langle\langle V_H^3 \rangle\rangle$.

configuration the third cumulant $C^{(3)}_{V_M V_M V_M}$ of V_M is given by

$$\frac{C^{(3)}_{V_M V_M V_M}}{Z_{MG}^3} = C^{(3)}_{I_G I_G I_G} + \frac{Z_{GM} + Z_{MG}}{2 Z_{GM}} \left(\frac{C^{(3)}_{V_G V_G V_G}}{Z_{GG}^3} - C^{(3)}_{I_G I_G I_G} \right). \tag{3.6.1}$$

It contains the correlator $\langle\langle \delta V_M(\omega) \delta V_G(\omega') \rangle\rangle = 2\pi\delta(\omega + \omega') C_{GM}$ of the voltage fluctuations over the two pairs of terminals of the macroscopic conductor, which according to the fluctuation-dissipation theorem (3.2.2) is given in the zero-frequency limit by

$$C_{GM} = kT_2 (Z_{GM} + Z_{MG}). \tag{3.6.2}$$

The correlator C_{GM} enters since $C^{(3)}_{V_M V_M V_M}$ depends on how thermal fluctuations in the measured variable V_M correlate with the thermal fluctuations of V_G which induce extra current noise in G_1.

We conclude from Eq. (3.6.1) that the voltage correlator $C^{(3)}_{V_M V_M V_M}$ becomes proportional to the current correlator $C^{(3)}_{I_G I_G I_G}$ if $Z_{GM} + Z_{MG} = 0$. This can be realized if V_M is the Hall voltage V_H in a weak magnetic field B. Then $Z_{MG} = -Z_{GM} = R_H$, with $R_H \propto |B|$ the Hall resistance. The magnetic field need only be present in the macroscopic conductor G_2, so it need not disturb the transport properties of the mesoscopic conductor G_1. If, on the other hand, V_M is the longitudinal voltage V_L, then $Z_{MG} = Z_{GM} = R_L$, with R_L the longitudinal resistance. The two-terminal impedance Z_{GG} is the sum of Hall and longitudinal resistances, $Z_{GG} = R_L + R_H$. So one has

$$C^{(3)}_{V_L V_L V_L} = \left(\frac{R_L}{R_L + R_H} \right)^3 C^{(3)}_{V_G V_G V_G}, \tag{3.6.3}$$

$$C^{(3)}_{V_H V_H V_H} = R_H^3 C^{(3)}_{I_G I_G I_G}. \tag{3.6.4}$$

One can generalize all this to an arbitrary measurement variable X that is linearly related to the current I_G through G_1. In a linear circuit the off-diagonal elements of the response tensor $\mathbf{Z}$ relating (X, V_G) to the conjugated sources are linked by Onsager-Casimir relations [20]. If X is even under time-reversal, then

$Z_{XG} = Z_{GX}$, while if X is odd, then $Z_{XG} = -Z_{GX}$. In the first case $C^{(3)}_{XXX} \propto C^{(3)}_{V_G V_G V_G}$, while in the second case $C^{(3)}_{XXX} \propto C^{(3)}_{I_G I_G I_G}$.

3.7 Environmental Coulomb blockade

The saddle-point approximation to the path integral (3.4.1) for a mesoscopic conductor G_1 in series with a macroscopic conductor G_2 (impedance Z) breaks down when the impedance at the characteristic frequency scale $\Lambda = 1/\max(\tau_1, \tau_2)$ discussed in section 3.4 is not small compared to the resistance quantum h/e^2. It can then react fast enough to affect the dynamics of the transfer of a single electron. These single-electron effects amount to a Coulomb blockade induced by the electromagnetic environment [4]. In our formalism they are accounted for by fluctuations around the saddle point of Eq. (3.4.1).

In Ref. [17] it has been found that the Coulomb blockade correction to the mean current calculated to leading order in Z is proportional to the second cumulant of current fluctuations in the isolated mesoscopic conductor ($Z = 0$). More recently, the Coulomb blockade correction to the second cumulant of current fluctuations has been found to be proportional to the third cumulant [18]. It was conjectured in Ref. [18] that this relation holds also for higher cumulants. Here we give a proof of this conjecture.

We show that at zero temperature and zero frequency the leading order Coulomb blockade correction to the n-th cumulant of current fluctuations is proportional to the voltage derivative of the $(n+1)$-th cumulant. To extract the environmental Coulomb blockade from the other effects of the environment we assume that Z vanishes at zero frequency, $Z(0) = 0$. The derivation is easiest in terms of the pseudo-probabilities discussed in Sec. 3.3.

According to Eq. (3.3.19), cumulant correlators of current have the generating functional

$$\mathcal{F}_{G_1+G_2}[\vec{\Phi} = (V, \varphi)] = \ln \int \mathcal{D}I \, e^{-i\int dt\, I\varphi} \, \mathcal{P}_{G_1+G_2}[V, I]. \tag{3.7.1}$$

Zero frequency current correlators are obtained from

$$\langle\langle I(0)^n \rangle\rangle_{G_1+G_2} = i^n \frac{\delta^n}{\delta[\varphi(0)]^n} \mathcal{F}_{G_1+G_2}[\vec{\Phi}]\Big|_{\varphi=0}. \tag{3.7.2}$$

We employ now Eq. (3.4.7) and expand $\mathcal{F}_{G_1+G_2}[\vec{\Phi}]$ to first order in Z,

$$\begin{aligned} \mathcal{F}_{G_1+G_2}[\vec{\Phi}] &= \mathcal{F}_{G_1}[\vec{\Phi}] - \frac{\int \mathcal{D}I \, e^{-i\int dt\, I\varphi} \int \frac{d\omega}{2\pi} Z(\omega) I(\omega) \frac{\delta}{\delta V(\omega)} \mathcal{P}_{G_1}[V, I]}{\int \mathcal{D}I \, e^{-i\int dt\, I\varphi} \, \mathcal{P}_{G_1}[V, I]} \\ &= \mathcal{F}_{G_1}[\vec{\Phi}] - i \int \frac{d\omega}{2\pi} Z(\omega) \frac{\delta^2}{\delta V(\omega) \delta\varphi(\omega)} \mathcal{F}_{G_1}[\vec{\Phi}]. \end{aligned} \tag{3.7.3}$$

The last equality holds since single derivatives of $\mathcal{F}_{G_1}[\vec{\Phi}]$ with respect to a variable at finite frequency vanish because of time-translation symmetry. Substitution into Eq. (3.7.2) gives

$$\langle\langle I(0)^n\rangle\rangle_{G_1+G_2} = \langle\langle I(0)^n\rangle\rangle_{G_1} - \int \frac{d\omega}{2\pi} Z(\omega) \frac{\delta}{\delta V(\omega)} \langle\langle I(\omega) I(0)^n\rangle\rangle_{G_1}, \tag{3.7.4}$$

which is what we had set out to prove.

3.8 Conclusion

In conclusion, we have presented a fully quantum mechanical derivation of the effect of an electromagnetic environment on current and voltage fluctuations in a mesoscopic conductor, going beyond an earlier study at zero temperature [9]. The results agree with those obtained from the cascaded Langevin approach [10], thereby providing the required microscopic justification.

From an experimental point of view, the nonlinear feedback from the environment is an obstacle that stands in the way of a measurement of the transport properties of the mesoscopic system. To remove the feedback it is not sufficient to reduce the impedance of the environment. One also needs to eliminate the mixing in of environmental thermal fluctuations. This can be done by ensuring that the environment is at a lower temperature than the conductor, but this might not be a viable approach for low-temperature measurements. We have proposed here an alternative method, which is to ensure that the measured variable changes sign under time reversal. In practice this could be realized by measuring the Hall voltage over a macroscopic conductor in series with the mesoscopic system.

The field theory developed here also provides for a systematic way to incorporate the effects of the Coulomb blockade which arise if the high-frequency impedance of the environment is not small compared to the resistance quantum. We have demonstrated this by generalizing to moments of arbitrary order a relation in the literature [17,18] for the leading-order Coulomb blockade correction to the first and second moment of the current. We refer to Ref. [19] for a renormalization group analysis of the Coulomb blockade corrections of higher order.

Appendix A: Derivation of the environmental action

To derive Eq. (3.3.10) we define a generating functional for the voltages $\mathbf{V} = (V_M, V_G)$ in the environmental circuit of Fig. 3-2,

$$\mathcal{Z}_e[\vec{\boldsymbol{Q}}] = \left\langle T_- e^{i\int dt\, [H+\boldsymbol{Q}^-(t)\boldsymbol{V}]} T_+ e^{-i\int dt\, [H+\boldsymbol{Q}^+(t)\boldsymbol{V}]} \right\rangle . \tag{A.1}$$

We have introduced sources $\boldsymbol{Q} = (Q_M, Q_G)$. Since the environmental Hamiltonian is quadratic, the generating functional is the exponential of a quadratic form in $\vec{\boldsymbol{Q}}$,

$$\mathcal{Z}_e[\vec{\boldsymbol{Q}}] = \exp\left(-\frac{i}{2}\int \frac{d\omega}{2\pi}\,\vec{\boldsymbol{Q}}^{\dagger}(\omega)\check{\boldsymbol{G}}(\omega)\vec{\boldsymbol{Q}}(\omega)\right). \tag{A.2}$$

The off-diagonal elements of the matrix $\check{\boldsymbol{G}}$ are determined by the impedance of the circuit,

$$i\frac{\delta^2}{\delta Q_\beta^{cl}(\omega')\delta Q_\alpha^{q*}(\omega)}\ln\mathcal{Z}_e\Big|_{\vec{Q}=0} = \frac{\delta}{\delta I_\beta(\omega')}\langle V_\alpha(\omega)\rangle = 2\pi\delta(\omega-\omega')Z_{\alpha\beta}(\omega). \tag{A.3}$$

The upper-diagonal (cl,cl) elements in the Keldysh space vanish for symmetry reasons ($\mathcal{Z}_e|_{Q^q=0} = 0$, cf. Ref. [21]). The lower-diagonal (q,q) elements are determined by the fluctuation-dissipation theorem (3.2.2),

$$\begin{aligned}-\frac{\delta^2}{\delta Q_\alpha^{q*}(\omega)\delta Q_\beta^{q*}(\omega')}\ln\mathcal{Z}_e\Big|_{\vec{Q}=0} &= \langle\delta V_\alpha(\omega)\delta V_\beta(\omega')\rangle \\ &= \pi\delta(\omega+\omega')\omega\coth\left(\frac{\omega}{2kT}\right)[Z_{\alpha\beta}(\omega)+Z^*_{\beta\alpha}(\omega)].\end{aligned} \tag{A.4}$$

Consequently we have

$$\check{\boldsymbol{G}}(\omega) = \begin{pmatrix} 0 & \boldsymbol{Z}^{\dagger}(\omega) \\ \boldsymbol{Z}(\omega) & -\frac{i}{2}\omega\coth\left(\frac{\omega}{2kT}\right)[\boldsymbol{Z}(\omega)+\boldsymbol{Z}^{\dagger}(\omega)] \end{pmatrix}. \tag{A.5}$$

The environmental action S_e is defined by

$$\mathcal{Z}_e[\vec{\boldsymbol{Q}}] = \int \mathcal{D}[\vec{\boldsymbol{\Phi}}_{\boldsymbol{G}}]\exp\left(-iS_e[\vec{\boldsymbol{Q}}_{\boldsymbol{M}},\vec{\boldsymbol{\Phi}}_{\boldsymbol{G}}] - i\vec{\boldsymbol{\Phi}}_{\boldsymbol{G}}\times\vec{\boldsymbol{Q}}_{\boldsymbol{G}}\right). \tag{A.6}$$

One can check that substitution of Eq. (3.3.10) into Eq. (A.6) yields the same $\mathcal{Z}_e$ as given by Eqs. (A.2) and (A.5).

Appendix B: Derivation of Eq. (3.3.14)

In the limit $R \to \infty$ a voltage measurement in the circuit of Fig. 3-8 corresponds to a voltage measurement at contacts M and M' of the circuit C. We obtain the generating functional $\mathcal{Z}_V$ of this voltage measurement from Eq. (3.3.9). The influence functional is now due to C and it equals the generating functional $\mathcal{Z}_I$ of a current measurement at contacts M and M' of C. From Eq. (3.3.10) with $Z_{MM} = Z_{GG} = -Z_{MG} = -Z_{GM} = R$ we find in the limit $R \to \infty$ that the environmental action takes the simple form $S_e[\vec{Q}_M,\vec{\Phi}_G] = \vec{\Phi}\times\vec{Q}$, with the cross-product defined in Eq. (3.3.15). Consequently, we have

$$\mathcal{Z}_V[\vec{Q}] = \int \mathcal{D}[\vec{\Phi}]\,e^{-i\vec{\Phi}\times\vec{Q}}\,\mathcal{Z}_I[\vec{\Phi}]. \tag{B.1}$$

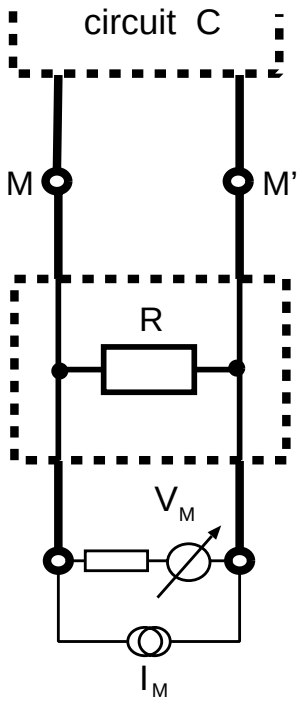

Figure 3-8. Circuit to relate voltage to current measurements.

This equation relates the generating functionals of current and voltage measurements at any pair of contacts of a circuit.

Appendix C: Derivation of Eq. (3.4.1)

To derive Eq. (3.4.1) from Eq. (3.3.9) we need the environmental action S_e of the circuit shown in Fig. 3-3. The impedance matrix is

$$\boldsymbol{Z} = \frac{1}{R_1+R_2+R_3}\begin{pmatrix} R_1(R_2+R_3) & -R_1R_2 & -R_1(R_2+R_3) & -R_1R_3 \\ -R_1R_2 & R_2(R_1+R_3) & -R_1R_2 & -R_2R_3 \\ -R_1(R_2+R_3) & -R_1R_2 & R_1(R_2+R_3) & -R_1R_3 \\ -R_1R_3 & -R_2R_3 & -R_1R_3 & R_3(R_1+R_2) \end{pmatrix}. \tag{C.1}$$

We seek the limit $R_1, R_2, R_3 \to \infty$. The environmental action (3.3.10) takes the form

$$S_e[\vec{\boldsymbol{Q}}_{\boldsymbol{M}}, \vec{\boldsymbol{\Phi}}_{\boldsymbol{G}}] = \vec{\Phi}_{G_1} \times \vec{Q}_{M_1} + \vec{\Phi}_{G_1} \times \vec{Q}_{M_2} + \vec{\Phi}_{G_2} \times \vec{Q}_{M_2}. \tag{C.2}$$

Substitution into Eq. (3.3.9) gives $\mathcal{Z}_{VV}$. Employing Eq. (3.3.14) to obtain $\mathcal{Z}_{VI}$ from $\mathcal{Z}_{VV}$ we arrive at Eq. (3.4.1).

Bibliography

[1] E. Ben-Jacob, E. Mottola, and G. Schön, Phys. Rev. Lett. **51**, 2064 (1983).

[2] G. Schön, Phys. Rev. B **32**, 4469 (1985).

[3] M. H. Devoret, D. Esteve, H. Grabert, G.-L. Ingold, H. Pothier, and C. Urbina, Phys. Rev. Lett. **64**, 1824 (1990).

[4] G.-L. Ingold and Yu. V. Nazarov, in *Single Charge Tunneling*, edited by H. Grabert and M. H. Devoret, NATO ASI Series B294 (Plenum, New York, 1992).

[5] H. Lee and L. S. Levitov, Phys. Rev. B **53**, 7383 (1996).

[6] Sh. Kogan, *Electronic Noise and Fluctuations in Solids* (Cambridge University, Cambridge, 1996).

[7] Ya. M. Blanter and M. Büttiker, Phys. Rep. **336**, 1 (2000).

[8] C. W. J. Beenakker and C. Schönenberger, Physics Today **56** (5), 37 (2003).

[9] M. Kindermann, Yu. V. Nazarov, and C. W. J. Beenakker, Phys. Rev. Lett. (in press).

[10] C. W. J. Beenakker, M. Kindermann, and Yu. V. Nazarov, Phys. Rev. Lett. **90**, 176802 (2003).

[11] L. S. Levitov and M. Reznikov, cond-mat/0111057.

[12] D. B. Gutman and Y. Gefen, cond-mat/0201007.

[13] K. E. Nagaev, Phys. Rev. B **66**, 075334 (2002).

[14] B. Reulet, J. Senzier, and D. E. Prober, cond-mat/0302084; B. Reulet, private communication.

[15] Yu. V. Nazarov, Ann. Phys. (Leipzig) **8**, 507 (1999).

[16] Yu. V. Nazarov and M. Kindermann, cond-mat/0107133.

[17] A. Levy Yeyati, A. Martin-Rodero, D. Esteve, and C. Urbina, Phys. Rev. Lett. **87**, 046802 (2001).

[18] A. V. Galaktionov, D. S. Golubev, and A. D. Zaikin, cond-mat/0212494.

[19] M. Kindermann and Yu. V. Nazarov, cond-mat/0304078.

[20] H. B. G. Casimir, Rev. Mod. Phys. **17**, 343 (1945).

[21] A. Kamenev, in *Strongly Correlated Fermions and Bosons in Low-Dimensional Disordered Systems*, edited by I. V. Lerner, B. L. Altshuler, V. I. Fal'ko, and T. Giamarchi, NATO Science Series II Vol. 72 (Kluwer, Dordrecht, 2002); cond-mat/0109316.

[22] M. Kindermann and Yu. V. Nazarov, in *Quantum Noise*, edited by Yu. V. Nazarov and Ya. M. Blanter, NATO Science Series II Vol. 97 (Kluwer, Dordrecht, 2003); cond-mat/0303590.

[23] W. Belzig and Yu. V. Nazarov, Phys. Rev. Lett. **87**, 197006 (2001).

[24] U. Gavish, Y. Imry, L. Levinson, and B. Yurke, in *Quantum Noise*, edited by Yu. V. Nazarov and Ya. M. Blanter, NATO Science Series II Vol. 97 (Kluwer, Dordrecht, 2003); cond-mat/0211646.

[25] L. S. Levitov and G. B. Lesovik, JETP Lett. **58**, 230 (1993).

[26] L. S. Levitov, H. Lee, and G. B. Lesovik, J. Math. Phys. **37**, 4845 (1996).

[27] K. E. Nagaev, cond-mat/0302008.

4 Distribution of voltage fluctuations in a current-biased conductor

The current–voltage or charge–phase duality plays a central role in the theory of single-electron tunneling through tunnel junctions of small capacitance [1]. At the two extremes one has a voltage-biased junction (in which the voltage is kept fixed by a source with zero internal resistance, while the current fluctuates) and a current-biased junction (fixed current from a source with infinite internal resistance, fluctuating voltage). The two current–voltage characteristics are entirely different. In the current-biased case the Coulomb blockade introduces a jump in the voltage at low current [2], while in the voltage-biased case the Coulomb blockade is inoperative.

Quantum mechanically, the duality appears because current I and voltage V are noncommuting operators [3]. This is conveniently expressed by the canonical commutator $[\Phi, Q] = ie$ of the transferred charge $Q = \int_0^\tau I(t)dt$ and accumulated phase $\Phi = (e/\hbar)\int_0^\tau V(t)dt$ (in a given detection time τ). Moments of charge and phase determine the measured correlators of current and voltage, respectively [4].

While all moments of Q in a voltage-biased conductor are known ([5]), the dual problem (moments of Φ under current bias) has only been studied for the first two moments [6, 7]. In the absence of Coulomb-blockade effects, the first two moments in the dual problems are simply related by rescaling $I(t) \to V(t) \times G$ (with G the conductance). One might surmise that this linear rescaling carries over to higher moments, so that the dual problems are trivially related in the absence of the Coulomb blockade. However, the rescaling (as derived for example in Ref. [8]) follows from a Langevin approach that is suspect for moments higher than the second [9, 10] — so that one might expect a more complex duality relation.

The resolution of this issue is particularly urgent in view of recent proposals to measure the third moment of shot noise in a mesoscopic conductor [9–11]. Does it matter if the circuit is voltage biased or current biased, or can one relate one circuit to the other by a linear rescaling? That is the question addressed in this chapter.

We will demonstrate that, quite generally, the rescaling breaks down beyond the second moment. We calculate all moments of the phase (hence all correlators of the voltage) for the simplest case of a single-channel conductor (transmission probability Γ) in the zero-temperature limit. In this case the charge $Q \equiv qe$ for

voltage bias $V_0 \equiv h\phi_0/e\tau$ is known to have the binomial distribution [5]

$$P_{\phi_0}(q) = \binom{\phi_0}{q}\Gamma^q(1-\Gamma)^{\phi_0-q}. \tag{4.0.1}$$

We find that the dual distribution of phase $\Phi \equiv 2\pi\phi$ for current bias $I_0 \equiv eq_0/\tau$ is the Pascal distribution [12]

$$P_{q_0}(\phi) = \binom{\phi-1}{q_0-1}\Gamma^{q_0}(1-\Gamma)^{\phi-q_0}. \tag{4.0.2}$$

(Both q and ϕ are integers for integer ϕ_0 and q_0.)

In the more general case we have found that the distributions of charge and phase are related in a remarkably simple fashion for $q, \phi \to \infty$:

$$\ln P_q(\phi) = \ln P_\phi(q) + \mathcal{O}(1). \tag{4.0.3}$$

(The remainder $\mathcal{O}(1)$ equals $\ln(q/\phi)$ in the zero-temperature limit.) This manifestation of charge-phase duality, valid with logarithmic accuracy, holds for any number of channels and any model of the conductor. Before presenting the derivation we give an intuitive physical interpretation.

The binomial distribution (4.0.1) for voltage bias has the interpretation [5] that electrons hit the barrier with frequency eV_0/h and are transmitted independently with probability Γ. For current bias the transmission rate is fixed at I_0/e. Deviations due to the probabilistic nature of the transmission process are compensated for by an adjustment of the voltage drop over the barrier. If the transmission rate is too low, the voltage $V(t)$ rises so that electrons hit the barrier with higher frequency. The number of transmission attempts ("trials") in a time τ is given by $(e/h)\int_0^\tau V(t)dt \equiv \phi$. The statistics of the accumulated phase ϕ is therefore given by the statistics of the number of trials needed for $I_0\tau/e$ successful transmission events. This stochastic process has the Pascal distribution (4.0.2).

Starting point of our derivation is a generalization to time-dependent bias voltage $V(t) = (\hbar/e)\dot{\Phi}(t)$ of an expression in the literature [5, 13] for the generating functional $\mathcal{Z}[\Phi(t), \chi(t)]$ of current fluctuations:

$$\begin{aligned}\mathcal{Z}[\Phi,\chi] = \Big\langle \overleftarrow{\mathrm{T}} \exp\Big\{\frac{i}{e}\int dt[\Phi(t) + \tfrac{1}{2}\chi(t)]\hat{I}(t)\Big\} \\ \times \overrightarrow{\mathrm{T}} \exp\Big\{\frac{i}{e}\int dt[-\Phi(t) + \tfrac{1}{2}\chi(t)]\hat{I}(t)\Big\}\Big\rangle .\end{aligned} \tag{4.0.4}$$

(The notation $\overrightarrow{T}(\overleftarrow{T})$ denotes time-ordering of the exponentials in ascending (descending) order.) Functional derivatives of the Keldysh action $\ln\mathcal{Z}$ with respect to $\chi(t)/e$ produce cumulant correlators of the current operator $\hat{I}(t)$ to any order desired. To make the transition from voltage to current bias we introduce

a second conductor B in series with the mesoscopic conductor A (see Fig. 4-1). The generating functional $\mathcal{Z}_{A+B}$ of current fluctuations in the circuit is a (path integral) convolution of $\mathcal{Z}_A$ and $\mathcal{Z}_B$,

$$\mathcal{Z}_{A+B}[\Phi,\chi] = \int \mathcal{D}\Phi_1 \mathcal{D}\chi_1 \, \mathcal{Z}_A[\Phi_1,\chi_1]\mathcal{Z}_B[\Phi-\Phi_1,\chi-\chi_1]. \tag{4.0.5}$$

One can understand this expression as the average over fluctuating phases Φ_1, χ_1 at the node of the circuit shared by both conductors.

In general the functional dependence of $\mathcal{Z}_A, \mathcal{Z}_B$ is rather complicated and non-local in time, but we have found an interesting and tractable low-frequency regime: The non-locality may be disregarded for sufficiently slow realizations of the fluctuating phases. In this regime the functional $\mathcal{Z}$ can be expressed in terms of a function S,

$$\ln \mathcal{Z}[\Phi(t),\chi(t)] = \int dt \, S(\dot{\Phi}(t),\chi(t)). \tag{4.0.6}$$

The path integral (4.0.5) can be taken in saddle-point approximation, with the result

$$S_{A+B}(\dot{\Phi},\chi) = S_A(\dot{\Phi}_s,\chi_s) + S_B(\dot{\Phi}-\dot{\Phi}_s,\chi-\chi_s). \tag{4.0.7}$$

Here $\dot{\Phi}_s$ and χ_s stand for the (generally complex) values of $\dot{\Phi}_1$ and χ_1 at the saddle point (where the derivatives with respect to these phases vanish).

The validity of the low-frequency and saddle-point approximations depends on two time scales. The first time scale $\tau_1 = \min(\hbar/eV, \hbar/kT)$ (with T the temperature) sets the width of current pulses associated with the transfer of individual electrons. The second time scale $\tau_2 = e/I$ sets the spacing of the pulses. Let ω be the characteristic frequency of a particular realization of the fluctuating phase. For the low-frequency approximation we require $\omega\tau_1 \ll 1$ and for the saddle-point approximation $\omega\tau_2 \ll 1$. Both conditions are satisfied if frequencies greater than $\Omega_c = \min(1/\tau_1, 1/\tau_2)$ do not contribute to the path integral. To provide this cut-off we assume that $|Z(\omega)| \ll \hbar/e^2$ at frequencies $\omega \gtrsim \Omega_c$. The small high-frequency impedance acts as a "mass term" in the Keldysh action, suppressing high-frequency fluctuations. The low-frequency impedance can have any value. Since the frequency dependence of $Z(\omega)$ is typically on scales much below Ω_c, it can be readily accounted for within the range of validity of our approximations.

Eqs. (4.0.6) and (4.0.7) are quite general and now we apply them to the specific circuit of Fig. 4-1. We assume that the mesoscopic conductor A (conductance G) is in series with a macroscopic conductor B with frequency dependent impedance $Z(\omega)$. We denote the zero-frequency limit by $Z(0) \equiv Z_0 \equiv z_0 h/e^2$. The circuit is driven by a voltage source with voltage V_0. Both the voltage drop V at the mesoscopic conductor and the current I through the conductor fluctuate in time for finite Z_0, with averages $\bar{I} = V_0 G(1+Z_0G)^{-1}$, $\overline{V} = V_0(1+Z_0G)^{-1}$. Voltage bias corresponds to $Z_0G \ll 1$ and current bias to $Z_0G \gg 1$, with $I_0 = V_0/Z_0$ the imposed current.

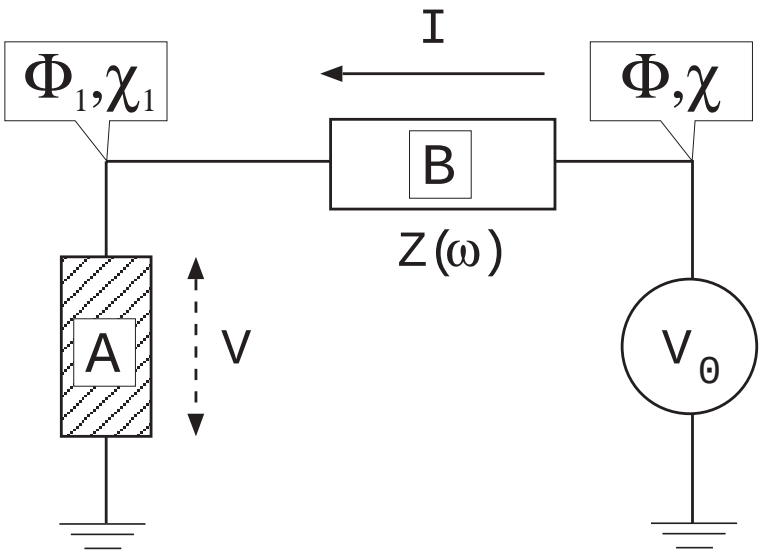

Figure 4-1. Mesoscopic conductor (shaded) in a circuit containing a voltage source V_0 and series impedance $Z(\omega)$. Both the current I through the circuit and the voltage drop V over the conductor may fluctuate in time. The dual problems contrasted here are: voltage bias ($Z \to 0$, fixed $V = V_0$, fluctuating I) and current bias ($Z \to \infty$, fixed $I = V_0/Z$, fluctuating V). The phases Φ, χ appearing in Eq. (4.0.5) are indicated.

We assume that the temperature of the entire circuit is sufficiently low ($kT \ll e\overline{V}$) to neglect thermal noise relative to shot noise. (See Ref. [14] for the effects of a finite temperature of mesoscopic conductor and/or series impedance.) We will also restrict ourselves to frequencies below the inverse RC-time of the circuit, where $Z(\omega) \approx Z_0$. The low-temperature, low-frequency Keldysh action of the external impedance is simply $S_B(\dot{\Phi}, \chi) = i\chi\dot{\Phi}/2\pi z_0$, while the action S_A of the mesoscopic conductor is given by [5]

$$S_A(\dot{\Phi}, \chi) = \frac{\dot{\Phi}}{2\pi} S(i\chi), \quad S(\xi) = \sum_{n=1}^{N} \ln[1 + (e^{\xi} - 1)T_n]. \tag{4.0.8}$$

The T_n's are the transmission eigenvalues, with $\sum_n T_n = Gh/e^2 \equiv g$ the dimensionless conductance.

We seek the cumulant generating function of charge

$$\mathcal{F}(\xi) = \ln\left(\sum_{q=0}^{\infty} e^{q\xi} P(q)\right) = \sum_{p=1}^{\infty} \langle\langle q^p \rangle\rangle \frac{\xi^p}{p!}, \tag{4.0.9}$$

where $\langle\langle q^p \rangle\rangle$ is the p-th cumulant of the charge transferred during the time interval τ. It is related to the Keldysh action (4.0.7) by

$$\mathcal{F}(\xi) = \tau S_{A+B}(eV_0/\hbar, -i\xi). \tag{4.0.10}$$

We also require the cumulant generating function of phase, $\mathcal{G}(\xi)$. Since $V = V_0 - Z_0 I$ (in the absence of thermal noise from the external impedance), it is related to $\mathcal{F}(\xi)$ by a change of variables (from q to $\phi = \phi_0 - q z_0$). The relation is

$$\mathcal{G}(\xi) = \sum_{p=1}^{\infty} \langle\langle \phi^p \rangle\rangle \frac{\xi^p}{p!} = \phi_0 \xi + \mathcal{F}(-z_0 \xi). \tag{4.0.11}$$

In the limit $Z_0 \to 0$ of voltage bias the saddle point of the Keldysh action is at $\dot{\Phi}_s = \dot{\Phi}$, $\chi_s = \chi$, and from Eqs. (4.0.7), (4.0.9), and (4.0.11) one recovers the results of Ref. [5]: The cumulant generating function $\mathcal{F}_0(\xi) = \tau S_A(eV_0/\hbar, -i\xi) = \phi_0 S(\xi)$ and the corresponding probability distribution

$$P_{\phi_0}(q) = \lim_{x \to 0} \frac{1}{q!} \frac{d^q}{dx^q} \prod_{n=1}^{N} [1 + (x-1)T_n]^{\phi_0}. \tag{4.0.12}$$

The parameter $\phi_0 = eV_0\tau/h$ is the number of attempted transmissions per channel, assumed to be an integer $\gg 1$. The first few cumulants are $\langle q \rangle_0 = \phi_0 g$, $\langle\langle q^2 \rangle\rangle_0 = \phi_0 \sum_n T_n(1-T_n)$, $\langle\langle q^3 \rangle\rangle_0 = \phi_0 \sum_n T_n(1-T_n)(1-2T_n)$. In the single-channel case ($N = 1$, $T_1 \equiv \Gamma$) the distribution (4.0.12) has the binomial form (4.0.1).

After these preparations we are now ready to generalize all of this to finite Z_0, and in particular to derive the dual distribution of phase (4.0.2) under current bias. The key equation that allows us to do that follows directly from Eqs. (4.0.7) and (4.0.10):

$$\mathcal{F}(\xi) = \frac{\phi_0}{z_0}[\xi - \sigma(\xi)], \quad \sigma + z_0 S(\sigma) = \xi. \tag{4.0.13}$$

The implicit function $\sigma(\xi)$ (which determines the saddle point of the Keldysh action) provides the cumulant generating function of charge $\mathcal{F}$ for arbitrary series resistance $z_0 = (e^2/h)Z_0$. One readily checks that $\mathcal{F}(\xi) \to \phi_0 S(\xi)$ in the limit $z_0 \to 0$, as it should.

By expanding Eq. (4.0.13) in powers of ξ we obtain a relation between the cumulants $\langle\langle q^p \rangle\rangle$ of charge at $Z_0 \neq 0$ and the cumulants $\langle\langle q^p \rangle\rangle_0$ at $Z_0 = 0$. The Langevin approach discussed in the introduction predicts that the fluctuations are rescaled by a factor $1 + z_0 g$ as a result of the series resistance. Indeed, to second order we find $\langle\langle q^2 \rangle\rangle = (1 + z_0 g)^{-3} \langle\langle q^2 \rangle\rangle_0$, in agreement with Ref. [8]. However, if we go to higher cumulants we find that other terms appear, which can not be incorporated by any rescaling. For example, Eq. (4.0.13) gives for the third cumulant

$$\langle\langle q^3 \rangle\rangle = \frac{\langle\langle q^3 \rangle\rangle_0}{(1 + z_0 g)^4} - \frac{3 z_0 g}{(1 + z_0 g)^5} \frac{\left(\langle\langle q^2 \rangle\rangle_0\right)^2}{\langle q \rangle_0}. \tag{4.0.14}$$

The first term on the the right-hand-side has the expected scaling form, but the second term does not. This is generic for $p \geq 3$: $\langle\langle q^p \rangle\rangle = (1 + z_0 g)^{-p-1} \langle\langle q^p \rangle\rangle$ plus a nonlinear (rational) function of lower cumulants [15]. All terms are of the

same order of magnitude in $z_0 g$, so one can not neglect the nonlinear terms. The Langevin approach ignores the nonlinear feedback that causes the mixing in of lower cumulants. This deficiency can be corrected, see Ref. [14].

Turning now to the limit $z_0 g \to \infty$ of current bias, we see from Eq. (4.0.13) that $\mathcal{F} \to \mathcal{F}_\infty$ with

$$\mathcal{F}_\infty(\xi) = q_0 \xi - q_0 S^{\rm inv}(\xi/z_0) \tag{4.0.15}$$

defined in terms of the functional inverse $S^{\rm inv}$ of S. The parameter $q_0 = \phi_0/z_0 = I_0\tau/e$ (assumed to be an integer $\gg 1$) is the number of charges transferred by the imposed current I_0 in the detection time τ. Transforming from charge to phase variables by means of Eq. (4.0.11), we find that $\mathcal{G} \to \mathcal{G}_\infty$ with

$$\mathcal{G}_\infty(\xi) = -q_0 S^{\rm inv}(-\xi). \tag{4.0.16}$$

In the single-channel case Eq. (4.0.16) reduces to $\mathcal{G}_\infty(\xi) = -q_0 \ln[1+\Gamma^{-1}(e^{-\xi}-1)]$, corresponding to the Pascal distribution (4.0.2). The first three cumulants are $\langle\phi\rangle = q_0/\Gamma$, $\langle\langle\phi^2\rangle\rangle = (q_0/\Gamma^2)(1-\Gamma)$, $\langle\langle\phi^3\rangle\rangle = (q_0/\Gamma^3)(1-\Gamma)(2-\Gamma)$.

For the general multi-channel case a simple expression for $P_{q_0}(\phi)$ can be obtained in the ballistic limit (all T_n's close to 1) and in the tunneling limit (all T_n's close to 0). In the ballistic limit one has $\mathcal{G}_\infty(\xi) = q_0\xi/N + q_0(N-g)(e^{\xi/N} - 1)$, corresponding to a Poisson distribution in the discrete variable $N\phi - q_0 = 0, 1, 2, \ldots$. In the tunneling limit $\mathcal{G}_\infty(\xi) = -q_0 \ln(1 - \xi/g)$, corresponding to a chi-square distribution $P_{q_0}(\phi) \propto \phi^{q_0-1} e^{-g\phi}$ in the continuous variable $\phi > 0$. In contrast, the charge distribution $P_{\phi_0}(q)$ is Poissonian both in the tunneling limit (in the variable q) and in the ballistic limit (in the variable $N\phi_0 - q$).

For large q_0 and ϕ, when the discreteness of these variables can be ignored, we may calculate $P_{q_0}(\phi)$ from $\mathcal{G}_\infty(\xi)$ in saddle-point approximation. If we also calculate $P_{\phi_0}(q)$ from $\mathcal{F}_0(\xi)$ in the same approximation (valid for large ϕ_0 and q), we find that the two distributions have a remarkably similar form:

$$P_{\phi_0}(q) = N_{\phi_0}(q) \exp[\tau\Sigma(2\pi\phi_0/\tau, q/\tau)], \tag{4.0.17}$$

$$P_{q_0}(\phi) = N_{q_0}(\phi) \exp[\tau\Sigma(2\pi\phi/\tau, q_0/\tau)]. \tag{4.0.18}$$

The same exponential function

$$\Sigma(x, y) = S_A(x, -i\xi_s) - y\xi_s \tag{4.0.19}$$

appears in both distributions (with ξ_s the location of the saddle point). The pre-exponential functions N_{ϕ_0} and N_{q_0} are different, determined by the Gaussian integration around the saddle point.

Since these two functions vary only algebraically, rather than exponentially, we conclude that Eq. (4.0.3) holds with the remainder $\mathcal{O}(1) = \ln(q/\phi)$ obtained by evaluating $\ln[2\pi(\partial^2\Sigma/\partial x^2)^{1/2}(\partial^2\Sigma/\partial y^2)^{-1/2}]$ at $x = 2\pi\phi/\tau$, $y = q/\tau$.

The distributions of charge and phase are compared graphically in Fig. 4-2, in the tunneling limit $\Gamma \ll 1$. We use the rescaled variable $x = q/\langle q\rangle$ for the charge

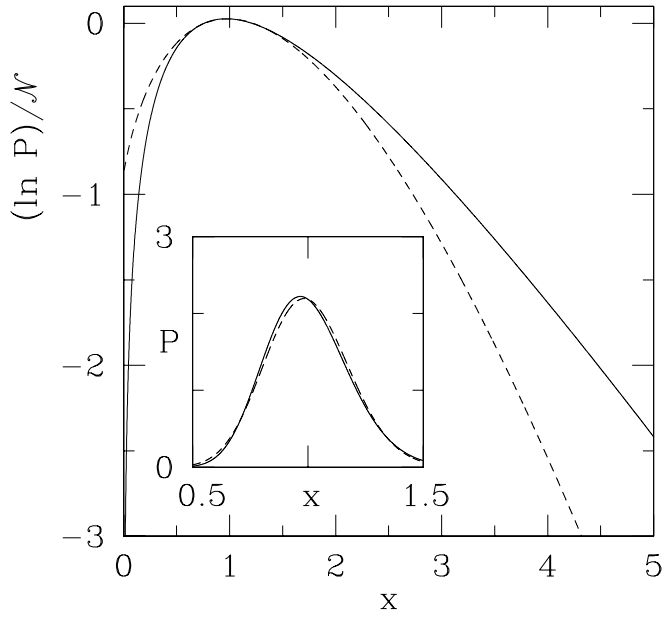

Figure 4-2. Comparison of the distributions of charge (dashed curve, with $x = q/\langle q\rangle$) and of phase (solid curve, with $x = \phi/\langle\phi\rangle$), calculated from Eqs. (4.0.20) and (4.0.21) for $\mathcal{N} = q_0 = \phi_0\Gamma = 30$ transferred charges in the tunneling limit $\Gamma \ll 1$. The main plot emphasizes the non-Gaussian tails on a semi-logarithmic scale, the inset shows on a linear scale that the Gaussian body of the distributions coincides.

and $x = \phi/\langle\phi\rangle$ for the phase, and take the same mean number $\mathcal{N} = q_0 = \phi_0\Gamma$ of transferred charges in both cases. We plot the asymptotic large-$\mathcal{N}$ form of the distributions,

$$P_{\text{charge}}(x) = (\mathcal{N}/2\pi)^{1/2} x^{-1/2} e^{\mathcal{N}(x-1-x\ln x)}, \tag{4.0.20}$$

$$P_{\text{phase}}(x) = (\mathcal{N}/2\pi)^{1/2} x^{-1} e^{\mathcal{N}(1-x+\ln x)}, \tag{4.0.21}$$

corresponding to the Poisson and chi-square distribution, respectively. Since the first two moments are the same, the difference appears in the non-Gaussian tails. The difference should be readily visible as a factor of two in a measurement of the third cumulant: $\langle\langle x^3\rangle\rangle = \mathcal{N}^{-2}$ for the charge and $\langle\langle x^3\rangle\rangle = 2\mathcal{N}^{-2}$ for the phase.

In summary, we have demonstrated theoretically that electrical noise becomes intrinsically different when the conductor is current biased rather than voltage biased. While the second moments can be related by a rescaling with the conductance, the third and higher moments can not. From a fundamental point of view, the limit of full current bias is of particular interest. The counterpart

of the celebrated binomial distribution of transferred charge [5] turns out to be the Pascal distribution of phase increments.

Bibliography

[1] G.-L. Ingold and Yu. V. Nazarov, in *Single Charge Tunneling*, edited by H. Grabert and M. H. Devoret, NATO ASI Series B294 (Plenum, New York, 1992).

[2] D. V. Averin and K. K. Likharev, in *Mesoscopic Phenomena in Solids*, edited by B. L. Altshuler, P. A. Lee, and R. A. Webb (Elsevier, Amsterdam, 1991).

[3] G. Schön and A. D. Zaikin, Phys. Rep. **198**, 237 (1990).

[4] For background reading on noise we refer to: C. W. J. Beenakker and C. Schönenberger, Physics Today, May 2003: p. 37. We summarize a few basic facts. The low-frequency noise spectral densities of current and voltage (also known as "noise power") are defined by $P_I = \int_{-\infty}^{\infty} dt\, \langle \delta I(0) \delta I(t) \rangle$, $P_V = \int_{-\infty}^{\infty} dt\, \langle \delta V(0) \delta V(t) \rangle$. They are given, respectively, by the second moments of charge and phase fluctuations in the limit of infinite detection time: $P_I = \lim_{\tau\to\infty} \tau^{-1} \langle \delta Q^2 \rangle$, $P_V = (\hbar/e)^2 \lim_{\tau\to\infty} \tau^{-1} \langle \delta \Phi^2 \rangle$. Third moments of δQ and $\delta\Phi$ are similarly related to third order correlators of δI and δV. For example, $\int dt \int dt'\, \langle \delta I(0) \delta I(t) \delta I(t') \rangle = \lim_{\tau\to\infty} \tau^{-1} \langle \delta Q^3 \rangle$. To fourth order and higher the relation holds for the cumulants, rather than for the moments themselves, because only the cumulants scale linearly with τ. The first four cumulants are related to the moments by $\langle\langle Q \rangle\rangle = \langle Q \rangle$, $\langle\langle Q^2 \rangle\rangle = \langle \delta Q^2 \rangle$, $\langle\langle Q^3 \rangle\rangle = \langle \delta Q^3 \rangle$, $\langle\langle Q^4 \rangle\rangle = \langle \delta Q^4 \rangle - 3 \langle \delta Q^2 \rangle^2$.

[5] L. S. Levitov and G. B. Lesovik, JETP Lett. **58**, 230 (1993); cond-mat/9401004; L. S. Levitov, H. Lee, and G. B. Lesovik, J. Math. Phys. **37**, 4845 (1996).

[6] E. Ben-Jacob, E. Mottola, and G. Schön, Phys. Rev. Lett. **51**, 2064 (1983); G. Schön, Phys. Rev. B **32**, 4469 (1985).

[7] H. Lee and L. S. Levitov, Phys. Rev. B **53**, 7383 (1996).

[8] Ya. M. Blanter and M. Büttiker, Phys. Rep. **336**, 1 (2000). The effect of a series resistance on the noise power is discussed in § 2.5.

[9] D. B. Gutman and Y. Gefen, cond-mat/0201007; D. B. Gutman, Y. Gefen, and A. D. Mirlin, cond-mat/0210076.

[10] K. E. Nagaev, Phys. Rev. B **66**, 075334 (2002); K. E. Nagaev, P. Samuelsson, and S. Pilgram, Phys. Rev. B **66**, 195318 (2002).

[11] L. S. Levitov and M. Reznikov, cond-mat/0111057.

[12] The Pascal distribution $P(m) = \binom{m-1}{M-1}\Gamma^M(1-\Gamma)^{m-M}$ is also called the "binomial waiting-time distribution", since it gives the probability of the number m of independent trials (with success probability Γ) that one has to wait until the M-th success. It is related to the negative-binomial distribution $P(n) = \binom{n+M-1}{n}\Gamma^M(1-\Gamma)^n$ by the displacement $n = m - M$.

[13] Yu. V. Nazarov, Ann. Phys. (Leipzig) **8**, 507 (1999); Yu. V. Nazarov and M. Kindermann, cond-mat/0107133.

[14] C. W. J. Beenakker, M. Kindermann, and Yu. V. Nazarov, Phys. Rev. Lett. **90**, 176802 (2003).

[15] We record the result for the fourth cumulant, obtained by expansion of Eq. (4.0.13) to order ξ^4: $\langle\langle q^4\rangle\rangle = (1+z_0g)^{-5}\mu_4 - 10z_0g(1+z_0g)^{-6}\mu_2\mu_3/\mu_1 + 15(z_0g)^2(1+z_0g)^{-7}\mu_2^3/\mu_1^2$, where we have abbreviated $\langle\langle q^p\rangle\rangle_0 = \mu_p$.

5 Temperature dependent third cumulant of tunneling noise

Shot noise of the electrical current was studied a century ago as a way to measure the fundamental unit of charge [1]. Today shot noise is used for this purpose in a wide range of contexts, including superconductivity and the fractional quantum Hall effect [2]. Already in the earliest work on vacuum tubes it was realized that thermal fluctuations of the current can mask the fluctuations due to the discreteness of the charge. In semiconductors, in particular, accurate measurements of shot noise are notoriously difficult because of the requirement to maintain a low temperature at a high applied voltage.

Until very recently, only the second cumulant of the fluctuating current was ever measured. The distribution of transferred charge is nearly Gaussian, because of the law of large numbers, so it is quite nontrivial to extract cumulants higher than the second. Much of the experimental effort was motivated by Levitov and Reznikov's prediction [3] that odd cumulants of the current through a tunnel junction should not be affected by the thermal noise that contaminates the even cumulants. This is a direct consequence of the Poisson statistics of tunneling events. The third cumulant should thus have the linear dependence on the applied voltage characteristic of shot noise, regardless of the ratio of voltage and temperature. In contrast, the second cumulant levels off at the thermal noise for low voltages.

The first experiments on the voltage dependence of the third cumulant of tunnel noise have now been reported [4]. The pictures are strikingly different from what was expected theoretically. The slope varies by an order of magnitude between low and high voltages, and for certain samples even changes sign. Such a behavior is expected for a diffusive conductor [5], but not for a tunnel junction. Although the data is still preliminary, it seems clear that an input of new physics is required for an understanding. It is the purpose of this chapter to provide such input.

We will show that the third cumulant of the measured noise (unlike the second cumulant [6]) is affected by the measurement circuit in a nonlinear way. The effect can be seen as a backaction of the electromagnetic environment [7]. We have found that the backaction persists even in the limit of zero impedance, when the measurement is supposed to be noninvasive. The temperature independent result for the third cumulant of tunneling noise is recovered only if the measurement circuit has both negligible impedance and negligible temperature.

The circuit is shown schematically in Fig. 5-1. Two resistors (impedances Z_1, Z_2 and temperatures T_1, T_2) are connected in series to a voltage source (voltage V_0). We will specialize later to the case that resistor 1 is a tunnel junction and

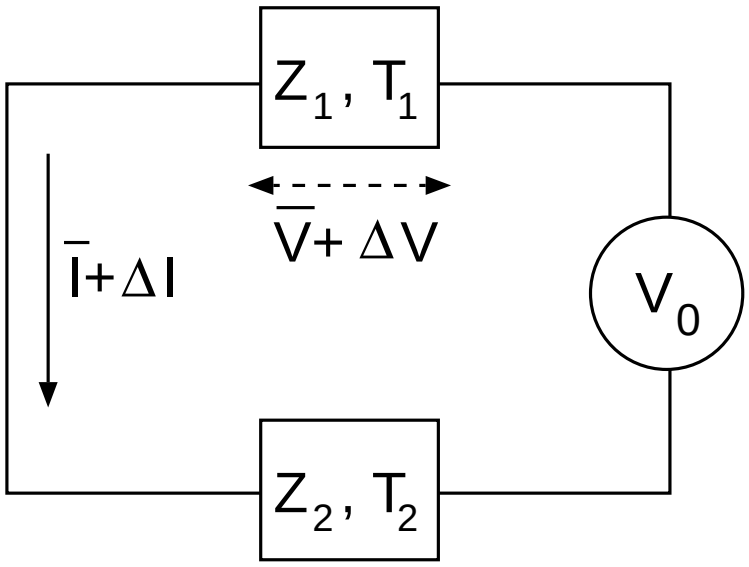

Figure 5-1. Two resistors in series with a voltage source. The fluctuating current and voltage are indicated.

that resistor 2 represents the macroscopic measurement circuit, but our main results hold for any two resistors. We disregard possible Coulomb blockade effects on fluctuations [8–10], which is justified if the impedances at frequencies of order $eV/\hbar$ are small compared to $\hbar/e^2$ [11].

We have calculated the temperature dependence of the third cumulant by two altogether different methods, the Keldysh formalism [12] and the Langevin approach [13]. The equivalence of the two methods has already been demonstrated for a single resistor in the absence of any measurement circuit [14]. Likewise, we have obtained the same results in both calculations of the backaction from the measurement. We choose to present the Langevin approach in this chapter, because it can be explained in elementary terms and provides an intuitive physical insight.

Starting point of the Langevin approach is the separation of the fluctuation ΔI_i of the current through resistor $i = 1, 2$ into an intrinsic fluctuation δI_i plus a term induced by a fluctuation ΔV_i of the voltage over the resistor: $\Delta I_i = \delta I_i + \Delta V_i/Z_i$. At low frequencies $\Delta I_1 = \Delta I_2 \equiv \Delta I$ and $\Delta V_1 = -\Delta V_2 \equiv \Delta V$. Upon substitution we arrive at the two equations

$$Z\Delta I = Z_1\delta I_1 + Z_2\delta I_2, \quad Z\Delta V = Z_1 Z_2(\delta I_2 - \delta I_1), \tag{5.0.1}$$

where $Z = Z_1 + Z_2$ is the total impedance of the circuit.

For simplicity we assume that Z_i is real and frequency independent in the frequency range of the measurement. All formulas have a straightforward generalization to complex $Z_i(\omega)$. We do not need to assume at this stage that the current-voltage characteristic of the resistors is linear. If it is not, then

one should simply replace $1/Z_i$ by the differential conductance evaluated at the mean voltage $\overline{V_i}$ over the resistor.

The mean voltages are given by $\overline{V_1} = (Z_1/Z)V_0 \equiv \overline{V}$ and $\overline{V_2} = V_0 - \overline{V}$. The intrinsic current fluctuations δI_i are driven by the fluctuating voltage $V_i = \overline{V_i} + \Delta V_i$, and therefore depend in a nonlinear way on ΔV. The nonlinearity has the effect of mixing in lower order cumulants of δI_i in the calculation of the p-th cumulant of ΔI, starting from $p = 3$.

Before addressing the case $p = 3$ we first consider $p = 2$, when all averages $\langle \cdots \rangle_{\overline{V}}$ can be performed at the mean voltage. At low frequencies one has

$$\langle \delta I_i(\omega) \delta I_i(\omega') \rangle_{\overline{V}} = 2\pi\delta(\omega + \omega') C_i^{(2)}(\overline{V_i}). \tag{5.0.2}$$

The noise power $C_i^{(2)}$ depends on the model for the resistor. We give two examples. In a macroscopic resistor the shot noise is suppressed by electron-phonon scattering and only thermal noise remains:

$$C_i^{(2)} = 2kT_i/Z_i \tag{5.0.3}$$

at temperature T_i, independent of the voltage. (The noise power is a factor of two larger if positive and negative frequencies are identified.) In a tunnel junction both thermal noise and shot noise coexist, according to [2]

$$C_i^{(2)}(\overline{V}_i) = (e\overline{V}_i/Z_i)\,\mathrm{cotanh}\,(e\overline{V}_i/2kT_i). \tag{5.0.4}$$

From Eq. (5.0.1) we compute the correlator

$$\langle \Delta X(\omega) \Delta Y(\omega') \rangle_{\overline{V}} = 2\pi\delta(\omega + \omega') S_{XY}(\overline{V}), \tag{5.0.5}$$

where X and Y can represent I or V. The result is

$$S_{II} = Z^{-2}[Z_1^2 C_1^{(2)}(\overline{V}) + Z_2^2 C_2^{(2)}(V_0 - \overline{V})], \tag{5.0.6a}$$

$$S_{VV} = Z^{-2}(Z_1 Z_2)^2 [C_1^{(2)}(\overline{V}) + C_2^{(2)}(V_0 - \overline{V})], \tag{5.0.6b}$$

$$S_{IV} = Z^{-2} Z_1 Z_2 [Z_2 C_2^{(2)}(V_0 - \overline{V}) - Z_1 C_1^{(2)}(\overline{V})]. \tag{5.0.6c}$$

Eq. (5.0.5) applies to a time independent mean voltage $\overline{V}$. For a time dependent perturbation $\nu(t)$ one has, to linear order,

$$\langle \Delta X(\omega) \Delta Y(\omega') \rangle_{\overline{V}+\nu} = \langle \Delta X(\omega) \Delta Y(\omega') \rangle_{\overline{V}} + \nu(\omega + \omega') \frac{d}{d\overline{V}} S_{XY}(\overline{V}). \tag{5.0.7}$$

We will use this equation, with $\nu = \Delta V$, to describe the effect of a fluctuating voltage over the resistors. This assumes a separation of time scales between ΔV and the intrinsic current fluctuations δI_i, so that we can first average over δI_i for given ΔV and then average over ΔV.

Turning now to the third cumulant, we first note that at fixed voltage the intrinsic current fluctuations δI_1 and δI_2 are uncorrelated, with third moment

$$\langle \delta I_i(\omega_1) \delta I_i(\omega_2) \delta I_i(\omega_3) \rangle_{\overline{V}} = 2\pi\delta(\omega_1 + \omega_2 + \omega_3) C_i^{(3)}(\overline{V_i}). \tag{5.0.8}$$

The spectral density $C_i^{(3)}$ vanishes for a macroscopic resistor. For a tunnel junction it has the temperature independent value [3]

$$C_i^{(3)}(\overline{V_i}) = e^2\overline{V_i}/Z_i = e^2\bar{I}, \tag{5.0.9}$$

with $\bar{I}$ the mean current.

We introduce the nonlinear feedback from the voltage fluctuations through the relation

$$\langle \Delta X_1 \Delta X_2 \Delta X_3 \rangle = \langle \Delta X_1 \Delta X_2 \Delta X_3 \rangle_{\overline{V}} + \sum_{\text{cyclic}} \langle \Delta X_j \Delta V(\omega_k + \omega_l) \rangle_{\overline{V}} \frac{d}{d\overline{V}} S_{X_k X_l}(\overline{V}). \tag{5.0.10}$$

The variable X_j stands for $I(\omega_j)$ or $V(\omega_j)$ and the sum is over the three cyclic permutations j,k,l of the indices $1,2,3$. These three terms account for the fact that the same voltage fluctuation ΔV that affects $S_{X_k X_l}$ also correlates with X_j, resulting in a cross-correlation.

Eq. (5.0.10) has the same form as the "cascaded average" through which Nagaev introduced a nonlinear feedback into the Langevin equation [13]. In that work the nonlinearity appears because the Langevin source depends on the electron density, which is itself a fluctuating quantity — but on a slower time scale, so the averages can be carried out separately, or "cascaded". In our case the voltage drop ΔV_i over the resistors is the slow variable, relative to the intrinsic current fluctuations δI_i.

Eq. (5.0.10) determines the current and voltage correlators

$$\langle \Delta X(\omega_1) \Delta Y(\omega_2) \Delta Z(\omega_3) \rangle = 2\pi\delta(\omega_1 + \omega_2 + \omega_3) C_{XYZ}(\overline{V}). \tag{5.0.11}$$

We find

$$C_{III} = Z^{-3}[Z_1^3 C_1^{(3)}(\overline{V}) + Z_2^3 C_2^{(3)}(V_0 - \overline{V})] + 3S_{IV}\frac{d}{d\overline{V}}S_{II}, \tag{5.0.12a}$$

$$C_{VVV} = Z^{-3}(Z_1 Z_2)^3[C_2^{(3)}(V_0 - \overline{V}) - C_1^{(3)}(\overline{V})] + 3S_{VV}\frac{d}{d\overline{V}}S_{VV}, \tag{5.0.12b}$$

$$C_{VVI} = Z^{-3}(Z_1 Z_2)^2[Z_1 C_1^{(3)}(\overline{V}) + Z_2 C_2^{(3)}(V_0 - \overline{V})] + 2S_{VV}\frac{d}{d\overline{V}}S_{IV} + S_{IV}\frac{d}{d\overline{V}}S_{VV}, \tag{5.0.12c}$$

$$C_{IIV} = Z^{-3} Z_1 Z_2[Z_2^2 C_2^{(3)}(V_0 - \overline{V}) - Z_1^2 C_1^{(3)}(\overline{V})] + 2S_{IV}\frac{d}{d\overline{V}}S_{IV} + S_{VV}\frac{d}{d\overline{V}}S_{II}. \tag{5.0.12d}$$

We apply the general result (5.0.12) to a tunnel barrier (resistor number 1) in series with a macroscopic resistor (number 2). The spectral densities $C_1^{(2)}$ and $C_1^{(3)}$ are given by Eqs. (5.0.4) and (5.0.9), respectively. For $C_2^{(2)}$ we use Eq. (5.0.3),

while $C_2^{(3)} = 0$. From this point on we assume linear current-voltage characteristics, so $\overline{V}$-independent Z_i's. We compare $C_I \equiv C_{III}$ with $C_V \equiv -C_{VVV}/Z_2^3$. The choice of C_V is motivated by the typical experimental situation in which one measures the current fluctuations indirectly through the voltage over a macroscopic series resistor. From Eq. (5.0.12) we find

$$C_x = \frac{e^2\bar{I}}{(1+Z_2/Z_1)^3}\left[1+\frac{3(\sinh u\cosh u-u)}{(1+Z_1/Z_2)\sinh^2 u}\left(\frac{T_2}{T_1}\frac{g_x}{u}-\operatorname{cotanh} u\right)\right], \quad (5.0.13)$$

with $g_I = 1$, $g_V = -Z_1/Z_2$, and $u = e\overline{V}/2kT_1$.

In the shot noise limit ($e\overline{V} \gg kT_1$) we recover the third cumulant obtained in Ref. [7] by the Keldysh technique:

$$C_I = C_V = e^2\bar{I}\frac{1-2Z_2/Z_1}{(1+Z_2/Z_1)^4}. \quad (5.0.14)$$

In the opposite limit of small voltages ($e\overline{V} \ll kT_1$) we obtain

$$C_I = e^2\bar{I}\frac{1+(Z_2/Z_1)(2T_2/T_1-1)}{(1+Z_2/Z_1)^4}, \quad (5.0.15)$$

$$C_V = e^2\bar{I}\frac{1-Z_2/Z_1-2T_2/T_1}{(1+Z_2/Z_1)^4}. \quad (5.0.16)$$

We conclude that there is a change in the slope $dC_x/d\bar{I}$ from low to high voltages. If the entire system is in thermal equilibrium ($T_2 = T_1$), then the change in slope is a factor $\pm(Z_1-2Z_2)(Z_1+Z_2)^{-1}$, where the + sign is for C_I and the − sign for C_V. In Fig. 5-2 we plot the entire voltage dependence of the third cumulants.

The limit $Z_2/Z_1 \to 0$ of a noninvasive measurement is of particular interest. Then $C_I = e^2\bar{I}$ has the expected result for an isolated tunnel junction [3], but C_V remains affected by the measurement circuit:

$$\lim_{Z_2/Z_1\to 0} C_V = e^2\bar{I}\left(1-\frac{T_2}{T_1}\frac{3(\sinh u\cosh u-u)}{u\sinh^2 u}\right). \quad (5.0.17)$$

This limit is also plotted in Fig. 5-2, for the case $T_2 = T_1 \equiv T$ of thermal equilibrium between the tunnel junction and the macroscopic series resistor. The slope then changes from $dC_V/d\bar{I} = -e^2$ at low voltages to $dC_V/d\bar{I} = e^2$ at high voltages. The minimum $C_V = -1.7\,ekT/Z_1 = -0.6\,e^2\bar{I}$ is reached at $e\overline{V} = 2.7\,kT$.

In conclusion, we have demonstrated that feedback from the measurement circuit introduces a temperature dependence of the third cumulant of tunneling noise. The temperature independent result $e^2\bar{I}$ of an isolated tunnel junction [3] acquires a striking temperature dependence in an electromagnetic environment, to the extent that the third cumulant may even change its sign. Precise predictions have been made for the dependence of the noise on the environmental impedance and temperature, which are in accordance with the recent experiment [4].

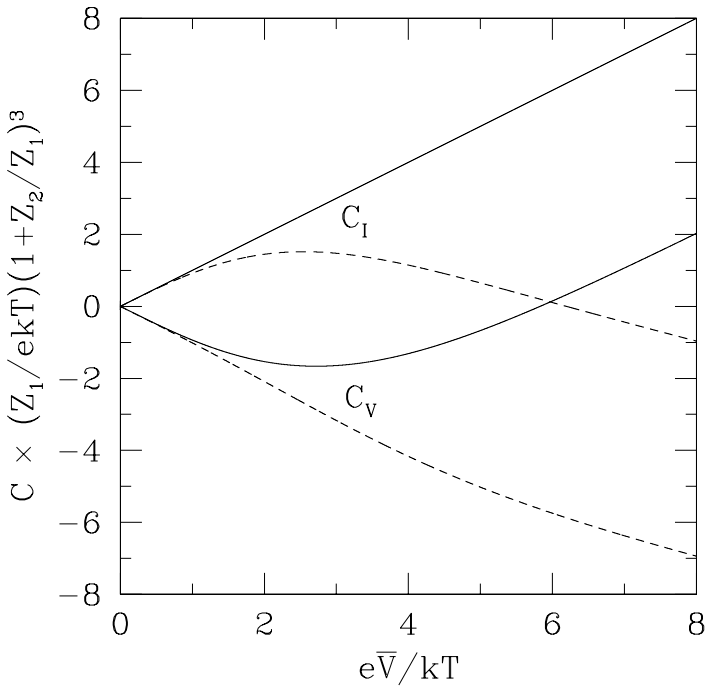

Figure 5-2. Voltage dependence of the third cumulants C_I and C_V of current and voltage for a tunnel junction (resistance Z_1) in series with a macroscopic resistor Z_2. The two solid curves are for $Z_2/Z_1 \to 0$ and the dashed curves for $Z_2/Z_1 = 1$. The curves are computed from Eq. (5.0.13) for $T_1 = T_2 \equiv T$. The high voltage slopes are the same for C_I and C_V, while the low voltage slopes have the opposite sign.

Bibliography

[1] W. Schottky, Ann. Phys. (Leipzig) **57**, 541 (1918); **68**, 157 (1922).

[2] Ya. M. Blanter and M. Büttiker, Phys. Rep. **336**, 1 (2000).

[3] L. S. Levitov and M. Reznikov, cond-mat/0111057.

[4] B. Reulet, J. Senzier, and D. E. Prober, cond-mat/0302084; B. Reulet, private communication.

[5] D. B. Gutman and Y. Gefen, cond-mat/0201007.

[6] U. Gavish, Y. Imry, L. Levinson, and B. Yurke, in *Quantum Noise*, edited by Yu. V. Nazarov and Ya. M. Blanter, NATO Science Series II Vol. 97 (Kluwer, Dordrecht, 2003); cond-mat/0211646.

[7] M. Kindermann, Yu. V. Nazarov, and C. W. J. Beenakker, cond-mat/0210617.

[8] E. Ben-Jacob, E. Mottola, and G. Schön, Phys. Rev. Lett. **51**, 2064 (1983); G. Schön, Phys. Rev. B **32**, 4469 (1985).

[9] H. Lee and L. S. Levitov, Phys. Rev. B **53**, 7383 (1996).

[10] A. V. Galaktionov, D. S. Golubev, and A. D. Zaikin, cond-mat/0212494.

[11] G.-L. Ingold and Yu. V. Nazarov, in *Single Charge Tunneling*, edited by H. Grabert and M. H. Devoret, NATO ASI Series B294 (Plenum, New York, 1992).

[12] Yu. V. Nazarov, Ann. Phys. (Leipzig) **8**, 507 (1999); Yu. V. Nazarov and M. Kindermann, cond-mat/0107133.

[13] K. E. Nagaev, Phys. Rev. B **66**, 075334 (2002); K. E. Nagaev, P. Samuelsson, and S. Pilgram, Phys. Rev. B **66**, 195318 (2002); S. Pilgram, A. N. Jordan, E. V. Sukhorukov, and M. Büttiker, Phys. Rev. Lett. **90**, 206801 (2003).

[14] D. B. Gutman, Y. Gefen, and A. D. Mirlin, cond-mat/0210076.

6 Interaction effects on counting statistics and the transmission distribution

It has been shown that at low energy scales the relevant part of the electron-electron interaction in mesoscopic conductors comes from their electromagnetic environment [1]. The resulting dynamical Coulomb blockade has been thoroughly investigated for tunnel junctions [2]. The measure of the interaction strength is the external impedance $Z(\omega)$ at the frequency scale $\Omega = \max(eV, k_B T)$ determined by either the voltage V at the conductor or its temperature T. If $z \equiv G_Q Z(\Omega) \ll 1$ (with the conductance quantum $G_Q = e^2/2\pi\hbar$) the interaction is weak, otherwise Coulomb effects strongly suppress electron transport.

A tunnel junction is the simplest mesoscopic conductor. An arbitrary mesoscopic conductor in the absence of interactions is characterized by its scattering matrix or, most conveniently, by a set of transmission eigenvalues T_n [3]. This Landauer-Büttiker approach to mesoscopic transport can be extended to access the full counting statistics (FCS) of charge transfer [4]. The FCS contains not only the average current but also current noise and all higher moments of current correlations in a compact and elegant form.

Interaction effects on general mesoscopic conductors are difficult to quantify for arbitrary z. For $z \ll 1$, one can employ perturbation theory to first order in z [5]. Recent work [6, 7] associates the resulting interaction correction to the conductance with shot noise properties of the conductor. The interaction correction to noise is associated with the third cumulant of charge transfer [8]. This motivates us to study the interaction correction to all cumulants of charge transfer, i.e. to the FCS. The recent experiment [9] addresses the correction to the conductance at arbitrary transmission.

A tunnel junction in the presence of an electromagnetic environment exhibits an anomalous power-law I-V characteristic, $I(V) \simeq V^{2z+1}$. The same power law behavior is typical for tunnel contacts between one-dimensional interacting electron systems, the so-called Luttinger liquids [10]. It has also been found for contacts with arbitrary transmission between single-channel conductors in the limit of weak interactions [11]. In this case, the interactions have been found to renormalize the transmission.

In this chapter we study the effects of weak interactions $z \ll 1$ on the FCS of a phase coherent multi-channel conductor. In the energy range below the Thouless energy that we restrict our analysis to, its transmission probabilities T_n are energy independent in the absence of interactions. We first analyze the interaction correction to first order in z. We identify an elastic and an inelastic contribution. The elastic contribution comes with a logarithmic factor that diverges

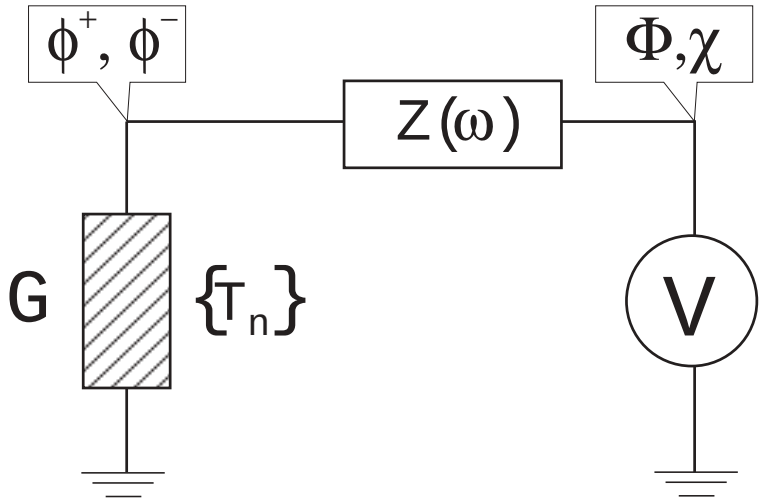

Figure 6-1. Phase-coherent conductor (conductance G) in an electromagnetic environment (impedance $Z(\omega)$). We formulate the quantum dynamics of the system in terms of the fluctuating fields $\phi^{\pm}(t)$.

at low energies suggesting that even weak interactions can suppress electron transport at sufficiently low energies. To quantify this we sum up interaction corrections to the FCS of all orders in z by a renormalization group analysis. We show that the result is best understood as a renormalization of the transmission eigenvalues similar to that proposed in [11]. The renormalization brings about an energy dependence of the transmission eigenvalues according to the flow equation

$$\frac{dT_n(E)}{d\ln E} = 2z\, T_n(E)[1 - T_n(E)]. \tag{6.0.1}$$

To calculate transport properties in the presence of interactions, one evaluates $T_n(E)$ at the energy $E \simeq \Omega$.

With relation (6.0.1) we explore the effect of interactions on the distributions of transmission probabilities for various types of mesoscopic conductors. In general, their conductance G and their noise properties display a complicated behavior at $z|\ln E| \simeq 1$ that depends on details of the conductor. However, in the limit of very low energies $z|\ln E| \gg 1$ we find only two possible scenarios. The first one is that the conductor behaves like a *single* tunnel junction with $G(V) \simeq V^{2z}$. In the other scenario, the transmission distribution approaches that of a symmetric *double* tunnel junction. The conductance scales then as $G(V) \simeq V^z$. Any given conductor follows one of the two scenarios. This divides all mesoscopic conductors into two broad classes.

We start out by evaluating the interaction correction to the FCS to first order in z. We analyze a simple circuit that consists of a mesoscopic conductor in series with an external resistor $Z(\omega)$ biased with a voltage source V (Fig. 1). For this we employ a non-equilibrium Keldysh action technique [12]. Within this

approach, one represents the generating function $\mathcal{F}(\chi)$ of current fluctuations in the circuit as a path integral over the fields $\phi^{\pm}(t)$ defined on the time interval $[0,\tau]$, that represent the fluctuating voltage in the node shared by mesoscopic conductor and external resistor. The path integral representation of $\mathcal{F}(\chi)$ reads

$$\begin{aligned}\mathcal{F}(\chi) &= \int \mathcal{D}\phi^{+}\mathcal{D}\phi^{-}\exp\{-iS_{\rm c}[\phi^{+},\phi^{-}] \\ &\quad -iS_{\rm env}[\Phi+\chi/2-\phi^{+},\Phi-\chi/2-\phi^{-}]\} \end{aligned} \tag{6.0.2}$$

where $d\Phi(t)/dt \equiv eV$. Derivatives of $\mathcal{F}(\chi)$ with respect to χ at $\chi = 0$ give the moments of the charge transferred through the circuit during a time interval of length τ. The Keldysh action is a sum of two terms $S_{\rm env}$ and $S_{\rm c}$ describing the environment and the mesoscopic conductor respectively.

We assume a linear electromagnetic environment that can be fully characterized by its impedance $Z(\omega)$ and its temperature T. Its action is bilinear in $\phi^{\pm}$,

$$\begin{aligned}S_{\rm env} &= \frac{1}{2\pi}\int_0^{\tau}dt\int_0^{\tau}dt'\,[\phi^{+}(t)A^{++}(t-t')\phi^{+}(t') \\ &\quad +\phi^{+}(t)A^{+-}(t-t')\phi^{-}(t')+\phi^{-}(t)A^{--}(t-t')\phi^{-}(t')]\end{aligned}$$

with

$$\begin{aligned}A^{++}(\omega) &= -i\omega[z^{-1}(\omega)+2N(\omega)\mathrm{Re}\,z^{-1}(\omega)] \\ A^{+-}(\omega) &= 4i\omega N(\omega)\mathrm{Re}\,z^{-1}(\omega) \\ A^{--}(\omega) &= -[A^{++}(\omega)]^{*}. \end{aligned} \tag{6.0.3}$$

Here, $N(\omega) \equiv \{\exp[\omega/k_BT]-1\}^{-1}$ is the Bose-Einstein distribution function and $z(\omega) = G_Q Z(\omega)$ the dimensionless frequency-dependent impedance.

The action $S_{\rm c}$ of the mesoscopic conductor can be expressed in terms of Keldysh Green functions $\check{G}_{R,L}$ (the "check"denotes 2×2 matrices in Keldysh space) of electrons in the two reservoirs adjacent to the conductor [13]. It takes the form of a trace over frequency and Keldysh indices,

$$S_{\rm c} = \frac{i}{2}\sum_n \mathrm{Tr}\,\ln\left[1+\frac{T_n}{4}\left(\left\{\check{G}_{\rm L},\check{G}_{\rm R}\right\}-2\right)\right] \tag{6.0.4}$$

and depends on the set of transmission eigenvalues T_n that characterizes the conductor. The fields $\phi^{\pm}(t)$ enter the expression as a gauge transform of $\check{G}$ in one of the reservoirs,

$$\check{G}_{\rm R} = \check{G}^{\rm res}, \tag{6.0.5}$$

$$\check{G}_{\rm L}(t,t') = \begin{bmatrix} e^{i\phi^{+}(t)} & 0 \\ 0 & e^{i\phi^{-}(t)}\end{bmatrix}\check{G}^{\rm res}(t-t')\begin{bmatrix} e^{-i\phi^{+}(t')} & 0 \\ 0 & e^{-i\phi^{-}(t')}\end{bmatrix}. \tag{6.0.6}$$

$G^{\rm res}$ is the equilibrium Keldysh Green function

$$\check{G}^{\rm res}(\epsilon) = \begin{pmatrix} 1-2f(\epsilon) & 2f(\epsilon) \\ 2[1-f(\epsilon)] & 2f(\epsilon)-1 \end{pmatrix}, \tag{6.0.7}$$

$f(\epsilon)$ being the equilibrium electron distribution function.

This defines our model that is valid for any external impedance but is hardly tractable in the general case. We proceed with perturbation theory in z assuming that $z \ll 1$. To zeroth order in z the fields $\phi^{\pm}(t)$ do not fluctuate and are fixed to $eVt \pm \chi/2$. Substituting this into Eq. (6.0.4) we recover Levitov's formula for non-interacting electrons,

$$\begin{aligned} \ln \mathcal{F}^{(0)}(\chi) \;\equiv\; -i\tau \mathcal{S}^{(0)}(\chi) = \tau \int \frac{d\epsilon}{2\pi} \sum_n \ln \{1 \\ + T_n \left[(e^{i\chi}-1) f_{\rm L}(1-f_{\rm R}) + (e^{-i\chi}-1) f_{\rm R}(1-f_{\rm L}) \right] \} \end{aligned} \tag{6.0.8}$$

($f_R \equiv f$ and $f_L(\epsilon) \equiv f(\epsilon - eV)$). Interaction effects manifest themselves at higher orders in z. To assess the first order correction, we expand the non-linear $S_{\rm c}$ to second order in the fluctuating fields $\phi^{\pm}(t)$. We integrate it over $\phi^{\pm}$ with the weight given by $S_{\rm env}$. The expression for the correction can be presented as [15]

$$\begin{aligned} \ln \mathcal{F}^{(1)}(\chi) \;=\; -i\tau \int_0^{\infty} d\omega \, \frac{{\rm Re}\, z(\omega)}{\omega} \Big\{ [2N(\omega)+1] S^{(1)}_{\rm el}(\chi) \\ + N(\omega) S^{(1)}_{\rm in}(\omega,\chi) + [N(\omega)+1] S^{(1)}_{\rm in}(-\omega,\chi) \Big\} . \end{aligned} \tag{6.0.9}$$

The three terms in square brackets correspond to *elastic* electron transfer, inelastic transfer with absorption of energy $\hbar\omega$ from the environment, and inelastic electron transfer with emission of this energy respectively. It is crucial to note that inelastic processes can only occur at frequencies $\omega \lesssim \Omega$ and that their contribution to the integral is thus restricted to this frequency range. In contrast, elastic contributions come primarily from frequencies exceeding the scale Ω. If $z = {\rm const}(\omega)$ for $\omega \lesssim \Lambda$, the elastic correction diverges logarithmically, its magnitude being $\simeq z \ln \Lambda/\Omega$. This suggests that i. the elastic correction is more important than the inelastic one and ii. a small value of z can be compensated for by a large logarithm, indicating the breakdown of perturbation theory. The upper cut-off energy Λ is set either by the inverse RC-time of the environment circuit or the Thouless energy of the electrons in the mesoscopic conductor.

The concrete expression for $S^{(1)}_{\rm in}$ reads

$$\begin{aligned} S^{(1)}_{\rm in}(\omega,\chi) \;=\; i \sum_n \int \frac{d\varepsilon}{2\pi} \Big\{ D_n D_n^+ \Big[T_n (f_L - f_L^+) + 2T_n (e^{i\chi}-1) f_L (1-f_R^+) \\ + 2T_n^2 (\cos\chi - 1) f_L (1-f_L^+)(f_R^+ - f_R) \Big] \\ + T_n D_n + (1-D_n)(1-D_n^+) \Big\} \\ + \left\{ \begin{array}{c} {\rm R} \leftrightarrow {\rm L} \\ \chi \leftrightarrow -\chi \end{array} \right\}, \end{aligned} \tag{6.0.10}$$

where we have introduced the functions

$$D_n = \left\{1 + T_n\left[f_L(1-f_R)(e^{i\chi}-1). + f_R(1-f_L)(e^{-i\chi}-1)\right]\right\}^{-1} \quad (6.0.11)$$

and the notation

$$f^+(\varepsilon) = f(\varepsilon+\omega), \;\; D_n^+(\varepsilon) = D_n(\varepsilon+\omega). \quad (6.0.12)$$

We do not analyze $S_{\rm in}^{(1)}$ further and instead turn to the analysis of the elastic correction.

It is important that the explicit form of the elastic correction can be presented as

$$\begin{aligned} S_{\rm el} &= \sum_n \delta T_n \frac{\partial S^{(0)}}{\partial T_n} \\ \text{with } \delta T_n &= -2T_n(1-T_n). \end{aligned} \quad (6.0.13)$$

This suggests that the main effect of interactions is to change the transmission coefficients T_n. It also suggests that we can go beyond perturbation theory by a renormalization group analysis that involves the T_n only. In such an analysis one concentrates at each renormalization step on the "fast"components of $\phi^\pm$ with frequencies in a narrow interval $\delta\omega$ around the running cut-off frequency E. Integrating out these fields one obtains a new action for the "slow"fields. Subsequently one reduces E by $\delta\omega$ and repeats the procedure until the running cut-off approaches Ω. We find that at each step of renormalization the action indeed retains the form given by Eq. (6.0.4) and only the T_n change, provided $z \ll \min\{1, G_Q/G\}$. The resulting energy dependence of the T_n obeys Eq. (6.0.1). The strict proof of this involves manipulations on the action (6.0.4) with time dependent arguments $\phi^\pm(t)$. It is very technical and we do not give it here. The approximations that we make in this renormalization procedure amount to a summation of the leading logarithms in every order of the perturbation series.

In the rest of the chapter we analyze the consequences of Eq. (6.0.1) for various mesoscopic conductors. Equation (6.0.1) can be explicitly integrated to obtain

$$T_n(E) = \frac{\xi T_n^\Lambda}{1 - T_n^\Lambda(1-\xi)}, \;\; \xi \equiv \left(\frac{E}{\Lambda}\right)^{2z} \quad (6.0.14)$$

in terms of the "high energy"(non-interacting) transmission eigenvalues T^Λ. A mesoscopic conductor containing many transport channels is most conveniently characterized by the distribution $\rho_\Lambda(T)$ of its transmission eigenvalues [14]. It follows from Eq. (6.0.14) that the effective transmission distribution at the energy scale E reads

$$\rho_E(T) = \frac{\xi}{[\xi + T(1-\xi)]^2}\rho_\Lambda\left(\frac{T}{\xi + T(1-\xi)}\right). \quad (6.0.15)$$

We now analyze its low energy limit $\xi \to 0$. Any given transmission eigenvalue will approach zero in this limit. Seemingly this implies that for any conductor the transmission distribution approaches that of a tunnel junction, so that all $T_n \ll 1$. The overall conductance would be proportional to ξ in accordance with Ref. [5].

Indeed, this is one of the possible scenarios. A remarkable exception is the case that the non-interacting ρ_Λ has an inverse square-root singularity at $T \to 1$. Many mesoscopic conductors display this feature, most importantly diffusive ones [14]. In this case, the low-energy transmission distribution approaches a limiting function

$$\rho_*(T) \propto \sqrt{\frac{\xi}{T^3(1-T)}}. \tag{6.0.16}$$

The conductance scales like $\xi^{1/2}$. ρ_* is known to be the transmission distribution of a *double* tunnel junction: two identical tunnel junctions in series [16]. Indeed, one checks that for a double tunnel junction the form of the transmission distribution is unaffected by interactions. This sets an alternative low-energy scenario. We are not aware of transmission distributions that would give rise to other scenarios.

We believe that this is an important general result in the theory of quantum transport and suggest now a qualitative explanation. The statement is that the conductance of a phase-coherent conductor at low voltage and temperature $\Omega \ll \Lambda$ asymptotically obeys a power law with an exponent that generically takes two values,

$$G \propto \left(\frac{\Omega}{\Lambda}\right)^{2z}, \quad \text{or} \quad G \propto \left(\frac{\Omega}{\Lambda}\right)^{z}. \tag{6.0.17}$$

For tunneling electrons the exponent is $2z$. An electron traverses the conductor in a single leap. The second possible exponent z has been discussed in the literature as well, in connection with *resonant* tunneling through a *double* tunnel barrier in the presence of interactions [10]. This resonant tunneling takes place via intermediate discrete states contained between the two tunnel barriers. The halved exponent $\alpha = z$ occurs in the regime of the so-called *successive* electron tunneling. In this case, the electron first jumps over one of the barriers ending up in a discrete state. Only in a second jump over the second barrier the charge transfer is completed. Since it takes two jumps to transfer a charge, the electron feels only half the counter voltage due to interactions with electrons in the environmental impedance Z at each hop. Consequently, the exponent at each jump takes half the value for direct tunneling. Our results strongly suggest that this transport mechanism is not restricted to resonant tunneling systems, or, in other words, that resonant tunneling can occur in systems of a more generic nature than generally believed. As far as transport is concerned, a mesoscopic conductor is characterized by its scattering matrix regardless of the details of its inner structure. In this approach it is not even obvious that the conductor can accommodate discrete states. Nevertheless, the transmission distribution of

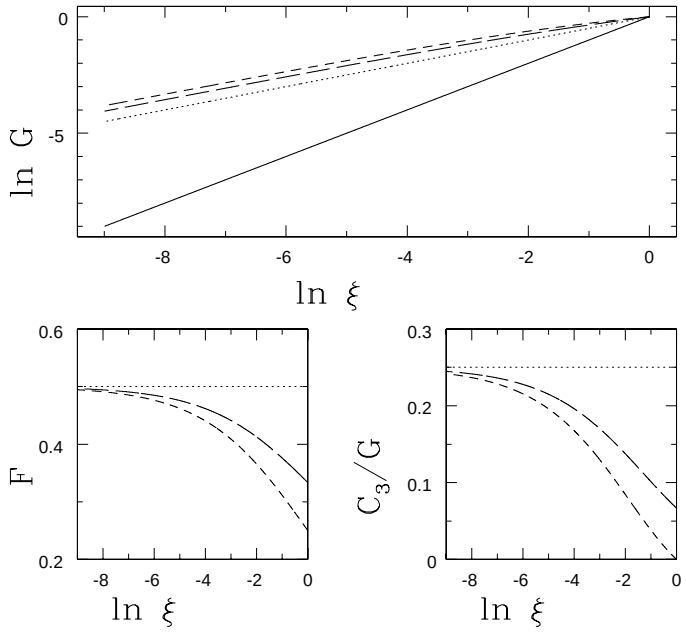

Figure 6-2. Renormalization of conductance G (logarithmically), Fano factor $F = C_2/G$ and third cumulant C_3 normalized by the conductance in a tunnel junction (solid line), a double tunnel barrier (dotted line), a double point contact (short dashed line), and a diffusive conductor (long lashed line).

this scattering matrix does depend on the internal structure of the conductor. The inverse square root singularity of this distribution at $T \to 1$ for a double tunnel barrier is due to the formation of Fabry-Perot resonances between the two barriers. Probably similar resonances are at the origin of the same singularity for more complicated mesoscopic conductors with multiple scattering. They are then the intermediate discrete states that give rise to the modified scaling of the conductance in presence of interactions. One may speculate that in diffusive conductors these resonances are the so-called "nearly localized states" found in [17].

From equation (6.0.14) one concludes that the resonant tunneling scaling holds only if $G(E) \gg G_Q$ so that many transport channels contribute to the conductance. At sufficiently small energies, $G(E)$ becomes of the order of G_Q. All transmission eigenvalues are then small and the conductance crosses over to the tunneling scaling.

With Eqs. (6.0.14) and (6.0.15) we can evaluate the transmissions and the FCS in the intermediate regime $\xi \sim 1$. Fig. 6-2 shows the results for the first three cumulants of charge transfer C_n for several types of conductors whose non-

interacting transmission distributions $\rho_\Lambda(T)$ are known. Apart from the tunnel contact all these conductors approach the resonant tunneling scaling with noise properties of a double tunnel barrier at very small bias voltage ($\xi \ll 1$).

We remark, that Eq. (6.0.13) generalizes the statements made in [7, 8]: At zero temperature, the interaction correction to the n-th cumulant of transferred charge is proportional to the (n+1)-th cumulant.

To conclude, we have investigated the effects of interactions on the FCS of a Landauer-Büttiker conductor and found that their main effect can be incorporated into an energy dependence of the transmission eigenvalues. For an arbitrary conductor, the conductance in the low-energy limit obeys one of two generic scaling laws.

Bibliography

[1] Yu. V. Nazarov, Zh. Eksp. Teor. Fiz. 95, 975 (1989); G.-L. Ingold and Yu. V. Nazarov, in *Single Charge Tunneling*, edited by H. Grabert and M. H. Devoret, NATO ASI Series B294 (Plenum, New York, 1992).

[2] M. H. Devoret, D. Esteve, H. Grabert, G.-L. Ingold, H. Pothier, and C. Urbina, Phys. Rev. Lett. **64**, 1824 (1990).

[3] C. W. J. Beenakker, Rev. Mod. Phys. **69**, 731 (1997).

[4] L. S. Levitov and G. B. Lesovik, JETP Lett. **58**, 230 (1993); cond-mat/9401004; L. S. Levitov, H. Lee, and G. B. Lesovik, J. Math. Phys. **37**, 4845 (1996).

[5] Yu. V. Nazarov, Sol. St. Comm. **75**, 669 (1990).

[6] D. S. Golubev, A. D. Zaikin, Phys. Rev. Lett. 86, 4887 (2001).

[7] A. Levy Yeyati, A. Martin-Rodero, D. Esteve, and C. Urbina, Phys. Rev. Lett. **87**, 046802 (2001).

[8] A. V. Galaktionov, D. S. Golubev, and A. D. Zaikin, cond-mat/0212494 (2002).

[9] R. Cron *et al.*, in *Electronic Correlations: From Meso-to Nano-Physics*, ed. by T. Martin, G. Montambaux, J. Trân Thanh Vân, EDP Sciences, 2001, p. 17.

[10] C. L. Kane and M. P. A. Fisher, Phys. Rev B 46, 15233 (1992).

[11] K. A. Matveev, D. Yue, and L. I. Glazman, Phys. Rev. Lett. 71, 3351 (1993).

[12] M. Kindermann, Yu. V. Nazarov, and C. W. J. Beenakker, cond-mat/0210617.

[13] Y. V. Nazarov, Ann. Phys. (Leipzig) **8**, 507 (1999).

[14] Yu. V. Nazarov, in: *Quantum Dynamics of Submicron Structures*, edited by H. A. Cerdeira, B. Kramer, G. Schön, Kluwer, 1995, p. 687; cond-mat/9410011.

[15] We disregard corrections $\propto z(0)$ that account for the division of the voltage between mesoscopic conductor and external impedance (see [12] for details).

[16] J. A. Melsen and C. W. J. Beenakker, Physica B **203**, 219 (1994); K. M. Schep and G. E. W. Bauer, Phys. Rev. Lett. **78**, 3015 (1997).

[17] B. A. Muzykantskii and D. E. Khmelnitskii, Phys. Rev. B **51**, 5480 (1995).

7 Quantum theory of electromechanical noise and momentum transfer statistics

7.1 Introduction

Electrical current is the transfer of charge from one end of the conductor to the other. The statistics of this charge transfer was investigated by Levitov and Lesovik [1]. It is binomial for a single-channel conductor at zero temperature and double-Poissonian at finite temperature in the tunneling regime [2]. The second cumulant, the noise power, has been measured in a variety of systems [3]. Ways of measuring the third cumulant have been proposed [2,4].

Electrical current also transfers momentum to the lattice. The second cumulant, the electromechanical noise power, determines the mean square displacement of an oscillator through which a current is driven. It has been studied theoretically [5–8] and is expected to lie within the range of sensitivity of nanomechanical oscillators [9]. No theory exists for higher order cumulants of the transferred momentum (which would determine higher cumulants of the oscillator displacement). It is the purpose of the present chapter to provide such a theory.

In the context of charge transfer statistics there exist two approaches: a fully quantum mechanical approach using Keldysh Green functions [1,10] and a semiclassical approach using the Boltzmann-Langevin equation [11]. Here we take the former approach, to arrive at a quantum theory of momentum transfer statistics. As a test, we show that the second moment calculated from Keldysh Green functions coincides in the semiclassical limit with the result obtained from the Boltzmann-Langevin equation by Shytov, Levitov, and one of the authors [8].

A calculation of the complete cumulant generating function of transferred momentum (or, equivalently, of oscillator displacement) is presented for the case of a single-channel conductor with a localized scatterer. The generating function in this case can be written entirely in terms of the transmission probability Γ of the scatterer. In the more general multi-channel case one also needs knowledge of the wavefunctions. This is an essential difference from the charge transfer problem, which can be solved in terms of transmission eigenvalues for any number of channels. At zero temperature the momentum statistics is binomial, just as for the charge. At finite temperature it is multinomial, even in the limit $\Gamma \to 0$, different from the double-Poissonian distribution of charge.

The outline of the chapter is as follows. In Sec. 7.2 we formulate the problem in a way that is suitable for further analysis. The key technical step in that section is a unitary transformation which eliminates the dependence of the

electron-phonon coupling Hamiltonian on the (unknown) scattering potential of the disordered lattice. The resulting coupling Hamiltonian contains the electron momentum flow and the phonon displacement. In the next section we use that Hamiltonian to derive a general formula for the generating function of the distribution of momentum transferred to a phonon (as well as the distribution of phonon displacements). It is the analogue of the Levitov-Lesovik formula for the charge transfer distribution [1]. For a localized scatterer we can evaluate this statistics in terms of the scattering matrix. We show how to do this in Sec. 7.4, and give an application to a single-channel conductor in Sec. 7.5. In Secs. 7.6 and 7.7 we turn to the case that the scattering region extends throughout the conductor. We follow the Keldysh approach to derive a general formula for the generating function and check its validity by rederiving the result of Ref. [8]. We conclude in Sec. 7.8 with an order of magnitude estimate of higher order cumulants of the momentum transfer statistics.

7.2 Formulation of the problem

The excitation of a phonon mode by conduction electrons is described by the Hamiltonian

$$H = \Omega a^\dagger a + \sum_i \mathbf{p}_i^2/2m + \sum_i V[\mathbf{r}_i - Q\mathbf{u}(\mathbf{r}_i)], \tag{7.2.1}$$

where we have set $\hbar = 1$. The phonon mode has annihilation operator a, frequency Ω, mass M, and displacement $Q\mathbf{u}(\mathbf{r})$, where $Q = (2M\Omega)^{-1/2}(a + a^\dagger)$ is the amplitude operator. The electrons have position $\mathbf{r}_i$, momentum $\mathbf{p}_i = -i\partial/\partial\mathbf{r}_i$, and mass m. Electrons and phonons are coupled through the ion potential $V(\mathbf{r})$. We assume zero magnetic field. Electron-electron interactions and the interactions of electrons and phonons with an external electric field have also been omitted.

We assume that electrons and phonons are uncoupled at time zero and measure moments of the observable A of the phonons after they have been coupled to the electrons for a time t. The operator $A(a, a^\dagger)$ could be the amplitude Q of the phonon mode, its momentum $P = -i(M\Omega/2)^{1/2}(a - a^\dagger)$, or its energy $\Omega a^\dagger a$. The moment generating function for A is

$$\mathcal{F}(\xi) = \sum_{m=0}^{\infty} \frac{\xi^m}{m!}\langle A^m(t)\rangle = \mathrm{Tr}\, e^{\xi A} e^{-iHt}\rho e^{iHt}. \tag{7.2.2}$$

The initial density matrix $\rho = \rho_e\rho_p$ is assumed to factorize into an electron and a phonon part.

We assume small displacements, so an obvious way to proceed would be to linearize $V(\mathbf{r} - Q\mathbf{u})$ with respect to the phonon amplitude Q. Such a procedure is complicated by the fact that the resulting coupling $-Q\mathbf{u}\cdot\nabla V$ of electrons and phonons depends on the ion potential V. Because of momentum conservation,

it should be possible to find the momentum transferred by the electrons to the lattice without having to consider explicitly the force $-\nabla V$. In the semiclassical calculation of Ref. [8] that goal is achieved by the continuity equation for the flow of electron momentum. The unitary transformation that we now discuss achieves the same purpose in a fully quantum mechanical framework.

What we need is a unitary operator U such that

$$U^\dagger V[\mathbf{r} - Q\mathbf{u}(\mathbf{r})]U = V(\mathbf{r}). \tag{7.2.3}$$

For constant $\mathbf{u}$ we have simply $U = \exp[-iQ\mathbf{u}\cdot\mathbf{p}]$. More generally, for space-dependent $\mathbf{u}$, we need to specify the operator ordering (denoted by colons $:\cdots:$) that all position operators $\mathbf{r}$ stand to the left of the momentum operators $\mathbf{p}$. We also need to include a Jacobian determinant $||J||$ to ensure unitarity of U. As shown in App. A, the desired operator is

$$U = ||J||^{1/2} : e^{-iQ\mathbf{u}(\mathbf{r})\cdot\mathbf{p}} :, \quad J_{\alpha\beta} = \delta_{\alpha\beta} - Q\partial_\alpha u_\beta(\mathbf{r}), \tag{7.2.4}$$

with $\partial_\alpha \equiv \partial/\partial r_\alpha$. All this was for a single electronic degree of freedom. The corresponding operator for many electrons is $U = \prod_i U_i$, where U_i is given by Eq. (7.2.4) with $\mathbf{r}$, $\mathbf{p}$ replaced by $\mathbf{r}_i$, $\mathbf{p}_i$.

The Hamiltonian (7.2.1) transforms as $U^\dagger H U = H_0 + H_{\rm int}$, with

$$H_0 = \Omega a^\dagger a + \sum_i [\mathbf{p}_i^2/2m + V(\mathbf{r}_i)], \tag{7.2.5a}$$

$$H_{\rm int} = -QF - \frac{1}{M}P\Pi + \mathcal{O}(\mathbf{u}^2). \tag{7.2.5b}$$

Here F is the driving force of the phonon mode,

$$F = \frac{1}{4m}\sum_i [u_{\alpha\beta}(\mathbf{r}_i)p_{i\alpha}p_{i\beta} + p_{i\alpha}u_{\alpha\beta}(\mathbf{r}_i)p_{i\beta}] + \text{H.c}, \tag{7.2.6}$$

and Π is the total electron momentum,

$$\Pi = \tfrac{1}{2}\sum_i \mathbf{u}(\mathbf{r}_i)\cdot\mathbf{p}_i + \text{H.c.}, \tag{7.2.7}$$

weighted with the (dimensionless) mode profile $\mathbf{u}(\mathbf{r})$. We have defined the shear tensor $u_{\alpha\beta} = \frac{1}{2}(\partial_\alpha u_\beta + \partial_\beta u_\alpha)$. The abbreviation H.c. indicates the Hermitian conjugate and a summation over repeated cartesian indices α, β is implied.

The interaction Hamiltonian $H_{\rm int}$ is now independent of the ion potential, as desired. In the first term $-QF$ we recognize the momentum flux tensor, while the second term $-P\Pi/M$ is an inertial contribution to the momentum transfer. The inertial contribution is of relative order $\Omega\lambda/v_F$ (λ being the wavelength of the phonon and v_F the Fermi velocity of the electrons) and typically $\ll 1$. In what follows we will neglect it. We also neglect the terms in $H_{\rm int}$ of second and higher order in $\mathbf{u}$, which contribute to order λ_F/L to the generating function (with L the

length scale on which **u** varies). These higher order interaction terms account for the momentum uncertainty of an electron upon a position measurement by the phonon.

If we apply the unitary transformation U to the generating function (7.2.2), we need to transform not only H but also $A \to U^\dagger A U = \tilde{A}$ and $\rho \to U^\dagger \rho U = \tilde{\rho}$, resulting in

$$\mathcal{F}(\xi) = \mathrm{Tr}\, e^{\xi \tilde{A}} e^{-it(H_0+H_{\rm int})} \tilde{\rho} e^{it(H_0+H_{\rm int})}. \tag{7.2.8}$$

In App. A we show that, quite generally, the distinction between ρ, A and $\tilde{\rho}, \tilde{A}$ is irrelevant in the limit of a long detection time t, and we will therefore ignore this distinction in what follows.

If **u** is smooth on the scale of λ_F, so that gradients of $u_{\alpha\beta}$ can be neglected, one can apply the effective mass approximation to the Hamiltonian (7.2.5). The ion potential $V = V_{\rm lat} + V_{\rm imp}$ is decomposed into a contribution $V_{\rm lat}$ from the periodic lattice and a contribution $V_{\rm imp}$ from impurities and boundaries that break the periodicity. The effects of $V_{\rm lat}$ can be incorporated in an effective mass m^* (assumed to be deformation independent [12,13]) and a corresponding quasimomentum p^*. The unperturbed Hamiltonian takes the usual form

$$H_0 \;=\; \Omega a^\dagger a + \sum_i [\mathbf{p}_i^{*2}/2m^* + V_{\rm imp}(\mathbf{r}_i)]. \tag{7.2.9}$$

As shown in App. B, the force operator in $H_{\rm int}$ is then expressed through the flow of quasi-momentum,

$$F = \frac{1}{m^*} \sum_i p^*_{i\alpha} u_{\alpha\beta}(\mathbf{r}_i) p^*_{i\beta}, \tag{7.2.10}$$

whereas the inertial contribution is still given by Eq. (7.2.7) in terms of the true electron momentum.

7.3 Momentum transfer statistics

7.3.1 Generating function

A massive phonon mode absorbs the momentum that electrons transfer to it without changing its displacement. We may therefore define a statistics of momentum transfer to the phonons without back action on the electrons by choosing the observable $A = P = -i(M\Omega/2)^{1/2}(a - a^\dagger)$ in Eq. (7.2.2) and taking the limit $M \to \infty$, $\Omega \to 0$ at fixed $M\Omega$. We assume that the phonon mode is initially in the ground state, so that $a\rho_p = 0$.

We transform to the interaction picture by means of the identity

$$e^{iH_0 t} e^{-iHt} = \mathcal{T} \exp\left[-i \int_0^t dt'\, H_{\rm int}(t') \right], \tag{7.3.1}$$

where $\mathcal{T}$ denotes time ordering (earlier times to the right of later times) of the time dependent operator $H_{\rm int}(t) = e^{iH_0 t} H_{\rm int} e^{-iH_0 t}$. In the massive phonon limit we have $H_{\rm int}(t) = -QF(t)$ with time independent Q (since Q commutes with H_0 when $\Omega \to 0$). Eq. (7.2.2) takes the form

$$\mathcal{F}(\xi) = \langle \mathcal{T}_\pm \exp[-iQK_-(t)] e^{\xi P} \exp[iQK_+(t)] \rangle, \tag{7.3.2}$$

where $K_\pm(t) = \int_0^t dt_\pm F(t_\pm)$ and $\mathcal{T}_\pm$ denotes the Keldysh time ordering: times t_- to the left of times t_+, earlier t_- to the left of later t_-, earlier t_+ to the right of later t_+.

Taking the expectation value of the phonon degree of freedom we find

$$\mathcal{F}(\xi) = e^{\xi^2 M\Omega/2} \left\langle \mathcal{T}_\pm \exp\left[\tfrac{1}{2}\xi(K_- + K_+) - \frac{(K_+ - K_-)^2}{4M\Omega} \right] \right\rangle. \tag{7.3.3}$$

The factor $\exp(\xi^2 M\Omega/2)$ originates from the uncertainty $(M\Omega)^{1/2}$ of the momentum of the phonon mode in the ground state (vacuum fluctuations). It is a time-independent additive contribution to the second cumulant and we can omit it for long detection times. The quadratic term $\propto K_\pm^2/M\Omega$ becomes small for a small uncertainty $(M\Omega)^{-1/2}$ of the displacement in the ground state. It describes a back action of the phonon mode on the electrons that persists in the massive phonon limit. (A similar effect is known in the context of charge counting statistics [14].) This term may be of importance in some situations, but we will not consider it here, assuming that the electron dynamics is insensitive to the vacuum fluctuations of the phonon mode.

With these simplifications we arrive at a formula for the momentum transfer statistics,

$$\mathcal{F}(\xi) = \langle \mathcal{T}_\pm \exp[\tfrac{1}{2}\xi K_-(t)] \exp[\tfrac{1}{2}\xi K_+(t)] \rangle, \tag{7.3.4}$$

that is of the same form as the formula for charge counting statistics due to Levitov and Lesovik [1],

$$\mathcal{F}_{\rm charge}(\xi) = \langle \mathcal{T}_\pm \exp[\tfrac{1}{2}\xi J_-(t)] \exp[\tfrac{1}{2}\xi J_+(t)] \rangle. \tag{7.3.5}$$

The role of the integrated current $J(t) = \int_0^t dt'\, I(t')$ is taken in our problem by the integrated force $K(t)$.

7.3.2 Relation to displacement statistics

Cumulants $\langle\langle \triangle P(t) \rangle\rangle$ of the momentum transferred in a time t are obtained from the cumulant generating function $\ln \mathcal{F}(\xi) = \sum_n \langle\langle \triangle P(t)^n \rangle\rangle \xi^n/n!$. Cumulants $\langle\langle F(\omega)^n \rangle\rangle$ of the Fourier transformed force $F(\omega) = \int dt\, e^{i\omega t} F(t)$ then follow from the relation $\triangle P(t) = \int_0^t dt'\, F(t')$. The limit $t \to \infty$ of a long detection time corresponds to the low frequency limit,

$$\left\langle\left\langle \prod_{i=1}^n F(\omega_i) \right\rangle\right\rangle \to 2\pi\delta\left(\sum_{i=1}^n \omega_i\right) \lim_{t\to\infty} \frac{1}{t} \langle\langle \triangle P(t)^n \rangle\rangle. \tag{7.3.6}$$

Cumulants of the Fourier transformed displacement $Q(\omega)$ of the oscillator follow from the phenomenological equation of motion

$$Q(\omega) = R(\omega)F(\omega),\ R(\omega) = \frac{1}{M}(\Omega^2 - \omega^2 - i\omega\Omega/\mathcal{Q})^{-1}, \tag{7.3.7}$$

where $\mathcal{Q}$ is the quality factor of the oscillator. Since the force noise is white until frequencies that are typically $\gg \Omega$, one has in good approximation

$$\left\langle\left\langle \prod_{i=1}^{n} Q(\omega_i) \right\rangle\right\rangle = 2\pi\delta\left(\sum_{i=1}^{n}\omega_i\right)\prod_{j=1}^{n} R(\omega_j)\lim_{t\to\infty}\frac{1}{t}\langle\langle \triangle P(t)^n\rangle\rangle\,. \tag{7.3.8}$$

Optical or magnetomotive detection of the vibration, as in Refs. [15–17], measures the probability distribution $P(Q)$ of the displacement at any given time. The cumulants of $P(Q)$ are obtained by Fourier transformation of Eq. (7.3.8),

$$\langle\langle Q^n\rangle\rangle = \mathcal{R}_n \lim_{t\to\infty}\frac{1}{t}\langle\langle \triangle P(t)^n\rangle\rangle, \tag{7.3.9}$$

$$\begin{aligned}\mathcal{R}_n &= \int\frac{d\omega_1}{2\pi}\cdots\int\frac{d\omega_n}{2\pi}R(\omega_1)\cdots R(\omega_n)2\pi\delta\left(\sum_{i=1}^{n}\omega_i\right)\\ &= \int_{-\infty}^{\infty} dt\, R(t)^n.\end{aligned} \tag{7.3.10}$$

For $\mathcal{Q} \gg 1$ the odd moments can be neglected, while the even moments are given by

$$\mathcal{R}_{2k} \approx \frac{1}{2k}(M\Omega)^{-2k}\frac{\mathcal{Q}}{\Omega},\ \ k \ll \mathcal{Q}. \tag{7.3.11}$$

7.3.3 Validity of the massive phonon approximation

These results were obtained in the massive phonon limit. Let us estimate how large M should be, for the simplest case of the scattering of an electron (mass m, velocity v_F) by a barrier (mass M, velocity $\dot{Q}$). Finite M corrections appear because a reflected electron transfers to the barrier not only a momentum $2p_F$ but also an energy $\delta E \simeq 2p_F\dot{Q}$. This energy transfer effectively changes the voltage drop over the barrier by an amount $\delta V = \delta E/e$, because reflected electrons suffer this energy change whereas transmitted electrons do not.

A voltage drop δV creates a feedback loop: The current is changed by $\delta I = G\delta V$, hence the force on the barrier is changed by $\delta F = (2p_F/e)\delta I$, hence the velocity of the barrier is changed by $\delta\dot{Q} = i\omega R(\omega)\delta F = 4i\omega(p_F/e)^2 R(\omega)G\dot{Q}$ (in Fourier representation). The feedback may be neglected if $\delta\dot{Q} \ll \dot{Q}$ at the resonance frequency Ω (where it is strongest). Since $R(\Omega) = i\mathcal{Q}/M\Omega^2$ the requirement for negligible feedback, and therefore for the validity of the massive phonon approximation, is

$$\alpha = \mathcal{Q}\frac{Gh}{e^2}\frac{E_F}{\hbar\Omega}\frac{m}{M} \ll 1. \tag{7.3.12}$$

The left-hand-side of this inequality is the product of three large ratios (quality factor, dimensionless conductance, and the ratio of Fermi energy over phonon energy) and one small ratio (electron mass over mass of the resonator). For typical parameter values of a single-channel conductor one has $Gh/e^2 < 1$, $M = 10^{-20}\,\mathrm{kg}$, $\Omega/2\pi = 5\,\mathrm{GHz}$, and $E_F/\hbar = 0.5 \cdot 10^{15}\,\mathrm{Hz}$, yielding $\alpha < 10^{-3}$ for $\mathcal{Q} = 10^3$.

7.4 Evaluation in terms of the scattering matrix

The Levitov-Lesovik formula (7.3.5) for the charge transfer statistics can be evaluated in terms of the scattering matrix of the conductor [1, 18, 19], without explicit knowledge of the scattering states. This is possible because the current operator depends only on the asymptotic form of the scattering states, far from the scattering region. The formula (7.3.4) for the momentum transfer statistics can be evaluated in a similar way, but only if the mode profile $\mathbf{u}(\mathbf{r})$ is approximately constant over the scattering region.

To this end, we first write the force operator (7.2.6) in second quantized form using a basis of scattering states $\psi_{n,\varepsilon}(\mathbf{r})$,

$$F(t) = \iint \frac{d\varepsilon d\varepsilon'}{2\pi} \sum_{n,n'} e^{i(\varepsilon-\varepsilon')t} c_n^\dagger(\varepsilon) M_{nn'}(\varepsilon,\varepsilon') c_{n'}(\varepsilon'), \tag{7.4.1}$$

$$M_{nn'}(\varepsilon,\varepsilon') = \frac{1}{m}\int d\mathbf{r}\, \psi^*_{n,\varepsilon}\big(p_\alpha u_{\alpha\beta} p_\beta + [[u_{\alpha\beta}, p_\alpha], p_\beta]\big)\psi_{n',\varepsilon'}. \tag{7.4.2}$$

The operator $c_n(\varepsilon)$ annihilates an electron in the n-th scattering channel at energy ε. The mode index n runs from 1 to N (or from $N+1$ to $2N$) for waves incident from the left (or from the right). (See Fig. 7-1 for a diagram of the geometry and see Ref. [20] for the analogous representation of the current operator.) The commutator $[[u_{\alpha\beta}, p_\alpha], p_\beta]$ can be neglected if $\mathbf{u}$ is smooth on the scale of the wavelength (hence if $\lambda_F/L \ll 1$). We assume that the derivative $u_{\alpha\beta}$ of the mode profile vanishes in the scattering region, so that for the scattering states we may use the asymptotic form

$$\psi_{n,\varepsilon}(\mathbf{r}) = \phi^{\mathrm{in}}_{n,\varepsilon}(\mathbf{r}) + \sum_m S_{mn}(\varepsilon)\phi^{\mathrm{out}}_{m,\varepsilon}(\mathbf{r}), \tag{7.4.3}$$

in terms of incident and outgoing waves $\phi^{\mathrm{in,out}}_{n,\varepsilon}$ (normalized to unit current) and the scattering matrix $S_{mn}(\varepsilon)$. Since we are neglecting the Lorentz force we may assume that $\phi^{\mathrm{out}}_{m,\varepsilon} = \phi^{\mathrm{in}*}_{m,\varepsilon}$. The scattering matrix has the block structure

$$S = \begin{pmatrix} r & t' \\ t & r' \end{pmatrix}, \tag{7.4.4}$$

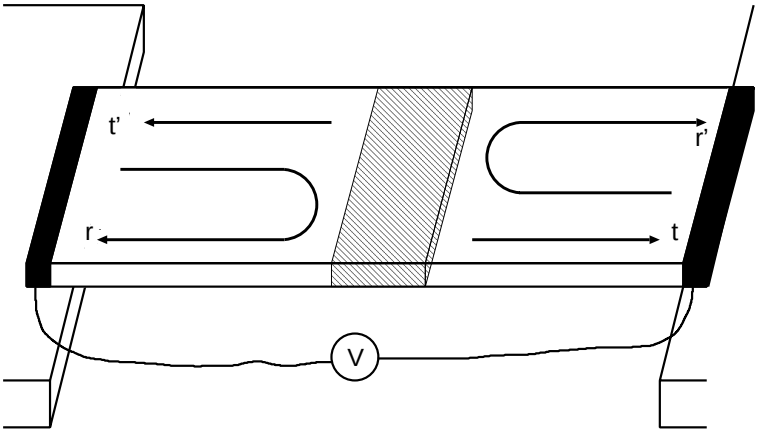

Figure 7-1. Sketch of a freely suspended wire. The matrices t, t' and r, r' describe transmission and reflection by a localized scatterer (shaded). A voltage V drives a current through the conductor, exciting a vibration.

with $N \times N$ transmission and reflection matrices t, t', r, r'. These matrices are related by unitarity ($S = S^\dagger$) and possibly also by time-reversal symmetry ($S = S^T$).

The operator $p_\alpha u_{\alpha\beta} p_\beta$ will couple only weakly the incident to the outgoing waves, provided $\mathbf{u}$ is smooth on the scale of λ_F, and we neglect this coupling. The matrix M then separates into an incident and outgoing part,

$$M(\varepsilon, \varepsilon') = M^{\rm in}(\varepsilon, \varepsilon') + S^\dagger(\varepsilon) M^{\rm out}(\varepsilon, \varepsilon') S(\varepsilon'). \tag{7.4.5}$$

The matrices $M^{\rm in}$ and $M^{\rm out}$ are defined as in Eq. (7.4.2) with ψ replaced by $\phi^{\rm in}$ and $\phi^{\rm out}$, respectively. (They are Hermitian and related by $M^{\rm out} = M^{\rm in*}$.) These two matrices vary with energy on the scale of the Fermi energy E_F, while the scattering matrix S has a much stronger energy dependence (on the scale of the Thouless energy). We may therefore replace $M^{\rm in}$, $M^{\rm out}$ by their value at $\varepsilon = \varepsilon' = E_F$ and assume that the energy dependence of M is given entirely by the scattering matrix.

The force operator can similarly be separated into $F = F^{\rm in} + F^{\rm out}$, where $F^{\rm in}$ and $F^{\rm out}$ are defined as in Eq. (7.4.1) with the matrix M replaced by $M^{\rm in}$ and $S^\dagger M^{\rm out} S$, respectively. We now proceed in the same way as in Ref. [19] for the current operator, by noting that the analyticity of $S(\varepsilon)$ in the upper half of the complex plane implies simple commutation relations:

$$\begin{aligned} &[F^{\rm in}(t), F^{\rm in}(t')] = 0, \;\; [F^{\rm out}(t), F^{\rm out}(t')] = 0, \;\; \forall\; t, t', \\ &[F^{\rm in}(t), F^{\rm out}(t')] = 0 \;\text{ if } t > t'. \end{aligned} \tag{7.4.6}$$

It follows that the Keldysh time ordering $\mathcal{T}_\pm$ of the force operators is the same as the so-called input-output ordering, defined by moving the operators $F_{\rm in}(t_-)$ to the left and $F_{\rm in}(t_+)$ to the right of all other operators — irrespective of the

value of the time arguments. The reason for preferring input-output ordering over time ordering is that Fourier transformation from time to energy commutes with the former ordering but not with the latter.

In the limit $t \to \infty$ different energies become uncoupled, and the cumulant generating function takes the simple form

$$\ln \mathcal{F}(\xi) = \frac{t}{2\pi} \int d\varepsilon \, \ln\langle e^{F^{\rm in}(\varepsilon)\xi/2} e^{F^{\rm out}(\varepsilon)\xi} e^{F^{\rm in}(\varepsilon)\xi/2}\rangle, \tag{7.4.7}$$

entirely analogous to the input-output ordered formula for charge transfer [19]. The Fourier transformed force is defined as

$$F^{\rm in}(\varepsilon) = c^\dagger(\varepsilon) M^{\rm in}(\varepsilon,\varepsilon) c(\varepsilon), \tag{7.4.8a}$$

$$F^{\rm out}(\varepsilon) = c^\dagger(\varepsilon) S^\dagger(\varepsilon) M^{\rm out}(\varepsilon,\varepsilon) S(\varepsilon) c(\varepsilon). \tag{7.4.8b}$$

(The operators c_n have been collected in a vector c.)

The matrices $M^{\rm in,out}$ are block diagonal,

$$M^{\rm in} = M^{\rm out *} = \begin{pmatrix} M_{\rm L} & 0 \\ 0 & M_{\rm R} \end{pmatrix}, \tag{7.4.9}$$

but the $N \times N$ matrices $M_{\rm L,R}$ are in general not diagonal themselves. They take a simple form for a longitudinal phonon mode, when $\mathbf{u}$ is a function of x in the x-direction (along the conductor), so that $u_{\alpha\beta}(\mathbf{r}) = \delta_{\alpha x}\delta_{\beta x} u'(x)$. The commutator $[[u', p_x], p_x]$ does not contribute because $\phi_n^{\rm in,out}$ is an eigenstate of p_x (with eigenvalue $p_n^{\rm in} = -p_n^{\rm out} \equiv p_n$). Hence for a longitudinal vibration one has

$$(M_{\rm L})_{nn'} = \delta_{nn'} |p_n| (u_0 - u_{\rm L}), \tag{7.4.10a}$$

$$(M_{\rm R})_{nn'} = \delta_{nn'} |p_n| (u_{\rm R} - u_0). \tag{7.4.10b}$$

The value of $u(x)$ in the scattering region is denoted by u_0, while $u_{\rm L}, u_{\rm R}$ denote the values at the left and right end of the conductor. The more complex situation of a transverse phonon mode, when the matrices $M_{\rm L,R}$ are no longer diagonal, is treated in Ref. [21].

We are now ready to calculate the expectation value in Eq. (7.4.7). We assume that the incident waves originate from reservoirs in thermal equilibrium at temperature T, with a voltage difference V between the left and right reservoir. The Fermi function in the left (right) reservoir is $f_{\rm L}$ ($f_{\rm R}$). We collect the Fermi functions in a diagonal matrix f and write

$$\langle c_n^\dagger(\varepsilon) c_{n'}(\varepsilon')\rangle = f_{nn'}(\varepsilon)\delta(\varepsilon - \varepsilon'), \quad f = \begin{pmatrix} f_{\rm L} & 0 \\ 0 & f_{\rm R} \end{pmatrix}. \tag{7.4.11}$$

All other expectation values of $c, c^\dagger$ vanish. We evaluate Eq. (7.4.7) with help of the determinantal identity

$$\left\langle \prod_i \exp(c^\dagger A_i c) \right\rangle = \Big|\Big| 1 - f + f \prod_i e^{A_i} \Big|\Big|, \tag{7.4.12}$$

valid for an arbitrary set of matrices A_i, and the identity

$$\exp(S^\dagger A S) = S^\dagger e^A S, \tag{7.4.13}$$

valid for unitary S. The result is

$$\ln \mathcal{F}(\xi) = \frac{t}{2\pi} \int d\varepsilon \, \ln ||1 - f + f e^{\xi M^{\rm in}} S^\dagger(\varepsilon) e^{\xi M^{\rm out}} S(\varepsilon)||, \tag{7.4.14}$$

where we have also used that the two matrices $M^{\rm in}$ and f commute.

At zero temperature $f_{\rm L} = \theta(E_F + eV - \varepsilon)$, $f_{\rm R} = \theta(E_F - \varepsilon)$. The energy range $\varepsilon < E_F$, where $f_{\rm L} = f_{\rm R} = 1$, contributes only to the first moment, while the energy range $E_F < \varepsilon < E_F + eV$, where $f_{\rm L} = 1$ and $f_{\rm R} = 0$, contributes to all moments. For small voltages we may neglect the energy dependence of $S(\varepsilon)$ in that range. Using the block structure (7.4.4), (7.4.9), of S, $M^{\rm in,out}$ the generating function for the second and higher cumulants takes the form

$$\ln \mathcal{F}(\xi) = \frac{eVt}{2\pi} \ln ||r^\dagger e^{\xi M_{\rm L}^*} r + t^\dagger e^{\xi M_{\rm R}^*} t|| + \mathcal{O}(\xi). \tag{7.4.15}$$

(By $\mathcal{O}(\xi)$ we mean terms linear in ξ.) This determinant can not be simplified further without knowledge of S. That is a major complication relative to the analogous formula for the charge transfer statistics [1], which can be cast entirely in terms of the transmission eigenvalues Γ_n (eigenvalues of $tt^\dagger$):

$$\begin{aligned} \ln \mathcal{F}_{\rm charge}(\xi) \;=\; & \frac{t}{2\pi} \int d\varepsilon \sum_n \ln \Big[1 + \Gamma_n (e^{e\xi} - 1) f_{\rm L}(1 - f_{\rm R}) \\ & + \Gamma_n (e^{-e\xi} - 1) f_{\rm R}(1 - f_{\rm L}) \Big]. \end{aligned} \tag{7.4.16}$$

In the case of momentum transfer, eigenvalues and eigenvectors both play a role.

7.5 Application to a one-dimensional conductor

7.5.1 Straight wire

Further simplification of Eqs. (7.4.14) and (7.4.15) is possible if the conductor is so narrow that it supports only a single propagating mode to the left and right of the scattering region ($N = 1$). The scattering matrix then consists of scalar transmission and reflection coefficients t, t', r, r' (related to each other by unitarity). We consider the case of a longitudinal vibration with

$$M^{\rm in} = M^{\rm out} = p_F \begin{pmatrix} u_0 - u_{\rm L} & 0 \\ 0 & u_{\rm R} - u_0 \end{pmatrix}, \tag{7.5.1}$$

cf. Eq. (7.4.10). Because of unitarity the result depends only on the transmission probability $\Gamma = |t|^2 = |t'|^2 = 1 - |r|^2 = 1 - |r'|^2$,

$$\begin{aligned}\ln \mathcal{F}(\xi) &= \frac{t}{2\pi}\int d\varepsilon\, \ln[1 + (e^{2\xi p_F(u_R - u_L)} - 1) f_L f_R \\ &\quad + \Gamma(e^{\xi p_F(u_R - u_L)} - 1)[f_L(1 - f_R) + f_R(1 - f_L)] \\ &\quad + (1 - \Gamma)(e^{2\xi p_F(u_0 - u_L)} - 1) f_L(1 - f_R) \\ &\quad + (1 - \Gamma)(e^{2\xi p_F(u_R - u_0)} - 1) f_R(1 - f_L)]. \end{aligned} \tag{7.5.2}$$

At zero temperature this simplifies further to

$$\ln \mathcal{F}(\xi) = \frac{eVt}{2\pi}\ln[1 + \Gamma e^{\xi p_F(u_R + u_L - 2u_0)} - \Gamma] + \mathcal{O}(\xi). \tag{7.5.3}$$

The zero temperature statistics (7.5.3) is binomial, just as for the charge. [The generating function $\mathcal{F}_{\text{charge}}(\xi)$ at $T = 0$ is obtained from Eq. (7.5.3) after substitution of $p_F(u_R + u_L - 2u_0)$ by e, cf. Eq. (7.4.16).] At finite temperatures one has the multinomial statistics (7.5.2), made up of stochastically independent elementary processes with more than two possible outcomes. The elementary processes may be characterized by the numbers $(n_{\text{in}}^L, n_{\text{in}}^R) \in \{0,1\}$ of electrons incident on the scatterer from the left, right and the numbers $(n_{\text{out}}^L, n_{\text{out}}^R) \in \{0,1\}$ of outgoing electrons to the left, right. The non-vanishing probabilities $P[(n_{\text{in}}^L, n_{\text{in}}^R) \to (n_{\text{out}}^L, n_{\text{out}}^R)]$ of scattering events evaluate to:

$$\begin{aligned} P[(0,0) \to (0,0)] &= (1 - f_L)(1 - f_R), \\ P[(0,1) \to (0,1)] &= (1 - f_L) f_R (1 - \Gamma), \\ P[(0,1) \to (1,0)] &= (1 - f_L) f_R \Gamma, \\ P[(1,0) \to (1,0)] &= f_L(1 - f_R)(1 - \Gamma), \\ P[(1,0) \to (0,1)] &= f_L(1 - f_R)\Gamma, \\ P[(1,1) \to (1,1)] &= f_L f_R. \end{aligned} \tag{7.5.4}$$

These probabilities appear in the generating function (7.5.3), multiplied by exponentials of ξ times the amount of transferred momentum.

A longitudinal vibration of a straight wire clamped at both ends would correspond to $u_L = u_R = 0$, $u_0 \neq 0$. In that special case Eq. (7.5.2) is equivalent to Eq. (7.4.16) for $\mathcal{F}_{\text{charge}}(\xi)$ under the substitution $\Gamma \to 1 - \Gamma$, $2p_F u_0 \to e$. In this case the multinomial statistics becomes a double-Poissonian in the limit $\Gamma \to 0$, corresponding to two independent Poisson processes originating from the left and right reservoirs [2]. A longitudinal vibration is difficult to observe, in contrast to a transverse vibration which can be observed optically [15, 16] or magnetomotively [17]. However, the direct excitation of a transverse mode is not possible in a single-channel conductor, while in a multi-channel conductor (width W) it is smaller than the excitation of a longitudinal mode by a factor $(W/L)^2$ [21]. So it would be desirable to find a way of coupling longitudinal electron motion to transverse vibration modes. In the following subsection we discuss how this can be achieved by bending the wire.

7.5.2 Bent wire

The bending of the wire is described as explained in Ref. [22], by means of a vector $\mathbf{\Omega}(s)$ that rotates the local coordinate system $\mathbf{e}_x(s), \mathbf{e}_y(s), \mathbf{e}_z(s)$ as one moves an infinitesimal distance ds along the wire: $\delta\mathbf{e}_\alpha = \mathbf{\Omega} \times \mathbf{e}_\alpha \delta s$. The local coordinate x is along the wire and y, z are perpendicular to it. The component $\Omega_{||}$ of $\mathbf{\Omega}$ along the wire describes a torsion (with $|\Omega_{||}|$ the torsion angle per unit length), while the perpendicular component $\Omega_\perp$ describes the bending (with $|\Omega_\perp|^{-1}$ the radius of curvature).

The momentum operators and wavefunctions, written in local coordinates, depend on the bending by terms of order $\lambda_F|\mathbf{\Omega}|$, which we assume to be $\ll 1$. These quantities may therefore be evaluated for a straight wire ($\mathbf{\Omega} = 0$). The dependence on the bending of the strain tensor is of order $L|\mathbf{\Omega}|$ and can not be neglected. For the interaction Hamiltonian (7.2.5) we need $\boldsymbol{\nabla}\mathbf{u}$ in the global coordinate system. It is obtained by differentiating the local coordinates of $\mathbf{u}$ as well as the local basis vectors. A bent wire can then be represented by a straight wire with an effective displacement $\mathbf{u}_{\rm eff}$ related to $\mathbf{u}$ (in local coordinates) by

$$\frac{\partial}{\partial x}\mathbf{u}_{\rm eff} = \frac{\partial}{\partial x}\mathbf{u} + \mathbf{\Omega} \times \mathbf{u}, \tag{7.5.5a}$$

$$\frac{\partial}{\partial y}\mathbf{u}_{\rm eff} = \frac{\partial}{\partial y}\mathbf{u}, \quad \frac{\partial}{\partial z}\mathbf{u}_{\rm eff} = \frac{\partial}{\partial z}\mathbf{u}. \tag{7.5.5b}$$

The second term on the right-hand-side of Eq. (7.5.5a) accounts for the centrifugal force exerted by an electron moving along the bent wire. It rotates a transverse mode, with $\mathbf{u}$ pointing in radial direction, into a fictitious longitudinal mode with $u_{{\rm eff},x}$ of order $L|\Omega_\perp|$. Note that in order for $\partial u_{{\rm eff},x}/\partial x$ to be non-zero, the displacement $\mathbf{u}$ needs to induce a stretching/compression of the wire. Only then is $\mathbf{e}_x \cdot \partial\mathbf{u}/\partial x = \partial u_x/\partial x + \mathbf{e}_x \cdot (\mathbf{\Omega} \times \mathbf{u}) = \partial u_{{\rm eff},x}/\partial x \neq 0$.

Fig. 7-2 shows two vibration modes in a bent wire with the corresponding longitudinal component $u_{{\rm eff},x}$ of the effective displacement. To apply the formulas of the previous subsection we need $u_{\rm L} = u_{{\rm eff},x}(x_{\rm L})$, $u_{\rm R} = u_{{\rm eff},x}(x_{\rm R})$, and $u_0 = u_{{\rm eff},x}(x_0)$. The first mode, Fig. 7-2a, has $u_{\rm L} = u_{\rm R} = 0$ and $u_0 \neq 0$. It measures the amount of electron momentum that has been transferred to the scatterer (located at x_0). The statistics of this process is equivalent to the charge transfer statistics (7.4.16), as mentioned at the end of the previous subsection.

The second mode, Fig. 7-2b, has $u_{\rm L} = 0$, $u_{\rm R} \neq 0$ and $u_0 \ll u_{\rm R}$ (assuming that the scatterer is located much closer to the left reservoir than to the right reservoir). It measures the amount of momentum transferred from the left to the right reservoir. Its statistics reads

$$\begin{aligned}\ln \mathcal{F}(\xi) = \frac{t}{2\pi}\int d\varepsilon \ln\{1 &+ (e^{2\xi p_F u_{\rm R}} - 1)[f_{\rm R} - \Gamma f_{\rm R}(1 - f_{\rm L})] \\ &+ \Gamma(e^{\xi p_F u_{\rm R}} - 1)[f_{\rm L}(1 - f_{\rm R}) + f_{\rm R}(1 - f_{\rm L})]\Big\}.\end{aligned} \tag{7.5.6}$$

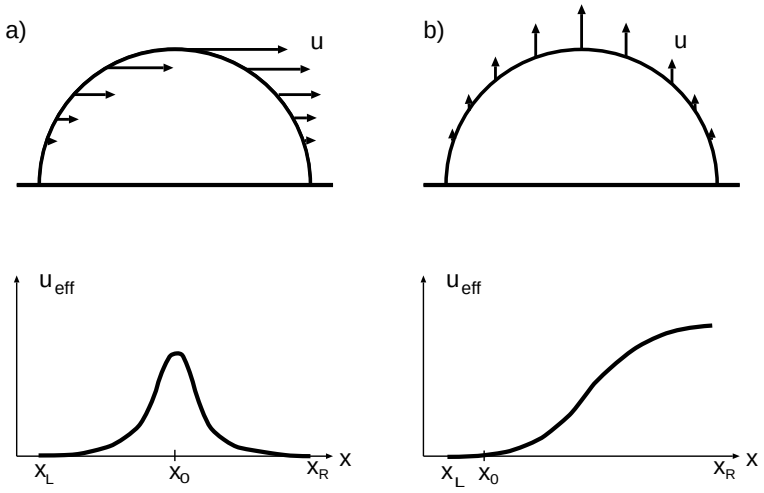

Figure 7-2. Two vibration modes in a bent wire (top) and the corresponding longitudinal displacements $\mathbf{u}_{\text{eff}}$ in the straight wire (bottom).

It cannot be reduced to the charge transfer statistics (7.4.16) by a substitution of variables, and in particular does not reduce to a double Poissonian in the limit $\Gamma \to 0$. (It remains multinomial in this limit.) Comparing the second cumulant $C^{(2)}$ of momentum with the second cumulant $C^{(2)}_{\text{charge}}$ of charge [the terms of order ξ^2 in Eqs. (7.4.16) and (7.5.6)], we find (setting $u_{\text{R}} \equiv 1$)

$$C^{(2)} - (p_F/e)^2 C^{(2)}_{\text{charge}} = \frac{2}{\pi} t p_F^2 k_B T (1-\Gamma). \tag{7.5.7}$$

The difference vanishes at zero temperature, in accordance with Eq. (7.5.3). It is independent of the voltage (as long as the energy dependence of Γ can be ignored), so the difference is an equilibrium property.

Eq. (7.5.7) can be given a physical interpretation by grouping the electrons to the right of the scattering region into $n_>$ right movers and $n_<$ left movers. The momentum transfer to the right reservoir is proportional to the sum $n_> + n_<$ while the charge transfer is proportional to the difference $n_> - n_<$, hence

$$\begin{aligned} C^{(2)} - \frac{p_F^2}{e^2} C^{(2)}_{\text{charge}} &\propto \langle\langle (n_> + n_<)^2 \rangle\rangle - \langle\langle (n_> - n_<)^2 \rangle\rangle \\ &= 4(\langle n_> n_< \rangle - \langle n_> \rangle \langle n_< \rangle). \end{aligned} \tag{7.5.8}$$

We see that the difference measures correlations between left and right-moving electrons. Such correlations are due to electrons that are backscattered with probability $1-\Gamma$. Eq. (7.5.7) describes the variance in the number of such backscattered electrons, given that electrons in an energy range $k_B T$ leave the right reservoir independently of each other.

7.6 Evaluation in terms of the Keldysh Green function

A scattering approach as in Sec. 7.4 is not possible if the displacement $\mathbf{u}(\mathbf{r})$ varies in the scattering region. Time ordering then no longer reduces to input-output ordering and we need the Keldysh technique to make progress [23]. Following the analogous formulation of the charge counting statistics [10], we write the generating function (7.3.4) as a single exponential of an integral along the Keldysh time contour,

$$\mathcal{F}(\xi) = \left\langle \mathcal{T}_\pm \exp\left[\tfrac{1}{2}\xi \int_0^t dt' \int d\mathbf{r}\, F_\pm(\mathbf{r},t')\right]\right\rangle, \tag{7.6.1a}$$

$$F_\pm(\mathbf{r},t) = \frac{1}{m}\sum_{\sigma=\pm} \psi^\dagger_\sigma(\mathbf{r},t) p_\alpha u_{\alpha\beta}(\mathbf{r}) p_\beta \psi_\sigma(\mathbf{r},t). \tag{7.6.1b}$$

We have written the force operator in second quantized form, as in Eq. (7.4.1), but do not assume that the electron field operator $\psi_\pm(\mathbf{r},t) \equiv \psi(\mathbf{r},t_\pm)$ takes its asymptotic form in terms of incident and outgoing states.

The generating function can be expressed in terms of the Keldysh Green function G,

$$\frac{d}{d\xi}\ln\mathcal{F}(\xi) = \frac{i}{2m}\sum_{\sigma=\pm}\sigma\int_0^t dt'\int d\boldsymbol{R}\, u_{\alpha\beta}(\boldsymbol{R})\frac{\partial^2}{\partial r_\alpha \partial r_\beta} G_{\sigma\sigma}(\mathbf{R},\mathbf{r},t',t';\xi)\Big|_{\mathbf{r}=0}. \tag{7.6.2}$$

The Green function $G_{\sigma\sigma'}$ is a 2×2 matrix in the indices $\sigma,\sigma' \in \{+,-\}$ that assure the correct time ordering of the operators. It is defined by

$$G_{\sigma\sigma'}(\mathbf{R},\mathbf{r},t,t';\xi) = \frac{-i\sigma\left\langle \mathcal{T}_\pm \psi_\sigma(\mathbf{R}+\frac{1}{2}\mathbf{r},t)\psi^\dagger_{\sigma'}(\mathbf{R}-\frac{1}{2}\mathbf{r},t')\exp\left[\frac{1}{2}\xi\int_0^t dt'\int d\mathbf{r}'\, F_\pm(\mathbf{r}',t')\right]\right\rangle}{\left\langle \mathcal{T}_\pm \exp\left[\frac{1}{2}\xi\int_0^t dt'\int d\mathbf{r}'\, F_\pm(\mathbf{r}',t')\right]\right\rangle}. \tag{7.6.3}$$

7.7 Application to a diffusive conductor

We apply the formalism of Sec. 7.6 to the example of diffusive electron transport through a freely suspended disordered wire. The semi-classical calculation of the transverse momentum noise in this geometry was done in Ref. [8], so we can compare results.

For long detection times we may assume that the Green function (7.6.3) depends only on the difference $\tau = t - t'$ of the time arguments. A Fourier transform gives

$$G_{\sigma\sigma'}(\boldsymbol{R},\boldsymbol{p},\varepsilon;\xi) = \int d\boldsymbol{r}\int d\tau\; e^{-i\boldsymbol{p}\cdot\boldsymbol{r}-i\varepsilon\tau} G_{\sigma\sigma'}(\boldsymbol{R},\boldsymbol{r},\tau;\xi). \tag{7.7.1}$$

We write $\mathbf{p} = |\mathbf{p}|\mathbf{n}$ and use the fact that in the semi-classical limit the Green function is peaked as a function of the absolute value $|\mathbf{p}|$ of the momentum. Integration over this variable yields the semi-classical Green function [23]

$$G_{\sigma\sigma'}(\boldsymbol{R},\mathbf{n},\varepsilon;\xi) = \frac{i}{\pi}\int d\varepsilon'\; G_{\sigma\sigma'}(\boldsymbol{R},\boldsymbol{n}\sqrt{2m\varepsilon'},\varepsilon;\xi). \tag{7.7.2}$$

We next make the diffusion approximation, expanding the $\mathbf{n}$-dependence in spherical harmonics,

$$\begin{aligned} G_{\sigma\sigma'}(\boldsymbol{R},\mathbf{n},\varepsilon;\xi) &= G^{(0)}_{\sigma\sigma'}(\boldsymbol{R},\varepsilon;\xi) + n_\alpha G^{(1)}_{\alpha\sigma\sigma'}(\boldsymbol{R},\varepsilon;\xi) \\ &\quad + (n_\alpha n_\beta - \tfrac{1}{3}\delta_{\alpha\beta})G^{(2)}_{\alpha\beta\sigma\sigma'}(\boldsymbol{R},\varepsilon;\xi). \end{aligned} \tag{7.7.3}$$

Substituting Eq. (7.7.3) into Eq. (7.6.2) we find

$$\begin{aligned} \frac{d}{d\xi}\ln F(\xi) &= \tfrac{1}{2}tE_F\nu\sum_{\sigma=\pm}\sigma\int d\varepsilon\int d\boldsymbol{R}\; u_{\alpha\beta}(\boldsymbol{R}) \\ &\quad\times\left[\frac{1}{3}\delta_{\alpha\beta}G^{(0)}_{\sigma\sigma}(\boldsymbol{R},\varepsilon;\xi) + \frac{2}{15}G^{(2)}_{\alpha\beta\sigma\sigma}(\boldsymbol{R},\varepsilon;\xi)\right], \end{aligned} \tag{7.7.4}$$

where $\nu = p_F^2/2\pi^2 v_F$ is the density of states.

The equation of motion for the semi-classical Green function in the diffusion approximation is derived in the same way as for the charge statistics [10]. We find

$$2ln_\alpha\frac{\partial}{\partial R_\alpha}G + [G^{(0)},G] + \xi p_F l u_{\alpha\beta}n_\alpha n_\beta[\tau_3,G] = 0. \tag{7.7.5}$$

The length l is the mean free path, assuming isotropic impurity scattering. The commutators $[..,..]$ are taken with respect to the Keldysh indices σ,σ' and τ_3 is the third Pauli matrix in these indices. The Green function satisfies the normalization condition $G^2 = 1$ that is respected by the differential equation (7.7.5). The boundary conditions at the left and right ends of the wire are [10]

$$\begin{aligned} G_{\rm L} &= \begin{pmatrix} 1-2f_{\rm L} & 2f_{\rm L} \\ 2-2f_{\rm L} & 2f_{\rm L}-1 \end{pmatrix}, \\ G_{\rm R} &= \begin{pmatrix} 1-2f_{\rm R} & 2f_{\rm R} \\ 2-2f_{\rm R} & 2f_{\rm R}-1 \end{pmatrix}. \end{aligned} \tag{7.7.6}$$

By projecting Eq. (7.7.5) onto spherical harmonics we find that, to leading order in l/L, the second harmonic $G^{(2)}$ depends only on the zeroth harmonic $G^{(0)}$:

$$G^{(2)}_{\alpha\beta} = \frac{\xi}{2}p_F l(u_{\alpha\beta} - \frac{1}{3}\delta_{\alpha\beta}u_{\gamma\gamma})G^{(0)}[\tau_3,G^{(0)}][1+\mathcal{O}(l/L)^2]. \tag{7.7.7}$$

Combining this relation with Eq. (7.7.4) we see that the momentum statistics of a transverse mode, with $u_{xx} = 0$, $u_{x\gamma} \neq 0$, follows from

$$\frac{d}{d\xi}\ln F(\xi) = \frac{\xi}{30}tp_F l E_F\nu\sum_{\sigma,\alpha,\beta}\int d\varepsilon\int d\boldsymbol{R}\; u^2_{\alpha\beta}\left(\tau_3 G^{(0)}[\tau_3,G^{(0)}]\right)_{\sigma\sigma}. \tag{7.7.8}$$

It remains to compute $G^{(0)}$. To calculate $\ln \mathcal{F}$ to order ξ^2, that is to calculate the variance $C^{(2)}$ of the force noise, it is sufficient to know $G^{(0)}$ for $\xi = 0$. The solution to the unperturbed diffusion equation (7.7.5) is known [10],

$$G^{(0)}(\mathbf{R}, \varepsilon; \xi = 0) = \begin{pmatrix} 1 - 2f(\mathbf{R}, \varepsilon) & 2f(\mathbf{R}, \varepsilon) \\ 2 - 2f(\mathbf{R}, \varepsilon) & 2f(\mathbf{R}, \varepsilon) - 1 \end{pmatrix}, \tag{7.7.9}$$

where $f(\boldsymbol{R}, \varepsilon) = f_{\mathrm{L}}(\varepsilon) + (x/L)[f_{\mathrm{R}}(\varepsilon) - f_{\mathrm{L}}(\varepsilon)]$. (The coordinate x runs along the wire, from $x = 0$ to $x = L$.) We find

$$C^{(2)} = t\frac{16}{15} p_F l E_F \nu A \int_0^L dx d\varepsilon \, u_{xy}^2(x) f(x, \varepsilon)[1 - f(x, \varepsilon)], \tag{7.7.10}$$

with A the cross-sectional area of the wire. This is the same result as in Ref. [8].

More complicated networks of diffusive wires, including tunnel barriers or point contacts, can be treated in the same way. In such situations the unperturbed Green function $G^{(0)}(\mathbf{R}, \varepsilon; \xi = 0)$ can be determined using Nazarov's circuit theory [24] and then substituted into Eq. (7.7.8).

7.8 Conclusion

We conclude by estimating the order of magnitude of the cumulants of the displacement distribution $P(Q)$ of a vibrating current-carrying wire. For an oscillator with a large quality factor only the even order cumulants $\langle\langle Q^{2k}\rangle\rangle$ are appreciable, given in good approximation by

$$\langle\langle Q^{2k}\rangle\rangle \approx \frac{1}{2k}(M\omega_0)^{-2k}\frac{\mathcal{Q}}{\omega_0}\lim_{t\to\infty}\frac{1}{t}\langle\langle \triangle P(t)^{2k}\rangle\rangle, \tag{7.8.1}$$

cf. Eqs. (7.3.9) and (7.3.11). The cumulants of transferred momentum $\triangle P$ have been calculated for a single-channel conductor with a localized scatterer in Sec. 7.5. At zero temperature one has

$$\lim_{t\to\infty}\frac{1}{t}\langle\langle \triangle P(t)^{2k}\rangle\rangle = \frac{eV}{2\pi\hbar}p_F^{2k}(u_{\mathrm{R}} + u_{\mathrm{L}} - 2u_0)^{2k}\frac{d^{2k}}{d\xi^{2k}}\ln[1 + \Gamma(e^{\xi} - 1)]\Big|_{\xi=0}, \tag{7.8.2}$$

cf. Eq. (7.5.3). (We have reinserted Planck's constant $\hbar$ for clarity.)

Combining Eqs. (7.8.1) and (7.8.2) we see that in order of magnitude $\langle\langle Q^{2k}\rangle\rangle \simeq (eV\mathcal{Q}/\hbar\omega_0)(p_F/M\omega_0)^{2k}$. Inserting parameter values (following Ref. [7]) $V = 1\,\mathrm{mV}$, $\mathcal{Q} = 10^3$, $\omega_0/2\pi = 5\,\mathrm{GHz}$, $p_F = 2 \cdot 10^{-24}\,\mathrm{Ns}$, and $M = 10^{-20}\,\mathrm{kg}$, we estimate

$$\langle\langle Q^{2k}\rangle\rangle^{1/2k} \approx 10^{4/2k} \times 10^{-4}\text{Å}. \tag{7.8.3}$$

Detectors with a 10^{-4}Å sensitivity have been proposed [25]. For a measurement of higher order cumulants one would want cumulants of different order to be of roughly the same magnitude. This can be achieved by choosing the number $eV\mathcal{Q}/\hbar\omega_0$ not too large. For the parameters chosen above, $\langle\langle Q^4\rangle\rangle^{1/4}/\langle\langle Q^2\rangle\rangle^{1/2} \approx 0.1$.

The theory presented in this work is more than a framework for the calculation of higher order cumulants in the momentum transfer statistics. It also provides for a formalism to treat quantum effects in electromechanical noise. A first application, to quantum size effects in a constriction, has been realized [21]. Other applications, including resonant tunneling, superconductivity, and interaction effects, are envisaged.

Appendix A: Derivation of the unitary transformation (7.2.4)

We demonstrate that the operator U given in Eq. (7.2.4) has the desired property (7.2.3) of eliminating the phonon displacement from the ion potential. By expanding the exponential in Eq. (7.2.4) we calculate the effect of U on a one-electron and one-phonon wavefunction in the position space representation:

$$U\psi(\boldsymbol{r},q) = ||J||^{1/2}\,\psi[\boldsymbol{r}-q\boldsymbol{u}(\boldsymbol{r}),q]. \tag{A.1}$$

We prove Eq. (7.2.3) by calculating matrix elements,

$$\begin{aligned}&\langle\psi_1|U^\dagger V[\boldsymbol{r}-Q\boldsymbol{u}(\boldsymbol{r})]U|\psi_2\rangle = \\ &\int d\mathbf{r}\int dq\,||J||\,\psi_1^*[\mathbf{r}-q\mathbf{u}(\mathbf{r}),q]V[\boldsymbol{r}-q\boldsymbol{u}(\boldsymbol{r})]\psi_2[\mathbf{r}-q\mathbf{u}(\mathbf{r}),q] \\ &= \int d\tilde{\mathbf{r}}\int dq\;\psi_1^*(\tilde{\mathbf{r}},q)V(\tilde{\boldsymbol{r}})\psi_2(\tilde{\mathbf{r}},q) = \langle\psi_1|V|\psi_2\rangle.\end{aligned} \tag{A.2}$$

The unitarity of U follows as the special case $V\equiv 1$.

We now justify the replacement of $\tilde{\rho}=U^\dagger\rho U$ with ρ and $\tilde{A}=U^\dagger AU$ by A in the generating function (7.2.8), in the limit of a long detection time t. Since Q commutes with U, it is sufficient to consider $A=P$. (Then $\tilde{A}=A(Q,\tilde{P})$ in the more general case that A is a function of both Q and P.) To first order in the displacement one has

$$\tilde{P} = P-\Pi+\mathcal{O}(\mathbf{u}^2). \tag{A.3}$$

The difference between $\tilde{P}$ and P is of the order of the total momentum Π inside the wire, which is t-independent in a stationary state. Since the expectation value (as well as higher cumulants) of P increases linearly with t, we can neglect the difference between $\tilde{P}$ and P for large t.

To justify the replacement of $\tilde{\rho}$ by ρ we note that the effect of U on the initial state is to shift the electron coordinates by the local phonon displacement [cf. Eq. (A.1)]. This initial shift has only a transient effect and can be neglected for large t.

Appendix B: Effective mass approximation

We start with the Hamiltonian (7.2.5) with $V = V_{\rm lat} + V_{\rm imp}$. In the absence of any deformation of the periodic lattice one has, in the effective mass approximation,

$$\frac{1}{2m}\mathbf{p}^2 + V_{\rm lat}(\mathbf{r}) = \frac{1}{2m^*}\mathbf{p}^{*2}. \tag{B.1}$$

The quasimomentum operator $\mathbf{p}^*$ is defined in terms of the Bloch function $g(\mathbf{r})$ by $\mathbf{p}^* = -ig\boldsymbol{\nabla}g^{-1}$. We seek a similar approximation to the same Hamiltonian in a distorted lattice, assuming that $\mathbf{u}$ is sufficiently smooth that we can neglect derivatives of the shear tensor $u_{\alpha\beta}$. The Hamiltonian (7.2.5) (for one electron) then has the form

$$H = \frac{1}{2m}p_\alpha(\delta_{\alpha\beta} - 2Qu_{\alpha\beta})p_\beta + V_{\rm lat} + V_{\rm imp} - \frac{1}{M}P\Pi + \Omega a^\dagger a. \tag{B.2}$$

For small displacements Q the real symmetric matrix $X_{\alpha\beta} = \delta_{\alpha\beta} - 2Qu_{\alpha\beta}$ is positive definite. We can therefore factorize $\mathbf{X} = \mathbf{T}\mathbf{T}^T$, with $\mathbf{T}$ real. We change coordinates to $\tilde{\mathbf{r}} = \mathbf{T}^{-1}\mathbf{r}$ and find

$$H = -\frac{1}{2m}\frac{\partial}{\partial\tilde{r}_\alpha}\frac{\partial}{\partial\tilde{r}_\alpha} + V_{\rm lat}(\mathbf{T}\tilde{\mathbf{r}}) + V_{\rm imp}(\mathbf{T}\tilde{\mathbf{r}}) - \frac{1}{M}P\Pi + \Omega a^\dagger a. \tag{B.3}$$

We now make the assumption of a deformation independent effective mass [12,13], that is to say, we assume that the Hamiltonian with the distorted lattice potential $V_{\rm lat}(\mathbf{T}\tilde{\mathbf{r}})$ is approximated as in Eq. (B.1) with distorted Bloch functions, but the same effective mass m^*. Hence

$$H = -\frac{1}{2m^*}\left[g(\mathbf{T}\tilde{\mathbf{r}})\frac{\partial}{\partial\tilde{r}_\alpha}\frac{1}{g(\mathbf{T}\tilde{\mathbf{r}})}\right]^2 + V_{\rm imp}(\mathbf{T}\tilde{\mathbf{r}}) - \frac{1}{M}P\Pi + \Omega a^\dagger a. \tag{B.4}$$

Transforming back to the original coordinates we arrive at the Hamiltonian

$$H = \frac{1}{2m^*}p^*_\alpha(\delta_{\alpha\beta} - 2Qu_{\alpha\beta})p^*_\beta + V_{\rm imp} - \frac{1}{M}P\Pi + \Omega a^\dagger a \tag{B.5}$$

given in Sec. 7.2.

Bibliography

[1] L. S. Levitov and G. B. Lesovik, JETP Lett. **58**, 230 (1993); L. S. Levitov, H. Lee, and G. B. Lesovik, J. Math. Phys. **37**, 4845 (1996).

[2] L. S. Levitov and M. Reznikov, cond-mat/0111057.

[3] Ya. M. Blanter and M. Büttiker, Phys. Rep. **336**, 1 (2000).

[4] D. B. Gutman and Y. Gefen, cond-mat/0201007.

[5] B. Yurke and G. P. Kochanski, Phys. Rev. B **41**, 8184 (1990).

[6] C. Presilla, R. Onofrio, and M. F. Bocko, Phys. Rev. B **45**, 3735 (1992).

[7] N. F. Schwabe, A. N. Cleland, M. C. Cross, and M. L. Roukes, Phys. Rev. B **52**, 12911 (1995).

[8] A. V. Shytov, L. S. Levitov, and C. W. J. Beenakker, Phys. Rev. Lett. **88**, 228303 (2002).

[9] M. L. Roukes, Phys. World **14**, 25 (2001); cond-mat/0008187.

[10] Yu. V. Nazarov, Ann. Phys. (Leipzig) **8**, 507 (1999).

[11] K. E. Nagaev, cond-mat/0203503.

[12] V. M. Kontorovich, Sov. Phys. Usp. **27**, 134 (1984).

[13] V. B. Fiks, Sov. Phys. JETP **48**, 68 (1978).

[14] Yu. V. Nazarov and M. Kindermann, cond-mat/0107133.

[15] G. Meyer and N. M. Amer, Appl. Phys. Lett. **53**, 1045 (1988).

[16] M. M. J. Treacy, T. W. Ebbesen, and J. M. Gibson, Nature (London) **381**, 678 (1996).

[17] A. N. Cleland and M. L. Roukes, Appl. Phys. Lett. **69**, 2653 (1996).

[18] B. A. Muzykantskii and D. E. Khmelnitskii, Phys. Rev. B **50**, 3982 (1994).

[19] C. W. J. Beenakker and H. Schomerus, Phys. Rev. Lett. **86**, 700 (2001).

[20] M. Büttiker, Phys. Rev. Lett. **65**, 2901 (1990).

[21] A. Tajic, M. Kindermann, and C. W. J. Beenakker, cond-mat/0206306.

[22] L. D. Landau and E. M. Lifshitz, *Theory of Elasticity* (Pergamon, Oxford, 1959): § 18.

[23] J. Rammer and H. Smith, Rev. Mod. Phys. **58**, 323 (1986).

[24] Yu. V. Nazarov, in: *Quantum Dynamics of Submicron Structures*, edited by H. A. Cerdeira, B. Kramer, and G. Sch/"on, NATO ASI Series E291 (Kluwer, Dordrecht, 1995).

[25] Y. Zhang and M. P. Blencowe, J. Appl. Phys. **91**, 4249 (2002).

8 Manipulation of photon statistics of highly degenerate incoherent radiation

Chaotic radiation is the name given in quantum optics to a gas of photons that has a Gaussian density matrix [1]. (To avoid misunderstanding, we note that chaotic radiation is not in any way related to chaos in classical mechanics.) The radiation emitted by a black body is a familiar example. The statistics of black-body radiation, as measured by a photodetector, is very close to the Poisson statistics of a gas of classical independent particles. Deviations due to photon bunching exist, but these are small corrections. To see effects of Bose statistics one needs a *degenerate* [2] photon gas, with an occupation number f of the modes that is $\gtrsim 1$. Black-body radiation at optical frequencies is non-degenerate to a large degree ($f \simeq e^{-\hbar\omega/kT} \ll 1$), even at temperatures reached on the surface of the Sun.

The degeneracy is no longer restricted by frequency and temperature if the photon gas is brought out of thermal equilibrium. The coherent radiation from a laser would be an extreme example of high degeneracy, but the counting statistics is still Poissonian because of the special properties of a coherent state [1]. One way to create non-equilibrium chaotic radiation is spectral filtering within the quantum-limited line width of a laser [3]. This will typically be single-mode radiation. For multi-mode radiation one can pass black-body radiation through a linear amplifier. The amplification might be due to stimulated emission by an inverted atomic population or to stimulated Raman scattering [4]. Alternatively, one can use the spontaneous emission from an amplifying medium that is well below the laser threshold [5], or parametric down-conversion in a non-linear crystal [1].

The purpose of this chapter is to show that the statistics of degenerate chaotic radiation can be manipulated by introducing scatterers, to an extent that would be impossible for both non-degenerate chaotic radiation and degenerate coherent radiation. We will illustrate the difference by examining in some detail a simple geometry consisting of one or two weakly transmitting barriers (in analogy with tunnel barriers for electrons) [6] embedded in a waveguide (see Fig. 8-1). For the single barrier the photocount distribution is close to Poissonian. The mean photocount $\bar{n}$ is only changed by a factor of two upon insertion of the second barrier. But the fluctuations around the mean are greatly enhanced, as a result of multiple scattering in a region of large occupation number. We find that the distribution $P(n)$ for the double-barrier geometry is not only much broader than a Poisson distribution, it also has a markedly different shape.

We consider a source of chaotic radiation that is not in thermal equilibrium. Chaotic radiation is characterized by a Gaussian density matrix ρ in the coherent

state representation [1]. For a single mode it takes the form

$$\rho = \int d\alpha d\alpha^* (\pi\mu)^{-1} \exp(-\alpha^* \mu^{-1} \alpha) |\alpha\rangle\langle\alpha|, \tag{8.0.1}$$

where μ is a positive real number and $|\alpha\rangle$ is a coherent state (eigenstate of the photon annihilation operator a) with complex eigenvalue α. If one takes into account more modes, α becomes a vector $\boldsymbol{\alpha}$ and μ a matrix $\boldsymbol{\mu}$ in the space of modes. (The factor $\pi\mu$ then becomes the determinant $||\pi\boldsymbol{\mu}||$.) We take a waveguide geometry and assume that the radiation is restricted to a narrow frequency interval $\delta\omega$ around ω_0. In this case the indices n,m of α_n, μ_{mn} label the N propagating waveguide modes at frequency ω_0.

In thermal equilibrium at temperature T, the covariance matrix $\boldsymbol{\mu} = f\,\underline{1}$ equals the unit matrix $\underline{1}$ times the scalar factor $f = (e^{\hbar\omega/kT} - 1)^{-1}$, being the Bose-Einstein distribution function. Multi-mode chaotic radiation out of thermal equilibrium has in general a non-scalar $\boldsymbol{\mu}$. We assume that $\boldsymbol{\mu}$ is a property of the amplifying medium, independent of the scattering properties of the waveguide to which it is coupled. Feedback from the waveguide into the amplifier is therefore neglected.

The radiation is fully absorbed at the other end of the waveguide by a photodetector. We seek the probability distribution $P(n)$ to count n photons in a time t. It is convenient to work with the cumulant generating function $F(\xi) = \ln[\sum_n e^{\xi n} P(n)]$. For long counting times $t\delta\omega \gg 1$ it is given by the Glauber formula [1, 7]

$$F(\xi) = \frac{t\delta\omega}{2\pi} \ln \mathrm{Tr}\, (\rho : \exp[(e^{\xi} - 1)\mathbf{a}^\dagger_{\mathrm{out}} \mathbf{a}_{\mathrm{out}}] :). \tag{8.0.2}$$

Here $\boldsymbol{a}_{\mathrm{out}}$ is the vector of annihilation operators for the modes going out of the waveguide and into the photodetector. The colons $:\ :$ indicate normal ordering (creation operators to the left of annihilation operators). The transmission matrix $\boldsymbol{t}$ relates $\boldsymbol{a}_{\mathrm{out}} = \boldsymbol{t}\boldsymbol{a}$ to the vector $\boldsymbol{a}$ of annihilation operators entering the waveguide. Substituting Eq. (8.0.1) for ρ, we find

$$\begin{aligned} F(\xi) &= \frac{t\delta\omega}{2\pi} \ln \int d\boldsymbol{\alpha} d\boldsymbol{\alpha}^* ||\pi\boldsymbol{\mu}||^{-1} \exp[-\boldsymbol{\alpha}^* \boldsymbol{\mu}^{-1} \boldsymbol{\alpha}) + (e^{\xi} - 1)\boldsymbol{\alpha}^* \boldsymbol{t}^\dagger \boldsymbol{t} \boldsymbol{\alpha}] \\ &= -\frac{t\delta\omega}{2\pi} \ln ||\underline{1} - (e^{\xi} - 1)\boldsymbol{\mu}\boldsymbol{t}^\dagger \boldsymbol{t}||. \end{aligned} \tag{8.0.3}$$

In thermal equilibrium, when $\boldsymbol{\mu} = f\,\underline{1}$, the determinant can be evaluated in terms of the eigenvalues T_n of the matrix product $\boldsymbol{t}^\dagger \boldsymbol{t}$. The resulting expression [5, 8]

$$F(\xi) = -\frac{t\delta\omega}{2\pi} \sum_{n=1}^{N} \ln[1 - (e^{\xi} - 1) f T_n)] \tag{8.0.4}$$

has a similar form as the generating function of the electronic charge counting distribution at zero temperature [9],

$$F_{\mathrm{electron}}(\xi) = \frac{teV}{2\pi\hbar} \sum_{n=1}^{N} \ln[1 + (e^{\xi} - 1) T_n], \tag{8.0.5}$$

where V is the applied voltage.

If the eigenvalues of $\boldsymbol{t\mu t}^\dagger$ are $\ll 1$, we may expand the logarithm in Eq. (8.0.3) to obtain $F(\xi) = \bar{n}(e^\xi - 1)$, with mean photocount $\bar{n} = (t\delta\omega/2\pi)\mathrm{Tr}\ \boldsymbol{\mu t}^\dagger \boldsymbol{t}$. The corresponding photocount distribution is Poissonian,

$$P_{\mathrm{Poisson}}(n) = \frac{1}{n!}\bar{n}^n e^{-\bar{n}}. \tag{8.0.6}$$

In thermal equilibrium the deviations from a Poisson distribution will be very small, because the Bose-Einstein function is $\ll 1$ at optical frequencies for any realistic temperature. There is no such restriction on the covariance matrix $\boldsymbol{\mu}$ out of equilibrium. This leads to striking deviations from Poisson statistics.

As a measure for deviations from a Poisson distribution we consider the deviations from unity of the Fano factor. From Eq. (8.0.4) we derive

$$\mathcal{F} = \frac{\mathrm{Var}\ n}{\bar{n}} = 1 + \frac{\mathrm{Tr}\ (\boldsymbol{\mu t}^\dagger \boldsymbol{t})^2}{\mathrm{Tr}\ \boldsymbol{\mu t}^\dagger \boldsymbol{t}}. \tag{8.0.7}$$

A Fano factor $\mathcal{F} > 1$ indicates photon bunching. For example, for black-body radiation $\mathcal{F} = 1 + f$. One might surmise that photon bunching is negligible if the waveguide is weakly transmitting, so that $N^{-1}\mathrm{Tr}\ \boldsymbol{t}^\dagger \boldsymbol{t} \ll 1$. That is correct if the weak transmission is due to a single barrier. Then each transmission eigenvalue $T_n \ll 1$, hence $\mathcal{F} \approx 1$. However, if a second identical barrier is placed in series with the first one a remarkable increase in the Fano factor occurs.

Let us first demonstrate this effect for a scalar $\boldsymbol{\mu} = f\mathbb{1}$, when it has a well-known electronic analogue [10, 11]. We assume that $N \gg 1$ so that we may replace traces in Eq. (8.0.7) by integrations over the transmission eigenvalue T with density $\rho(T)$,

$$\mathcal{F} = 1 + f\frac{\int_0^1 dT\rho(T)T^2}{\int_0^1 dT\rho(T)T}. \tag{8.0.8}$$

For a single barrier $\rho(T)$ is sharply peaked at a transmittance $\Gamma \ll 1$. Hence, $\mathcal{F} \approx 1$ for a single barrier. For two identical barriers in series the density is bimodal [12],

$$\rho(T) = \frac{N\Gamma}{2\pi}T^{-3/2}(1-T)^{-1/2}, \tag{8.0.9}$$

with a peak near $T = 0$ and at $T = 1$. From this distribution we find that

$$\mathcal{F} = 1 + \tfrac{1}{2}f. \tag{8.0.10}$$

While the second barrier reduces the mean photocount by only a factor of two, independently of the occupation number f of the modes of the incident radiation, it can greatly increase the Fano factor for large f (see Fig. 8-1). From the electronic analogue (8.0.5) we would find $\mathcal{F} = 1$ for a single barrier and $\mathcal{F} = 1 - \frac{1}{2} = \frac{1}{2}$ for a double barrier [10]. We conclude that for electrons the effect of the second barrier on the mean current and the Fano factor are comparable

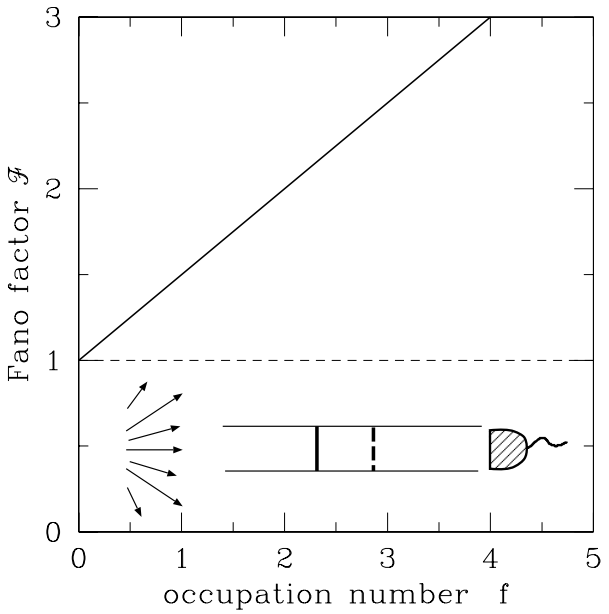

Figure 8-1. Dependence of the Fano factor on the occupation number of the modes, for transmission through one (dashed line) or two barriers (solid line). The inset shows schematically the photodetector (shaded) and the waveguide containing one or two barriers.

(both being a factor of two), while for photons the effect on the Fano factor can be orders of magnitude greater than on the mean current for $f \gg 1$.

The two terms 1 and $\frac{1}{2}f$ in Eq. (8.0.10) account, respectively, for the particle and the wave nature of the radiation. For a classical wave the mean of the squared intensity fluctuations is proportional to the mean intensity squared, hence a classical wave has a Fano factor that varies linearly with f. In the double barrier geometry there is a high intensity of the radiation in a region with strong multiple scattering and this enhances the wave contribution to $\mathcal{F}$ relative to the particle contribution. This explains in simple terms why $\mathcal{F} \propto f$ for $f \gg 1$, but to find the numerical coefficient $\frac{1}{2}$ and the crossover to particle-like behaviour relevant in the single barrier geometry requires an explicit calculation.

Changing the nature of the multiple scattering will change the numerical coefficient. For example, multiple scattering by disorder would give $\mathcal{F} = 1 + \frac{2}{3}f$, in analogy with the electronic result [13, 14] $\mathcal{F} = 1 - \frac{2}{3} = \frac{1}{3}$. What the double-barrier and the disordered case have in common is a $\rho(T)$ that is bimodal, with peaks at $T = 0, 1$. The shape of the peaks depends on the type of multiple scattering, and that in turn affects the numerical coefficients, but the coefficient remains of order unity. (The single barrier, in contrast, has a uni-modal $\rho(T)$, with a single peak at $T = \Gamma$.) The bimodal $\rho(T)$ can be understood as being a precursor of wave localization due to multiple scattering [16]. The bimodal

$\rho(T)$ does not depend on the separation L of the barriers, as long as it is large compared to the wavelength λ and short compared to the absorption length ξ. For $L \lesssim \lambda$ we are back to the single-barrier case and for $L \gg \xi$ the Fano factor tends to zero.

We now generalize Eq. (8.0.10) to a non-scalar $\boldsymbol{\mu}$. An extreme case is a covariance matrix of rank one having all eigenvalues μ_n equal to zero except a single one. This would happen if the waveguide is far removed from the source, so that its cross-sectional area A is smaller than the coherence area A_c [15]. Since Tr $(\boldsymbol{\mu}\boldsymbol{t}^\dagger\boldsymbol{t})^2 = (\text{Tr } \boldsymbol{\mu}\boldsymbol{t}^\dagger\boldsymbol{t})^2$ if $\boldsymbol{\mu}$ is of rank one, the Fano factor reduces to $\mathcal{F} = 1 + \text{Tr } \boldsymbol{\mu}\boldsymbol{t}^\dagger\boldsymbol{t}$. The trace of $\boldsymbol{\mu}\boldsymbol{t}^\dagger\boldsymbol{t}$ is $\ll 1$ for both a single and double barrier geometry, hence a second barrier has no large effect on the noise if $A \lesssim A_c$.

More generally, for a non-scalar $\boldsymbol{\mu}$ the Fano factor (8.0.7) depends not just on the eigenvalues T_n of $\boldsymbol{t}^\dagger\boldsymbol{t}$, but also on the eigenvectors. We write $\boldsymbol{t}^\dagger\boldsymbol{t} = \boldsymbol{U}^\dagger\boldsymbol{\tau}\boldsymbol{U}$, with $\boldsymbol{U}$ the unitary matrix of eigenvectors. We assume strong intermode scattering by disorder inside the waveguide. The resulting $\boldsymbol{U}$ will then be uniformly distributed in the unitary group, independent of $\boldsymbol{\tau}$ [16]. For $N \gg 1$ we can replace the traces in numerator and denominator in Eq. (8.0.7) by integrations over $\boldsymbol{U}$, with the result

$$\mathcal{F} = 1 + \langle\boldsymbol{\mu}\rangle\langle\boldsymbol{\tau}\rangle + \langle\boldsymbol{\mu}\rangle\frac{\langle\langle\boldsymbol{\tau}^2\rangle\rangle}{\langle\boldsymbol{\tau}\rangle} + \langle\boldsymbol{\tau}\rangle\frac{\langle\langle\boldsymbol{\mu}^2\rangle\rangle}{\langle\boldsymbol{\mu}\rangle}. \tag{8.0.11}$$

Here $\langle\boldsymbol{\mu}^p\rangle = N^{-1}\text{Tr } \boldsymbol{\mu}^p$, $\langle\boldsymbol{\tau}^p\rangle = N^{-1}\text{Tr } \boldsymbol{\tau}^p$ denote the spectral moments and $\langle\langle\boldsymbol{\mu}^p\rangle\rangle$, $\langle\langle\boldsymbol{\tau}^p\rangle\rangle$ the corresponding cumulants. [For example, $\langle\langle\boldsymbol{\tau}^2\rangle\rangle = \langle\boldsymbol{\tau}^2\rangle - \langle\boldsymbol{\tau}\rangle^2$.]

Instead of Eq. (8.0.10) we now have for the double barrier geometry a Fano factor

$$\mathcal{F} = 1 + \tfrac{1}{2}\langle\boldsymbol{\mu}\rangle(1+\kappa), \quad \kappa = \Gamma\frac{\langle\langle\boldsymbol{\mu}^2\rangle\rangle}{\langle\boldsymbol{\mu}\rangle^2}. \tag{8.0.12}$$

We may estimate the magnitude of the correction κ by noting that, typically, only $N_c \simeq A/A_c$ eigenvalues of $\boldsymbol{\mu}$ will be significantly different from 0. If we ignore the spread among these N_c eigenvalues, we have $\langle\boldsymbol{\mu}^2\rangle \approx (N/N_c)\langle\boldsymbol{\mu}\rangle^2$, hence $\kappa \approx \Gamma(N/N_c - 1)$. This correction will be negligibly small for $\Gamma \ll 1$, unless $\Gamma N \gtrsim N_c$.

In the final part of this chapter we consider the full photocount probability distribution $P(n) = (2\pi)^{-1}\int_0^{2\pi} d\xi \exp[F(i\xi) - in\xi]$. For large detection time this integral can be done in saddle point approximation. The result has the form $P(n) = \exp[\bar{n}g(n/\bar{n})]$. For small relative deviations of n from $\bar{n}$ the function $g(n/\bar{n})$ can be expanded to second order in $n/\bar{n}$. Thus the body of the distribution tends to a Gaussian for $t \to \infty$, in accordance with the central limit theorem. The same holds for the Poisson distribution (8.0.6). However, the tails of $P(n)$ for degenerate radiation remain non-Gaussian and different from the tails of $P_{\text{Poisson}}(n)$.

Let us first investigate this for a scalar $\boldsymbol{\mu} = f\mathbb{1}$. Replacing the sum over n in Eq. (8.0.4) by the integral $\int_0^1 dT\rho(T)$, which is allowed in the large-N limit, we

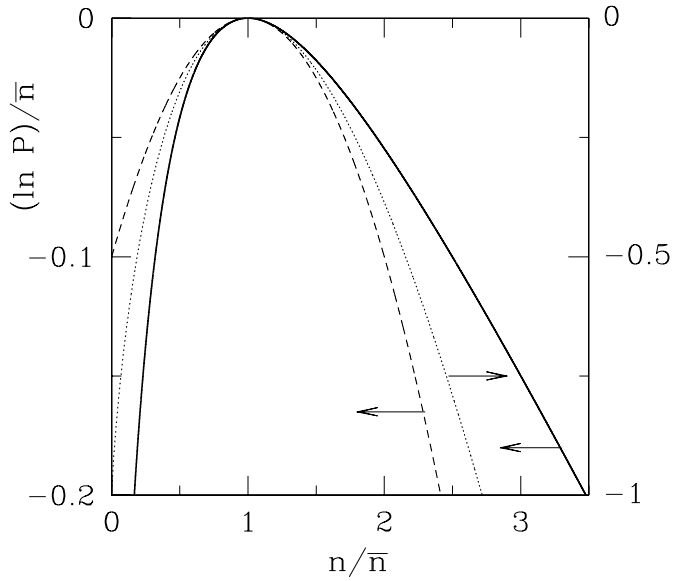

Figure 8-2. Logarithmic plot of the photocount distribution for $f = 8$ and $\bar{n} \to \infty$. The solid curve follows from Eq. (8.0.13) (describing the double barrier geometry) and is very close to the large-f limit (8.0.14). The dashed curve is a Gaussian with variance $(1 + \frac{1}{2}f)\bar{n}$ and the dotted curve is the Poisson distribution (8.0.6). (Notice the different vertical scale for the dotted curve, chosen such that the Gaussian body of the Poisson distribution becomes evident.)

find, using Eq. (8.0.9), the generating function

$$F(\xi) = \frac{t\delta\omega}{2\pi} N\Gamma\big[1 - \sqrt{1 - (e^{\xi} - 1)f}\big]. \tag{8.0.13}$$

The corresponding $P(n)$ is the K-distribution that has appeared before in a variety of contexts [7,8,17]. The K-distribution is usually considered only for $f \ll 1$, as is appropriate for thermal equilibrium. In the regime $1 \ll f \ll \bar{n}$ of interest here it has the form

$$P(n) = C\, n^{-3/2} \exp\left(-\frac{n}{f} - \frac{\bar{n}^2}{nf}\right), \tag{8.0.14}$$

with a normalization constant $C = \bar{n}(\pi f)^{-1/2} \exp(2\bar{n}/f)$. The essential singularity at $n = 0$ is cut off below $\bar{n}/\sqrt{f}$, where the distribution saturates at $P(0) = \exp(-2\bar{n}/\sqrt{f})$. In Fig. 8-2 we compare the distribution (8.0.14) with a Gaussian and with a Poisson distribution, which has the asymptotic form $P_{\text{Poisson}} = (2\pi n)^{-1/2} \exp\big[n - \bar{n} - n\ln(n/\bar{n})\big]$. The logarithmic plot emphasizes the tails, which are markedly different.

For a non-scalar $\boldsymbol{\mu}$ we find that the functional form of the large-n tail depends only on the largest eigenvalue $\lambda_{\max} \gg 1$ of the Hermitian positive definite matrix $\boldsymbol{t\mu t}^{\dagger}$,

$$\lim_{n\to\infty} P(n) \propto e^{-n/\lambda_{\max}}. \tag{8.0.15}$$

The number $\lambda_{\max}$ plays the role for a non-scalar $\boldsymbol{\mu}$ of the filling factor f in the result (8.0.14) for a scalar $\boldsymbol{\mu}$. While the large-n tail is exponential under very general conditions, the tail for $n \ll \bar{n}$ has no universal form.

In conclusion, we have calculated the effect of multiple scattering on the photodetection statistics of radiation that is both chaotic (like thermal radiation from a black body) and highly degenerate (like coherent radiation from a laser). Even for weak transmission there appear large deviations of the photocount distribution from Poisson statistics, that are absent in the radiation from a black body or a laser. They take the form of an enhancement of Var n above $\bar{n}$ by a factor $\propto f$ and a slowing down of the large-n decay rate of $P(n)$ by a factor $1/f$. Explicit results have been given for a double barrier geometry, but these findings are generic and would apply also, for example, to multiple scattering by disorder. Because of this generality we believe that experimental observation of our predictions would be both significant and feasible.

Bibliography

[1] L. Mandel and E. Wolf, *Optical Coherence and Quantum Optics* (Cambridge University Press, Cambridge, 1995).

[2] We use the word "degenerate" here by analogy with the degenerate electron gas.

[3] R. Centeno Neelen, D. M. Boersma, M. P. van Exter, G. Nienhuis, and J. P. Woerdman, Phys. Rev. Lett. **69**, 593 (1992).

[4] C. H. Henry and R. F. Kazarinov, Rev. Mod. Phys. **68**, 801 (1996).

[5] C. W. J. Beenakker, Phys. Rev. Lett. **81**, 1829 (1998).

[6] As a barrier one could use a "spatial filter" consisting of a metal perforated by a large number of sub-wavelength holes. Abrsorption by the metal should be minimized because it suppresses the multiple scattering that is at the origin of the effect predicted here. Another realization would be a layered medium with a refractive index that is randomly distributed along the direction of light propagation. There the light intensity would decay exponentially due to wave localization.

[7] R. J. Glauber, Phys. Rev. Lett. **10**, 84 (1963).

[8] C. W. J. Beenakker, in: *Diffuse Waves in Complex Media*, edited by J.-P. Fouque, NATO Science Series C531 (Kluwer, Dordrecht, 1999).

[9] L. S. Levitov and G. B. Lesovik, JETP Lett. **58**, 230 (1993).

[10] L. Y. Chen and C. S. Ting, Phys. Rev. B **43**, 4534 (1991).

[11] Ya. M. Blanter and M. Büttiker, Phys. Rep. **336**, 1 (2000).

[12] J. A. Melsen and C. W. J. Beenakker, Physica B **203**, 219 (1994). The distribution (8.0.9) requires $N \gg \Gamma^{(}-1) \gg 1$. For a spatial filter with one hole per wavelength squared one can identify Γ with the transmittance of a single hole and N with the total number of holes.

[13] C. W. J. Beenakker and M. Büttiker, Phys. Rev. B **46**, 1889 (1992).

[14] K. E. Nagaev, Phys. Lett. A **169**, 103 (1992).

[15] The coherence area $A_c \approx R^2/N_{\rm source}$ of multi-mode radiation increases quadratically with separation R from the source ($N_{\rm source}$ being the number of modes).

[16] C. W. J. Beenakker, Rev. Mod. Phys. **69**, 731 (1997).

[17] M. Bertolotti, B. Crosignani, and P. Di Porto, J. Phys. A **3**, L37 (1970); E. Jakeman and P. N. Pusey, Phys. Rev. Lett. **40**, 546 (1978). In these two papers the noise is due to time-dependent fluctuations in the scattering medium. In contrast, we consider time-dependent fluctuations of the photon flux in the presence of static scatterers.

Samenvatting

Fluctuaties in de elektrische stroom bevatten waardevolle informatie over de geleider. Bijvoorbeeld, de lading van de deeltjes die de stroom dragen volgt uit een meting van het gemiddelde van het kwadraat van de stroomfluctuaties. Dit soort ruismetingen zijn heel succesvol gebleken. Het valt te verwachten, dat verder inzicht in het ladingstransport verkregen kan worden door ook hogere machten van de fluctuaties te middelen. Uiteindelijk zou men de volledige kansverdeling van de stroomfluctuaties willen kennen en niet alleen de eerste paar momenten. Men noemt dit het probleem van de "elektronische telstatistiek", omdat men de kansverdeling van de stroomfluctuaties kan vinden door herhaaldelijk te tellen hoeveel elektronen er in een gegeven tijdsinterval passeren. Er is een analogie met de quantumoptica, waar het tellen van fotonen een heel effectieve manier is om de stralingsbron te karakteriseren. Echter, in de elektronica staat deze techniek nog in de kinderschoenen.

De elektronische telstatistiek is voor 't eerst onderzocht door Levitov en Lesovik. Zij beschouwden niet-wisselwerkende elektronen in een mesoscopische geleider (d.w.z. zonder inelastische verstrooiing) met een ideale spanningsbron. Het resultaat van die berekening is dat het aantal gepasseerde elektronen een binomiale kansverdeling heeft. (Eenzelfde statistiek treedt op bij "kruis of munt".) De binomiale telverdeling voor elektronen is analoog aan de negatief-binomiale telverdeling van fotonen uitgestraald door een zwart lichaam. Het verschil is te verklaren door het verschil in de quantumstatistiek van fermionen en bosonen.

In tegenstelling tot fotonen, zijn elektronen sterk wisselwerkende deeltjes. Men zou verwachten dat deze wisselwerking tot correlaties leidt die in de telstatistiek zichtbaar worden. Nu is de wisselwerking binnen de geleider zelf goed afgeschermd en dus niet zo effectief. Van groter belang is de elektromagnetische wisselwerking tussen de geleider en het circuit waar hij in is opgenomen. Een representatief voorbeeld, dat in dit proefschrift wordt behandeld, is de wisselwerking tussen een mesoscopische geleider G en een macroscopische serieweerstand R. De gemiddelde stroom (eerste moment) wordt gewoon met een factor $1 + RG$ verminderd door de serieweerstand. Het tweede moment wordt verminderd met een factor $(1 + RG)^2$. We hebben ontdekt dat deze simpele regel niet meer opgaat bij het derde en hogere moment. Zoals beschreven in hoofdstuk 3, treedt er een niet-lineaire terugkoppeling op die momenten van verschillende orde koppelt.

In hoofdstuk 5 tonen we aan dat deze terugkoppeling een drastisch effect heeft op de temperatuurafhankelijkheid van de stroomfluctuaties. We onderzoeken het geval van een tunnelbarrière, waar het derde moment temperatuuronafhankelijk zou zijn zonder serieweerstand. De eerste metingen uit Yale University lieten echter een sterke temperatuurafhankelijkheid zien, die zelfs gepaard ging met een tekenomslag. Onze terugkoppelingstheorie blijkt een kwantitatieve verklaring te geven van deze metingen.

In hoofdstuk 4 onderzoeken we het verschil tussen enerzijds spanningsfluctuaties met een ideale stroombron (oneindige inwendige weerstand) en anderzijds stroomfluctuaties met een ideale spanningsbron (nul inwendige weerstand). Dit verschil betreft de twee limieten $R \to \infty$ en $R \to 0$ van de theorie uit hoofdstuk 3. Zoals gezegd hebben stroomfluctuaties de binomiale verdeling. Voor spanningsfluctuaties vinden we de Pascalverdeling, ook wel bekend als de binomiale wachttijdverdeling. In het geval van "kruis of munt", geeft de binomiale verdeling de kans op het aantal malen kruis bij een vast aantal worpen van het muntstuk. De Pascalverdeling geeft de kans op het aantal keren dat men moet werpen om een vast aantal malen kruis te vinden. De berekening is nogal technisch, maar we geven ook een eenvoudige fysische verklaring.

De verschijnselen die we tot dit punt hebben beschreven zijn klassieke elektromagnetische verschijnselen. Quantummechanische effecten treden op als de serieweerstand groter is dan het quantum h/e^2 bij frequenties van orde $eV/\hbar$ (met V de aangelegde spanning). De serieweerstand is dan snel genoeg om het passeren van een enkel elektron te kunnen volgen. Er treedt dan een effect op dat de Coulomb blokkade wordt genoemd. De stroom wordt op een niet-lineaire manier onderdrukt als de spanning naar nul gaat. De onderdrukking wordt voor een tunnelbarrière beschreven door een machtswet. In hoofdstuk 6 onderzoeken we de onderdrukking voor een willekeurige mesoscopische geleider. Nog steeds geldt een machtswet, maar de exponent kan anders zijn dan voor de tunnelbarrière. Opmerkelijk genoeg vinden we dat er maar twee mogelijke waarden zijn voor de exponent. Er zijn dus maar twee universaliteitsklassen. Alle geleiders in dezelfde klasse gedragen zich hetzelfde bij lage spanningen. Een enkele tunnelbarrière zit in de eerste klasse, een dubbele tunnelbarrière in de tweede klasse.

De hoofdstukken 2, 7 en 8 betreffen ook telstatistiek, maar in een andere context.

Hoofdstuk 2 betreft telstatistiek in supergeleiders. We presenteren een oplossing voor de paradox van de "negatieve waarschijnlijkheden", die was opgetreden in een eerdere studie van de elektronische telstatistiek in een Josephson junctie. Dit is een supergeleidende ring, onderbroken door een zwakke schakel. De stroom door de ring vloeit in evenwicht, zonder een aangelegde spanning. We identificeren een quasiklassieke benadering in het model van Levitov en Lesovik als de oorzaak voor het optreden van negatieve waarschijnlijkheden en geven aan hoe die benadering vermeden kan worden.

Hoofdstuk 7 betreft de telstatistiek van impuls, in plaats van lading. Dit is een probleem uit de nanomechanica. Fluctuaties in de elektrische stroom door een vrij opgehangen geleider van nanometer-afmetingen kunnen een mechanische trilling veroorzaken, doordat de elektronen tegen verontreinigingen aanbotsen. Eerdere semiklassieke berekeningen van het tweede moment van de impulsoverdracht hadden aangetoond dat dit een waarneembaar effect zou moeten zijn. We geven een volledig quantummechanische theorie voor alle mo-

menten. Het is een klein effect, ten gevolge van de lage relatieve bijdrage van de elektronen aan de massa van de geleider. Deze elektromechanische trillingen kunnen worden onderscheiden van thermische trillingen via de spanningsafhankelijkheid en de niet-normale verdeling van de verplaatsing.

Hoofdstuk 8, ten slotte, behandelt een opvallend verschil tussen elektronische en fotonische telstatistiek. Dit verschil treedt op als de gemiddelde bezetting van de fotontoestanden groot is ten opzichte van 1, hetgeen uiteraard niet mogelijk is voor elektronen. In het geval van meervoudige verstrooiing ontstaat dan een grote toename van de fotonruis, die geen elektronisch analogon heeft.

List of publications

- *Phase transitions in liquid ^{3}He*, M. Kindermann and C. Wetterich, Phys. Rev. Lett. **86**, 1034 (2001).
- *Manipulation of photon statistics of highly degenerate incoherent radiation* , M. Kindermann, Yu. V. Nazarov, and C. W. J. Beenakker, Phys. Rev. Lett. **88**, 063601 (2002). [Chapter 8]
- *Full counting statistics of a general quantum mechanical variable*, Yu. V. Nazarov and M. Kindermann, preprint, cond-mat/0107133. [Chapter 2]
- *Quantum theory of electromechanical noise and momentum transfer statistics*, M. Kindermann and C. W. J. Beenakker, Phys. Rev. B **66**, 224106 (2002). [Chapter 7]
- *Momentum noise in a quantum point contact*, A. Tajic, M. Kindermann, and C. W. J. Beenakker, Phys. Rev. B **66**, 241301(R) (2002).
- *Distribution of voltage fluctuations in a current-biased conductor*, M. Kindermann, Yu. V. Nazarov, and C. W. J. Beenakker, Phys. Rev. Lett. **90**, 246805 (2003). [Chapter 4]
- *Full counting statistics in electric circuits*, M. Kindermann and Yu. V. Nazarov, in "Quantum Noise in Mesoscopic Physics", edited by Yu. V. Nazarov, NATO Science Series II Vol. 97, p. 403-427 (Kluwer, Dordrecht, 2003).
- *Temperature dependent third cumulant of tunneling noise*, C. W. J. Beenakker, M. Kindermann, and Yu. V. Nazarov, Phys. Rev. Lett. **90**, 176802 (2003). [Chapter 5]
- *Interaction effects on counting statistics and the transmission distribution*, M. Kindermann and Yu. V. Nazarov, preprint, cond-mat/0304078. [Chapter 6]
- *Production and detection of entangled electron-hole pairs in a degenerate electron gas*, C. W. J. Beenakker, C. Emary, M. Kindermann, and J. L. van Velsen, preprint, cond-mat/0305110.
- *Feedback of the electromagnetic environment on current and voltage fluctuations out of equilibrium*, M. Kindermann, Yu. V. Nazarov, and C. W. J. Beenakker, preprint, cond-mat/0306375. [Chapter 3]
- *Quantum teleportation by particle-hole annihilation in the Fermi sea*, C. W. J. Beenakker and M. Kindermann, preprint, cond-mat/0307103.

- *Dephasing of entangled electron-hole pairs in a degenerate electron gas*, J. L. van Velsen, M. Kindermann, and C. W. J. Beenakker , to appear in a special issue on “Quantum Computation at the Atomic Scale” of Turk. J. Phys (2003).

Curriculum Vitæ

Ik ben geboren op 6 augustus 1974 in Regensburg. In de herfst van 1981 ging ik naar de lagere school in Regenstauf en vervolgens in 1985 naar de middelbare school in Burglengenfeld. Mijn eindexamen (Abitur) deed ik in 1994. Daarna vervulde ik mijn civiele dienstplicht in een ziekenhuis in Burglengenfeld.

In de de herfst van 1995 begon ik de studie natuuurkunde aan de universiteit van Heidelberg, gesteund door een beurs van de staat Beieren. Mijn kandidaatsexamen (Vordiplom) legde ik af na het derde semester. Toen ontving ik tevens een beurs van de "Studienstiftung des deutschen Volkes".

Het collegejaar 1997–1998 bracht ik door aan de Universiteit van Illinois in Urbana-Champaign. Daar volgde ik colleges in de theoretische natuurkunde en deed experimenteel werk in de groep van Prof.dr. J.P. Wolfe.

Terug in Heidelberg legde ik in juni 1999 de drie doctoraalexamens in de natuuurkunde af. Mijn afstudeeronderzoek deed ik in de periode 1999–2000 in de groep van Prof.dr. C. Wetterich. De titel van mijn scriptie (Diplomarbeit) is "Matrix models in exact renormalization group equations". Het behandelt aspecten van veldentheorieën die een beschrijving geven van vloeibare kristallen en vloeibaar ^{3}He. Tijdens mijn afstudeeronderzoek nam ik deel aan een workshop over topologische defecten in Capri.

In oktober 2000 begon ik mijn promotieonderzoek aan de Universiteit Leiden in dienst van de Stichting voor Fundamenteel Onderzoek der Materie (FOM). Mijn begeleiders waren Prof.dr. C.W.J. Beenakker (Universiteit Leiden) en Prof.dr. Yu.V. Nazarov (Technische Universiteit Delft). De belangrijkste resultaten van dit onderzoek zijn beschreven in dit proefschrift.

Naast mijn onderzoek assisteerde ik in 2001 en 2002 bij het college Elektromagnetisme II. Ik volgde zomerscholen in Windsor (Engeland), Bad Honnef (Duitsland) en Erice (Italië) en presenteerde mijn werk op conferenties in Matrafured (Hongarije), Rome en Delft.

STELLINGEN

behorend bij het proefschrift
Electron counting statistics in nanostructures

1. A Hall bar in the quantum Hall regime is a non-invasive current meter.

   This thesis, chapter 3.

2. Voltage noise presents the first appearance in mesoscopic physics of the Pascal distribution.

   This thesis, chapter 4.

3. The environmental Coulomb blockade has two universality classes.

   This thesis, chapter 6.

4. The distribution of displacements of a suspended current-carrying nanowire is non-Gaussian.

   This thesis, chapter 7.

5. A tunnel barrier creates entangled electron-hole pairs in the Fermi sea.

   C. W. J. Beenakker, C. Emary, M. Kindermann, and J. L. van Velsen, preprint, cond-mat/0305110.

6. Electron-hole annihilation realizes quantum teleportation in condensed matter.

   C. W. J. Beenakker and M. Kindermann, preprint, cond-mat/0307103.

7. The fourth cumulant of current fluctuations through a conductor may be measured efficiently through the variance of the heat produced in a series resistor.

8. Transitions between the superfluid phases of liquid ^{3}He are first order.

   M. Kindermann and C. Wetterich, Phys. Rev. Lett. **86**, *1034 (2001).*

9. It is beneficial for the digestion to eat carbohydrates separately from proteins.

Markus Kindermann
Leiden, 3 september 2003